Stochastic Analysis of Wind Turbine Power Curves

Edgar Anahua

CARL VON OSSIETZKY
universität OLDENBURG

Oldenburg 2007

Stochastic Analysis of Wind Turbine Power Curves

Edgar Anahua

Von der Fakultät für Mathematik und Naturwissenschaften
der Carl von Ossietzky Universität Oldenburg
zur Erlangung des Grades und Titels eines

DOKTOR DER NATURWISSENSCHAFTEN
DR. RER. NAT.

angenommene Dissertation

von Herrn Edgar Anahua
geboren am 17.11.1971 in Tacna (Peru)

Gutachter: Prof. Dr. Joachim Peinke

Zweitgutachter: Prof. Dr. Alexander Rauh

Tag der Disputation: 05.10.2007

Abstract

This work shows a novel method to characterize the wind turbine's power performance directly from high frequency fluctuating measurements. In particular we show how to evaluate dynamic responses of the wind turbine system on fluctuating wind speed in the range of seconds. The method is based on the stochastic differential equations known as the Langevin equations of diffusive Markov processes. In this analysis the fluctuating wind turbine power output is decomposed into two functions: i) the relaxation, which describes the deterministic dynamic response of the wind turbine to its desired power production; and ii) the stochastic force (noise), which is an intrinsic feature of the system of wind power conversion. As a main result we show that independently of the turbulence intensity of the wind the characteristic of the wind turbine power performance is properly reconstructed. This characteristic is given by their fixed points (steady-states) from the deterministic dynamic relaxation conditioned for given wind speed values. The method to estimate these coefficients directly from the data is presented and applied to numerical model data, as well as, to real world measured power output data. The method is universal and not only more accurate than the current standard procedure of ensemble averaging (*IEC-61400-12*) but it also allows a faster and robust estimation of wind turbine's power curves. In addition, the stochastic power output of a wind turbine was analyzed in the response theory. To derive the delayed response from measured data a simple example for relaxation in the special case of constant power output is discussed.

Zusammenfassung

Diese Arbeit stellt eine neuartige Methode zur Bestimmung von Leistungskennlinien von Windkraftanlage auf Basis von hochfrequenten, fluktuierenden Messdaten dar. Insbesondere wird gezeigt, wie die Antwort einer Windkraftanlagen auf turbulente Windschwankungen im Sekundenbereich berechnet werden kann. Die Methode basiert auf einer stochastischen Differentialgleichung – bekannt als Langevin-Gleichung – für diffusive Markovprozesse. Zunächst wird die stochastische Leistungsabgabe in zwei Komponenten aufgeteilt: i) die deterministische Antwort einer Windkraftanlage, die die Relaxation auf die vorgegebene Regelleistung beschreibt und ii) die stochastische Kraft (Rauschen), die eine intrinsische Eigenschaft der Windenergiewandlung ist. Als Hauptergebnisse zeigen wir, dass unabhängig von der Turbulenzintensität die Leistungskennlinie genau rekonstruiert werden kann. Die Kennlinie ist dabei durch die stabilen Fixpunkte der deterministischen Dynamik gegeben. Die Methode zur Bestimmung dieser Koeffizienten aus Messdaten wird beschrieben und auf numerische Modelldaten sowie reale Leistungsdaten angewendet. Das Verfahren ist universell und nicht nur exakter als das Standardverfahren nach *IEC-61400-12*, sondern auch effizienter and robuster. Die stochastische Leistungsabgabe wird ausserdem mit Hilfe der „response theory“ analysiert. Um die zeitversetzte Antwort einer Windkraftanlage aus Messdaten abzuleiten, wird ein einfaches Beispiel für die Relaxation im Sonderfall konstanter Leistungsabgabe diskutiert.

Contents

List of Figures

Chapter 1

General Introduction

Wind energy is world-wide growing faster to be a mainstream power source and it is expected to contribute importantly into the existing electric power generation mix in the coming future. This enormous growth has been driven by climate changes and energy supply security aspects. The European Union, as wind energy leader, has already started with a directive for the energy integration policies of the renewable energy sources in order to reduce CO_2 emissions. Currently the overall European renewable energy shares abruptly in the electric power generation 13.4% and the target is for 21% by 2010. For example, the installed wind capacity reached 40.5 GW at 2005 and this is already achieved, five years ahead of time, because the target set by the European Union was at the end of ninety-years for 40 GW by 2010 [1, 2, 3]. Thus an important market for the wind turbine industry and investors from the mainstream finance and traditional sectors has been established.

Although wind energy developments increase rapidly wind turbines designs have also improved fast in the last twenty years. The planning, building and operating of wind energy projects are still a challenge. Because for the power productive capacity assessment of wind power plants the power performance of a wind turbine, namely the power curve, is crucial. Therefore several technical and economical risks in specific sites with higher turbulent wind fields (e.g. complex and off-shore areas) have been brought forward, especially by project developers and manufacturers. One of their main problems is the lack of accurate methods for the estimating power curves at the site specific which is very important for such assessment. Actually current methods to estimate power curves are only provided in an ideal site, namely flat terrain, under standard conditions according to the official approval of a wind turbine.

As the power output of a wind turbine depends mainly on the turbulent winds, and, also on the wind turbine dynamics, high uncertainties of the order of 10%-20%, even for sites of

flat terrains, are usually found in the power assessment. Those significant results are due to the fact that those dynamics effects had not been well understood for such assessments and are, therefore, the main risk parameter of importance in the feasibility of projects. This is a relevant basic problem which concern with the method to determine properly the true power curve of wind turbines in the wind fields and which has to be investigated in detail in order to separate the definition of the actual power performance and the power yield potential of a wind turbine.

1.1 Propose of the thesis

This thesis concerns with the method to characterize power curves of wind turbines in the wind fields. The power curve is the most important characteristics of a wind turbine. Actually the method to estimate power curves, which is given by the standard (*officially regularized in the IEC 61400-12*), is based on measured 10 - minute average values of wind and power. In fact, there are several problems concerning to this method. For example, the averaging time of those mean values, which is applied over the collected data, is too long for the purpose of power performance estimation. Furthermore, the basic problem of those mean values are that in principle they are affected by turbulent winds due to the nonlinearity of the power and to wind turbine responses. That is why measured power curves are actually wind turbulence dependent, especially for sites of complex terrains. To add in this point this procedure is inaccurate for estimating power curves and, hence, the wind power potential. Therefore, it is important to investigate a new procedure by means of the dynamics for the stochastic power output. Hence, the new method, which considers all dynamics of the power output to the turbulent winds, should provide wind turbulence independent power curves, fast measurement period and the separation of the wind and power production. This is an important procedure for the manufacturers as it allows to estimate, more reliably, accurate power curves for arbitrary specific sites and, thus optimize costs in the power performance verification, calibration and assessment phases.

In this work we introduce the definition of wind turbine power conversion for given wind speeds of a given site by the stochastic power output. We focus on how to evaluate the dynamic response of the wind turbine power output on fluctuating wind speeds in the range of seconds. This include the assessment of the overall dynamical behavior of the the stochastic power to its true steady power production in terms of their fixed-points (attractor). Also the decomposition of the stochastic power by of its relaxation, which describe the deterministic dynamic response of the turbine on sudden wind speed changes, to its desired power operation state, and the stochastic force (noisy), which is intrinsic feature of the

power production system. A new stochastic *Markov* power output model is introduced, which is based on a stochastic differential equations known as *diffusive Langevin* equation of Markov processes. Special attention is paid to the deterministic dynamic relaxation, which is the main parameter for finding those fixed-points. The result of this new method, so-called *Markovian power curves*, can be used to reconstruct properly wind turbulence independent power curves of specific wind turbines of an arbitrary site in an optimized way.

In addition, the stochastic power output of a wind turbine is also analyzed in the response theory. A more general relaxation model, which take into account the power response as a non-linear function and the wind field is introduced. The results can be applied to predict power output for arbitrary turbulence wind fields.

1.2 Structure

The structure of this thesis is organized as follows. Following this introduction, in Chapter 2 the basic concepts of stochastic for describing the power output process of wind turbines is briefly described. The standard procedure (*IEC 61400-12*) for power performance characterization of a single wind turbines is shown. An overview of a selection of the more relevant existing power output prediction approaches which take into account the turbulence of the wind and, lately, the dynamical characteristics of the wind turbine are discussed.

In Chapter 3 the data used in this work are briefly described. Also a standard analysis of the data and the respective measured power curve of a large wind turbine by the standard method is illustrated.

In Chapter 4 the Markovian method to characterize power curves directly from high-frequency measurement data is explained. An illustration of stochastic power output from numerical model are reproduced by measured wind fields from different sites and turbulence intensities. The procedure of the stochastic analysis is described in detail. Results of the Markovian method and standard method are shown.

In Chapter 5 the relaxation function of the wind turbine in the wind field to predict power output is analyzed in the response theory. The preliminary results of this method from measurement data is discussed.

And, in Chapter 6 a summary of this thesis with the conclusions and an outlook are given.

Chapter 2

Theoretical Fundament

This chapter briefly shows basic concepts of stochastic that are needed as background for the description of the power output process of wind turbines developed lately in the wind energy field.

In the steady wind situation, the theoretical wind power extraction approach of a wind turbine is presented. To show the importance of the aerodynamics properties of the wind turbine rotor, given by its performance coefficient, into the power production, the power output characteristics of a real wind turbine is presented. The standard method (*IEC 61400-12*) to characterize the power performance of wind turbines from measurement data is shortly discussed.

As atmospheric wind flows are turbulent, the effects of wind turbulence intensity to the expected wind power extraction is introduced. In order to take into account these wind fluctuations the mean power value from a wind turbine in the case of weak turbulence on the wind is described by a Taylor series approach. In addition, to include the inherent dynamical wind turbine interaction with the fluctuating winds the Taylor approach for the mean power is modified. The generalization of this modified Taylor approach for the case of arbitrary turbulence is given by a dynamical response model based in a differential equation is presented.

2.1 Basic statistics wind turbine power output

Since the energy available in the wind depends basically by the variability of the wind basic concepts of random variable and its distributions are used. Also the concepts of stationarity, characterization by the two-points-autocorrelation function as well as its relation with the power spectrum are briefly described.

2.1.1 Random variable and distributions

Let U be a *random variable* of a physical (stochastic) process, whose outcomes is a collection of U-random values, gives the real numerical value u. We call the *distribution function* $F(u)$ as the probability W of the random variable U that would take the value u satisfying the following inequality $U < u$ of set of points

$$F(u) \quad = \quad W(U < u) \quad \forall U \in \mathrm{R}. \tag{2.1}$$

If the random variable is continuous in a range of values then the distribution function is defined as the *probability density function* $f(u)$ by

$$F(u) \quad = \quad \int_{-\infty}^{u} f(u')du'. \tag{2.2}$$

This implies that the total integral from $-\infty$ to $+\infty$ is equal to 1. Thus it follows that $f(u) \geq 0$ and the normalization condition satisfies the following equality

$$1 = \lim_{u \to +\infty} W(U < u) = \int_{-\infty}^{+\infty} f(u)du. \tag{2.3}$$

The nth *moments* u of the stochastic variable U are defined as

$$\langle u^n \rangle = \int_{-\infty}^{+\infty} u^n f(u)du. \tag{2.4}$$

The brackets $\langle\ \rangle$ indicate the ensemble average. The first moment is the *mean value*, called also the expected value $E(U)$

$$\langle u \rangle = E(U) = \int_{-\infty}^{+\infty} uf(u)du. \tag{2.5}$$

As an important quantity, the nth central-moment of U is defined by

$$\mu_n = \int_{-\infty}^{+\infty} (u - E(U))^n f(u)du. \tag{2.6}$$

Obviously, the first central moment is thus zero. The second central moment is the *variance*,

$$\mu_2 = \sigma_u^2 = \int_{-\infty}^{+\infty} (u - E(U))^2 f(u) du, \tag{2.7}$$

where its square root σ_u is the known *standard deviation*. In general, odd-orders central moments of Eq. (2.6) give the asymmetry property of the distribution while even-orders describe the broad property of the distribution. If all the central moments of the random variable are known then its distribution is completely characterized.

The most known probability density function of a random variable U is the *Gauss* (or normal) distribution which is given by

$$f(u) = \frac{1}{\sqrt{2\pi\sigma}} exp\left(-\frac{(u-a)^2}{2\sigma^2}\right). \tag{2.8}$$

This distribution is completely characterized only by its first two moments, the expected value a and the variance σ^2. The importance of the Gauss distribution is its property attributed to the *central limit theorem*, which states that the distribution of a sum of a large number of independent variables is approximately normal [4].

In the case of two functional random variables U and X and considering Eq. (2.3) the probability density function of $f(x)$ is defined by

$$f(x) = f(u(x)) \frac{du}{dx}. \tag{2.9}$$

Now, considers the case of N random variables $U_1, U_2, ..., U_N$, the distribution function, called the *joint distribution function*, is defined similarly as it is presented in Eq. (2.1)

$$F(u_1, u_2, ..., u_N) = W(U_1 < u_1, U_2 < u_2, ..., U_N < u_N) \tag{2.10}$$

and their probability density function by

$$F(u_1, u_2, ..., u_N) = \int_{-\infty}^{u_1'} \int_{-\infty}^{u_2'} ... f(u_1', u_2', ..., u_N') du_1' du_2' ... du_N'. \tag{2.11}$$

From Eq. (2.3) it follows that the integration of N dimensional probability satisfies the normalization condition

$$1 = \int_{-\infty}^{u_1} \int_{-\infty}^{u_2} ... f(u_1, u_2, ..., u_N) du_1 du_2 ... du_N. \tag{2.12}$$

If all different pairs of the normally distributed random variables are independent then these random variables have independent probability densities

$$f(u_1, u_2, ..., u_N) = f(u_1) f(u_2) ... f(u_N). \tag{2.13}$$

The advanced form for analyzing the relationship between random variables is given by the conditional probability, $f(u_1|u_2)$, see Ref. [5]. Let U_1 and U_2 be two random variables. The conditional probability in terms of the joint probability density, $f(u_1,u_2)$, is written as follows

$$f(u_1|u_2) = \frac{f(u_1,u_2)}{f(u_2)}, \tag{2.14}$$

which states that if the probability density of the variable u_2 is known too, then the probability density of the first variable u_1 conditioned at u_2 can be determined.

The *covariance*, defined as

$$cov(u_i,u_j) = \langle (u_i - E(U_i))(u_j - E(U_j)) \rangle \tag{2.15}$$

is an important quantity to measure dependencies of two random variables U_i and U_j with expected values $E(U_i)$ and $E(U_j)$ respectively.

The *correlation coefficient*, in the usual normalized form is

$$R_{i,j}(u_i,u_j) = \frac{cov(u_i,u_j)}{\sigma_{u_i}\sigma_{u_j}} = \frac{\langle (u_i - E(U_i))(u_j - E(U_j)) \rangle}{\sigma_{u_i}\sigma_{u_j}}. \tag{2.16}$$

If the two variables are independent then the correlation is zero. But the inverse is not true in general sense because the correlation coefficient shows only linear dependencies. However, in the especial case when U_i and U_j are jointly normal, independence is equivalence to uncorrelatedness.

In the statistic of the fluctuating $u(t)$ time variable, often the correlation function at two different times is of interest. The quantity of the two-point-correlations function is called *autocorrelation function* and is defined, in the normalized form, as

$$R_{uu}(t,t+\tau) = \frac{\langle u(t)u(t+\tau) \rangle}{\sigma_u^2}. \tag{2.17}$$

For the special case of stationary $u(t)$, as defined later, the quantity $R_{uu}(t,t+\tau)$ becomes independent of the time t, i.e. $R_{uu}(\tau)$. The values $R_{uu}(\tau)$ are within the range between $-1 \leq R_{uu} \leq 1$. If $R_{uu}(\tau) = 1$ then $u(t)$ and $u(t+\tau)$ are perfectly correlated. If $R_{uu}(\tau) = -1$ then they are perfectly anticorrelated and if $R_{uu}(\tau) = 0$ then they are not correlated.

A general and applied quantity to characterize turbulent flows is given by the *power spectra* or *Fourier analysis*. The Fourier transform of a variable $u(t)$ is defined by

$$H_u(f) = \int_{-\infty}^{+\infty} u(t) e^{2\pi i f t} dt \ , \tag{2.18}$$

where the the amplitude $H_u(f)$ is a function of f frequency. The power spectral density function is given by

$$S_u(f) \propto |H_u(f)|^2 \,, \tag{2.19}$$

which describes how the energy (or variance) of a time series is distributed with the frequency f function. Note that the power spectral $S_u(f)$ is proportional to the Fourier transform of the two-point autocorrelation function $R_{uu}(\tau)$, [4].

Now, let $h(t)$ and $g(t)$ be two random variables and their corresponding Fourier transforms $H(f)$ and $G(f)$ respectively. The convolution of these two variables, denoted g$*$h, is defined by

$$g * h = \int_{-\infty}^{\infty} g(\tau)h(t-\tau)d\tau. \tag{2.20}$$

The product $g*h$ is a function in the time domain and the $g*h = h*g$. It turns out that the function $g*h$ is one member of a simple transform pair

$$g * h \Leftrightarrow G(f) * H(f). \tag{2.21}$$

This is known as the "convolution theorem". In other words, the Fourier transform of the convolution is just the product of the individual Fourier transforms.

2.1.2 Stationarity

An essential simplification of the stochastic process ($u = u(t_1),...,u(t_n),\ \forall n = 1,...,n$) is if the time dependence is taken out of the distribution function. So that the stochastic values of $u(t)$ remains itself essentially invariable at the time evolution of t. Hence, the stochastic $u(t)$ variable satisfies the following restriction

$$E(U(t)) = E(U(t+\tau)) = \mu_u, \tag{2.22}$$

$$R_{uu}(t,t+\tau)) = R_{uu}(\tau),\ \ \forall\tau \in \mathrm{R}\,. \tag{2.23}$$

A process with this characteristics is called *stationarity process*. That means that the probability function at a fixed time is the same for all the times, [4].

2.1.3 Turbulence intensity

An basic quantity to measure the turbulence of a stochastic variable $u(t)$, which is defined by its mean μ_u and fluctuating $u'(t)$ components, i.e. $u(t) = \mu_u + u'(t)$, is given by its

turbulence intensity. The turbulence intensity is defined as the ratio of the σ_u standard deviation of u, given by Eq. (2.7), in relation to its mean μ_u value

$$I_u = \frac{\sigma_u}{\mu_u}\,, \tag{2.24}$$

and describes the overall level of turbulence of the stochastic $u(t)$ variable. Note that the value I_u does not contain any dynamical or time-resolved information about the fluctuation itself. In this case an advanced analysis in the small-scale turbulence can be given by the statistic of increments, see Ref. [6]. However, applications of Eq. (2.24) in the wind energy field are given in Ref. [9, 12].

2.2 The power of wind turbines

2.2.1 Theoretical power extraction from the wind

The primarily purpose of the wind turbines is the conversion of the kinetic energy from the wind into (usually) electrical energy. This is achieved by the moments and energy wind flows that are considered in a stream-tube that encloses the rotor disc, see Ref. [9]. The mechanical wind power extraction by a horizontal wind turbine converter, at the steady-state and uniformly flow on the loaded rotor area, is given by the following expression

$$P_s(V) \;=\; \frac{1}{2}\,\rho\,A_r\,C_p\,V^3, \tag{2.25}$$

where ρ is the air mass density and the constant A_r is the wind turbine's rotor swept area.

The quantity $C_p < 1$ and is the power (or performance) coefficient of the wind turbine system and is in general a function of the wind speed V. The maximum value of $C_{p,max} = 16/27$, so-called *Betz limit*, is the theoretical achievable value into the free-stream airflow when the wind speed slows down to $2/3$ at the actuator rotor disc, see Ref. [8, 9].

In fact, the power C_p coefficient of real wind turbines achieves lower values than theoretical value because the aerodynamics losses, which depend on the rotor construction or characteristics (e.g. number and shape of blades, weight, stiffness, etc).

The wind speed V represent the actual wind velocity at the hub height, or center of rotor as reference, of the wind turbine. Note that Eq. (2.25) gives the theoretical expected power output $P_s(V)$ that one obtains if the wind speed is frozed (constant) in at the steady V value, i.e. fluctuating winds are not considered.

2.2.2 Power performance of real wind turbines

In Eq. (2.25) we have shown that for a given wind speed V the power extraction of a given wind turbine also depends on the aerodynamics properties of the rotor. These aerodynamics properties, which are given by its power C_p coefficient, are important for the power performance characteristics of the specific wind turbine.

In the mechanical wind turbine power extraction the usual way to controll power production is achieved by stall (flow separation) effects[1] on the rotor blades, [9]. In modern larger wind turbines machines this is achieved by so-called *active stall* controll or *pitch control*, see Ref. [9, 10]. This consists by rotation of the blades into the plane of rotation and the blade cross-section. The blade rotation angle is known as blade pitch angle ϑ. The power C_p coefficient, in this case, is denoted as function of the tip-speed ratio[2] λ and the blade pitch angle ϑ parameter, i.e. $C_p(\lambda, \vartheta)$. Thus, the power extraction of wind turbines is optimized to a desired power production as well as it protects of damages in the turbine design in cases of excessive wind conditions (over power production).

In the wind energy conversion to achive an effective pitch control the wind turbine is equipped by an power controller system. This is, in general, composed by several composite mechanical-electrical components that, depending on the type of design, it operates actively for the optimum power performance. As consequence the power output operation for active stall wind turbine systems can be distinguished into two states: *partial load* and *full load*. A complet detail about the overall structure of the power operation system for different wind turbine types is described in Ref. [9, 10]. In the case of numerical wind turbine simulation this can be found, as example, in Ref. [11]. In Figure 2.1 the static power curve characteristics of a wind turbine system and the partial and full load operating states is depicted.

The partial load, $V > V_{cut-in}$, where V_{cut-in} is the minimum wind speed for power production, the wind turbine yields the maximum wind energy extraction by power optimization operation. This is achieved by an effective power control system, which adjust to the desired pitch angle ϑ at a given wind speed V value in order to optimize the power C_p coefficient and hence the power production. In practice a simple lookup table is the most used method for this operation, see Ref. [11].

The partial load of the power curve is limited to the range $V_{cut-in} \leq V \leq V_r$. The wind speed V_r is the rated wind velocity. For $V > V_r$ the wind turbine generates the rated P_r.

[1] In aerodynamics, a stall is a sudden reduction in the lift forces generated by an airfoil when the critical angle of attack for the airfoil is exceeded.

[2] The tip-steep ratio λ at the wind turbine rotor is defined as $\lambda = \omega R/V$, where ω is the angular velocity of rotor, R the rotor radius ($\approx$ blade length) and V the wind speed

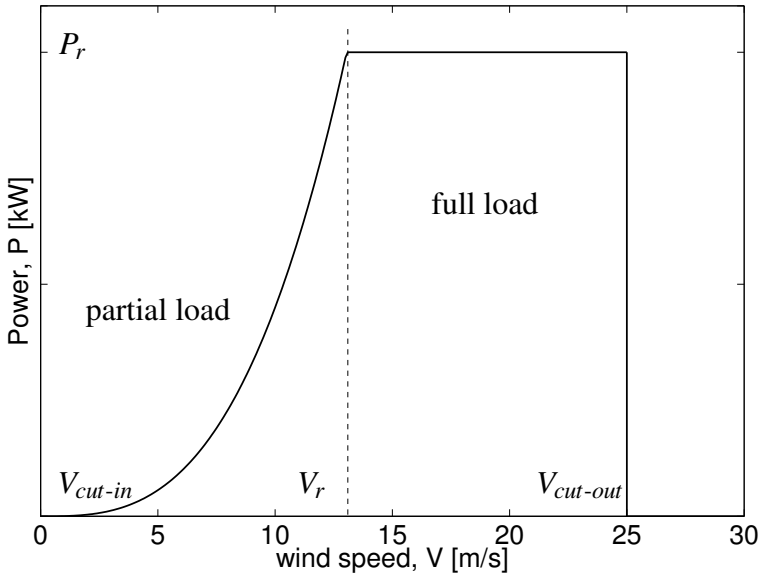

Figure 2.1: *Static (steady-state) power curve $P_s(V)$ of an active stall controlled wind turbine showing the two power operation states: partial and full load*

The full load $V_r \leq V \leq V_{cut-out}$, where $V_{cut-out}$ is the maximum wind speed, or also shut-down wind speed, for power production, the wind turbine power output is limitated to nominal power. In this power operation the pitch angle ϑ is adjusted to control the stall effect and hence the power output is reduced to its rated P_r power.

For $V > V_{cut-out}$ the pitch angle ϑ is maximized (minimizing the angle attack) to the feathered position in order to get full stall effect on the rotor blades. As consequence power generation is switched off (stopped).

2.2.3 Standard power curve

In wind energy applications, to assess the power performance of a given specific wind turbine generator system in the long-term energy production expected on a given site, an estimation of its power curve characteristic from measurements is required. The standard procedure to achieve such evaluation is currently given by the standard *IEC 61400-12* [3] [12].

In this standard procedure the power curve of a single wind turbine is estimated by collected mean values, which are taken from instantanenous short-term measurements of the

[3] The International Electro-technical Commission (IEC) is the current developing of standards specifically applicable to wind turbines.

horizontal wind speed $u(t)$ at the hub height as reference with a certain distance upwind from the wind turbine and their corresponding electrical power output response $P(u(t))$, as recommended in [12].

The empirical power curve from those measured mean values are found by a functional mean values relation. This is written as, if the air density is assumed constant in Eq. (2.25), else air density corrections has to be considered properly see [9, 12]

$$P : \langle u(t)\rangle_T \to \langle P(u(t))\rangle_T. \tag{2.26}$$

On this base the measured power curve of the specific wind turbine is determined. The $\langle\cdot\rangle$ brackets denotes the short-time ensemble averages, commonly over a time period $T = 10$ minutes is used.

In this procedure the following notation for the fluctuating $u(t)$ wind variable with 10 minute mean value $V = \langle u(t)\rangle$ and stochastic u' contribution with $\langle u'(t)\rangle = 0$ is considered. In the same way, the corresponding fluctuating output power $P(t) = P + p'(t)$ with mean value $P = \langle P(u(t))\rangle$ and stochastic p' with $\langle p'(t)\rangle = 0$ is also adopted.

In the analysis, the ensemble mean relation (2.26) for the power curve is usually given by the known *method of bins*, [33]. This consists in calculating the corresponding ensemble mean values as

$$V_i = \frac{1}{N_i}\sum_{j=1}^{N_j} V_{ij}\ , \qquad P_i = \frac{1}{N_i}\sum_{j=1}^{N_j} P_{ij} \tag{2.27}$$

into the wind speed intervals of 0.5 m/s as width of wind speed bins. The terms V_{ij} and P_{ij} are just the jth 10 min averages of wind speed and the coresponding power output in the ith bin, respectively. The ensemble averages (V_i, P_i), which is given by (2.27), describes the measured power curve for the specific wind turbine generator system [9, 12].

However, one of the the main problem of the ensemble averaging procedure (IEC standard) for evaluating measured power curves (2.26) is the fundamental non-linearity characteristics of the power curve, i.e. $P(u) \propto u^3$, see Eq. (2.25), that in combination with short-term turbulent wind situations yield the following inequality at the expected power value: $P_s(V) \neq \langle P(u)\rangle$. In Figure 2.2 the effects of the non-linearity on the standard power curve for 10%, 20% and 30% of turbulence intensities of the wind (2.24) are depicted.

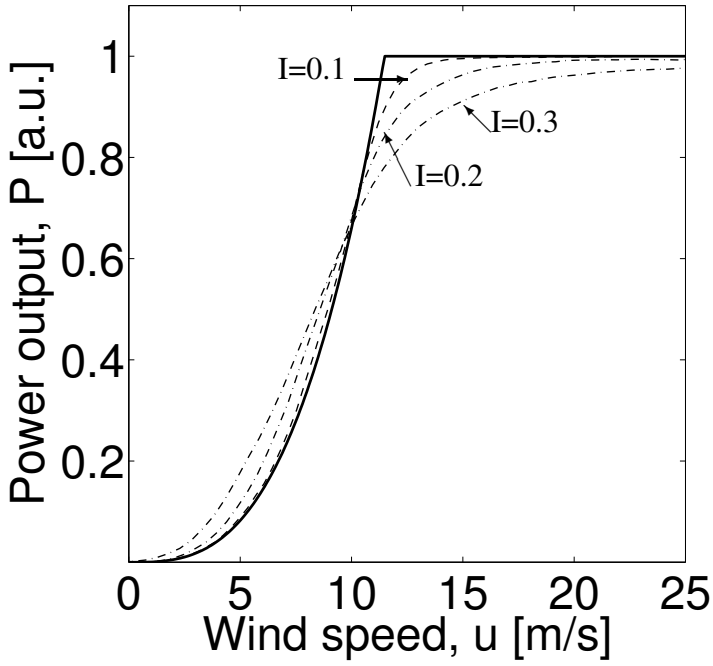

Figure 2.2: *The non-linearity effects of the power curve for 10%, 20% and 30% turbulence intensities (2.24) of the wind. The (full line) is the ideal power curve and the (dotted line) is the standard power curves given by the IEC procedure. The data have been obtained from numerical model simulations [15].*

2.2.4 Turbulent wind effects

As mentioned above, turbulent winds refer to the fluctuations in the wind speed variable over periods much shorter than the time-scale T, (i.e. $\leq 1sec$). These faster turbulent wind fluctuations are not only responsible for the high mechanical loads (fatigue) on the wind turbines components, which are importants in the aerodynamic designs, but also to variations on the power output production, which contribute to the expected power output value and therefore non-linearity effects of Eq. (2.25) has to be taken into account for the power assessment.

To show these influences to the basic mean wind power production we replace the following stochastic wind speed $u(t)$ instead of the steady wind speed V value of Eq. (2.25). Then, if the air density of Eq. (2.25) is assumed constant, the expected wind power production for a wind turbine

$$\langle P(u(t))\rangle \quad \propto \quad \langle (V+u'(t))^3\rangle \,,$$

becomes to be proportional to the average value of third order power of the fluctuating wind speed.

Solving $\langle (V+u'(t))^3 \rangle$ term and considering that wind fluctuations are symmetrically normal Gauss distributed to mean value $\langle u'(t) \rangle = 0$, the expected power value is reduced to $V^3 + 3V\langle u'^2(t) \rangle + \langle u'^3(t) \rangle$. In this expression mean fields and fluctuating higher order moments of the wind are separated. Using Eq. (2.24) and $\langle u'^2(t) \rangle \equiv \sigma_u^2$ this expression is written as

$$\langle P(u(t)) \rangle \quad \propto \quad V^3[1+3I_u^2] + \langle u'^3(t) \rangle \, . \tag{2.28}$$

Thus the averaged power value is determined by the third order mean V^3 value with the correction factor $3I_u^2$ plus the contribution of the higher nonlinear term $\langle u'^3(t) \rangle$ of the wind. This approach (2.28) shows, for example, that in the special case of laminar wind flows (i.e. zero turbulent intensity, $I_u = 0$) the expected power would simply be proportional to steady V^3 value, as shown above in Eq. (2.25), while that for the case of turbulent winds would be not.

It is clear, that the correction factor given in (2.28) for calculating the averaged power is stronger for large turbulence intensity of the wind fluctuations. For instance, the correction factor will amount to around 11% for a turbulence intensity value of 20%, which is a typical wind turbulence intensity value of complex sites [9, 12] Therefore, to predict the mean power output of wind turbines more accurately higher order of moments of the fluctuating wind speed, i.e. $\langle u'^3(t) \rangle$, has to be known previously.

Furthermore, dealing in the especial case of free atmospheric winds the problem of the turbulence intensity is that this quantity cannot characterize uniquely the real fluctuating variable of the wind signal. Because turbulence of free atmospheric winds are much more intermittent in the small-time scales than those stationary, see examples in [13, 52]. Hence, the turbulency intensity approach is mathematically applicable only if the wind signal is a pour random variable number with zero-correlation. In this case the corresponding wind turbine power lost these correlation.

In the following we will introduce the current statistical approaches to predict power production of wind turbines considering the influences of the turbulence intensity of wind.

2.3 Taylor series for the power output

In order to reduce the dynamics of the power output $P(u(t))$ at the stochastic wind $u(t)$ to its static form and considering that to characterize a fluctuating nonlinear quantity higher

order of moments has to be known in advance. Due to the determination of proper power curves this means that the functional relation of an averaged power to an averaged wind speed is not unique but will depend at least on the turbulence intensity of the wind.

The power $P(u)$ variable of a wind-turbine for any average V value can be described by the following (general) power series, so-called *Taylor series* [16]

$$P(u) = \sum_{n=0}^{\infty} \frac{P^{(n)}(V)}{n!}(u-V)^n \tag{2.29}$$

with their convergences around to the fixed V value within the interval of the wind fluctuations $(V-u', V+u')$. Here, the notation $P^{(n)}(V)$ is the nth derivative of the power P function defined at the mean V wind speed value.

This approach (2.29) shows that as the nth derivative degree of the Taylor series rises on the $P(u)$ variable, it approaches to the theoretical $P_s(V)$ power value.

An application of the Taylor approach (2.29) for wind turbine power assessments in turbulent winds has been already introduced in order to unfold from measured mean values, as suggested in IEC standard, the unknown steady power curve $P_s(V)$. In this application the approach (2.29) is suggested to be expanded up to its third derivative in the fluctuating wind $u' = u - V$. Thus it follows that Eq. (2.29) reads the form [18, 19, 20, 21])

$$P(u) = P(V) + P'(V)(u-V) + \frac{1}{2}P''(V)(u-V)^2 + O(u-V)^3, \tag{2.30}$$

where, the fluctuating wind speed $u(t) = V + u'(t)$ with $V = \langle u(t) \rangle$ and $\langle u'(t) \rangle = 0$ is assumed to be weakly turbulent, i.e. for small turbulence intensities I_u.

Now, in order to calculate the stationary average power output from the dynamic approach (2.30) and after neglecting higher order moments, i.e. $O(u-V)^3 \to 0$, one averages (2.30). The result approach is written in the following form

$$\langle P(u) \rangle = P_s(V) + \frac{1}{2}P''(V) \cdot \sigma_u^2 \,, \tag{2.31}$$

where $\sigma_u^2 = \langle (u-V)^2 \rangle$ denotes the variance of the wind fluctuations as defined in Eq. (2.7).

Eq. (2.31) shows that the mean $\langle P(u) \rangle$ power is decomposed into the two terms: the steady $P_s(V)$ power at the mean wind speed V and the corresponding second derivative of the power output $\frac{1}{2}P''(V)$ at the standard deviation σ_u of the fluctuating wind speed u.

It is clear that the steady power $P_s(V)$, as given in Eq. (2.25), has to be modified. This modification depends on the second derivative of the power curve and the turbulence intensity, which is denoted by the σ_u^2 variance. It is strong for large wind fluctuations. In the

case of a positive curvature by the second derivative of the power curve, i.e. in the partial load states as illustrated in Figure 2.1, the steady $P_s(V)$ power curve is overestimated while in a negative curvature the power curve is underestimated.

The common procedure of Eq. (2.31) to evaluate the correction of measured IEC power curves by their wind turbulence intensities, is given by the well-known least-square (linear regression) method, see Ref. [19, 20, 21]. This analysis estimate the steady $P_s(V)$ power curve simply by extrapolating beyond the range of the measured turbulence intensities to the zero turbulence value, i.e. $I_u = 0$.

However, one of the main problems of Eq. (2.31) is the non-linearity characteristic of the power curve (2.25). This characteristic yield that the relationship between the power values and wind turbulence intensity values are also affected, which gives as result independence and uncorrelation [16], even though both variables are dependent, see examples in [19, 20, 21]. Therefore, linear regression (variance) analysis is limited to be applied on non-linear systems such as the wind turbine power output.

In fact, to approach properly from measured power curves to the steady power curve $P_s(V)$, higher derivative degrees on the Taylor series approach (2.29), than the given in Eq. (2.31), have to be applied. Because the steady power curve, see Figure (2.1), presents, furthermore of their affected full and load parts, at the rated wind velocity V_r value a singular vertex (corner) curve at the P_r value. Unfortunately this is the most affected part by measured IEC power curves, which in turbulent winds situations the ensemble mean values of power and wind are extremely influenced by the dynamics power control responses of the wind turbine, especially in modern machines, as seen in section 2.2.2.

2.3.1 Modification of the Taylor series

Hitherto we have included the effects of the fluctuating wind through of the turbulence intensity quantity in the mean value of the power output of a wind turbine, as described Eq. (2.31). But we have said nothing about the interaction of the dynamical characteristics of the wind-turbine due to wind turbulence in the averaged value of power.

It is a fact, that wind turbines are systems with complex dynamical responses, as mentioned in section 2.2.2, which mainly depend on the suddenly changes of the wind speed. In order to take into account those coupled effects of the wind and wind turbine dynamics in the mean value of the power for the case of weak wind turbulence. The Taylor approach, given by Eq. (2.31), was modified in the following form

$$\langle P(u)\rangle \;:=\; P(V)+\lambda_2\cdot\sum_{i=1}^{N}\Delta f\; S(f_i)G(f_i,V)\;, \tag{2.32}$$

which corresponds to a coupling between the dynamic characteristics of the *specific* wind turbine, through of G function, and the wind field, in analytic form, through of S function, see Ref. [17, 18]. The $G(f_i,V)$ term is a function of the frequency ($f_i = i\Delta f,\ \forall i = 1,...,N$) and the average wind velocity V.

This G function is usually obtained, empirically, by numerical simulations by means of a specific rotor-gearbox-generator models for wind turbines systems as shown in [17, 18].

The variance of the wind fluctuations is written explicitly as $\sigma_u^2 \equiv \sum_{i=1}^{N}\Delta f\; S(f_i)$, where the term $S(f_i)$ denotes the spectral density of the turbulent wind speed $u = V + u'$ that in general depends on the short-term mean wind speed V and at the hub height of the wind turbine. The turbulence intensity of the wind is defined by Eq. (2.24) and the stochastic fluctuating wind u' is described by the function of distribution $S(f)$ which can be given, for example, by the Kaimal spectral analysis, for details about this analysis, see Ref. [7, 9].

In this approach numerical calculations using the spectral G and S functions for calculating correction terms into the Eq. (2.32) can be performed as input in order to predicting power output of a given specific wind turbine on conditions of weak turbulent winds. The first numerical applications of this approach for the power output of specific wind turbine can be found in Ref. [17, 18].

However one of the disadvantages of this modified Taylor approach (2.32) is that the corresponding dynamical response $g(t)$ function can be uniquely determined by the empirical G function which is obtained by numerical simulations for the specific wind turbine, which commonly is not always available. Therefore in order to overcome this difficulty a generalized response model has been developed. The $g(t)$ function can be obtained by a differential equation of the instantaneous power value, which is characterized, in a nonlinear way, by a time-dependent relaxation function and the stochastic wind field [22]. In the following section this new approach is described.

2.4 Dynamic response model

In the previous section we have described the mean value for the power output (2.32) and the coupling between the wind turbine dynamic characteristics and the wind field dynamics. Following this ansatz a more general approach in the condition to obtain the form of Eq. (2.32) and in the limit of weak turbulence has been recently proposed by Rauh [22]. This

new ansatz, which is a dynamic response model to predict power output of a wind turbine and which takes into account the delayed response function of the turbine to turbulent winds as well as the wind fields of arbitrary turbulence intensity.

This response model is based in a linear differential equation for the instantaneous stochastic power output $P(t)$, given by the wind turbine, at the time t, which corresponds to be uniquely related to the longitudinal short-time wind fluctuations $u(t)$ variable. This general relaxation model is written in the following form

$$\frac{d}{dt}P(t) = \alpha(t) \cdot [P_s(u(t)) - P(t)] \tag{2.33}$$

and is characterized by the time-dependent relaxation function $\alpha(t)$. Here the function $P_s(u(t))$ corresponds to the steady $P_s(V)$ power curve, see Figure 2.1, where the stochastic power output $P(t)$ variable would relax to $P_s(V)$, if the particular wind speed $u(t)$ was frozed in the steady V value. In this approach (2.33) the steady power $P_s(V)$ function have to be known in advance[4]. The solution (2.33) depends on the wind turbine response and the wind field in a nonlinear way.

The Eq. (2.33) was basically motivated by the need that it should reproduce the dynamical power response of Eq. (2.32) in the limit of weak turbulence, as was presented above in [17, 18], and that it should be more general in order to include wind fields of arbitrary turbulence intensities.

The relaxation $\alpha(t)$ function, in general, depends on the fluctuating wind speed variable $u(t) = V + u'(t)$ and in the time derivative of the fluctuating wind $\dot{u} = \dot{u}'$. Here, it was assumed to have the following form

$$\alpha(t) = \alpha_1(u(t)) + \alpha_2(\dot{u}') \,, \tag{2.34}$$

where the term $\alpha_1(t)$ describes the relaxation function, on constant wind speed $\dot{u} = 0$, to the steady power $P_s(u)$ from a nonestationary value $P(t=0) \neq P_s(u)$. In this analysis the relaxation term α_1 is assumed, for simplicity, as a constant factor, i.e. depending on the mean wind speed V only with $\alpha_1(u) = \alpha_1(V) = \alpha_0$. The other function α_2 is described from the linear response theory by the following convolution form, see (2.20)(2.21)

$$\alpha_2(t) = \int_{-\infty}^{t} \dot{u}'(t')g(t-t')dt' \,, \tag{2.35}$$

where g describes, in the non-linear way, the response function of the wind turbine. It depends, in general, on the mean wind speed V and the turbulence intensity I_u (2.24) as

[4] In the next chapter we will shown in a simplied stochastic method to describe properly the steady $P_s(u)$ power curve directly from instantaneos measurement data

control parameters. Those parameters can be simply obtained if a short-term period $t \in [0,T]$ is considered. The function term $\alpha_2 = \alpha_2(\dot{u}')$ is used to describe the instantaneous interaction between the wind-turbine with the turbulent wind velocity.

Obviously, the response $g(t)$ has to be causal, this implies that $g(t-t') = 0$ if $t' > t$.

Now, assuming that the steady power curve $P_s(V)$ depends on the turbulence it follows that

$$P_s(u) \rightarrow P_s(u, I_u) = \begin{cases} P_s(u,0) & , \text{ if } I_u \leq I^* \\ 0 & , \text{ if } I_u > I^* \ . \end{cases} \tag{2.36}$$

As an application of the model, the effects of large turbulence intensities in the especial case of a simplied idealized shutdown model, for details see Ref. [22], at time $t = 0$ and instantaneous power output $P(0)$ in the turbulent wind field. Thus, the general solution for the differential equation given in (2.33) is written as follows

$$P(t) = \exp[-\alpha_0 t - R(t) + R(0)]P(0) + \int_0^t dt' \exp[-\alpha_0(t-t')]P(t,t'), \tag{2.37}$$

$$P(t,t') = \alpha(t')\exp[-R(t) + R(t')]P_s(V + u'(t')) \ , \tag{2.38}$$

with the definition $R(t) = \int_0^t dt' \alpha_2(t')$. Then, given for the shoutdown case the stationary power $P_s \equiv 0$ for $t > 0$. As the phase averaging of the initial value term (2.37), as shown in [22], it decays exponentially to zero, due to the stochastic wind field rise to an effectively larger relaxation time, i.e. shutdown is slowed down to some extend. Thus, the described solution, shown above, is simplied in the following form

$$P(t) \quad = \quad \int_0^t dt' \exp[-\alpha_0(t-t')]P(t,t') \ . \tag{2.39}$$

The relaxation time $1/\alpha_0$ commonly is, for example, in the order of a few seconds in the case of the response measurements of blade root bending moments to sudden changes of the blade pitch angle system of a wind turbine [9]. The phase averaged $P(t,t')$ function depends on the time difference only, i.e. $\tau = t - t'$. After the phase averaging is developed, see Ref. [22]. The following expression is obtained

$$\langle P(t) \rangle \quad = \quad \int_0^t d\tau \exp[-\alpha_0 \tau] \langle P(\tau) \rangle \ . \tag{2.40}$$

As is seen the ensemble average of the power output depends in a nonlinear way on the spectrum of the wind gusts and the turbine response function. Anyway, it turns out that phase averaging with respect to the stochastic wind field can rigorously be reduced to an one-dimensional integral containing a Gaussian distribution function.

In order to derivate from Eq. (2.40) in the weak turbulence intensity and thus to achieve the connection of the turbine function $g(t)$ of the response model (2.33) to the spectral

function $G(f)$ defined in the ansatz (2.32) according to [17, 18]. The following expression is obtained in a formal way, see more details in [22]

$$\langle P(t)\rangle \;=\; P_s(V)+\lambda_2\sum_{i=1}^{N}\Delta f\; S(f_i)+\Delta P_{dyn}=\langle P_s(V)+u'(t)\rangle+\Delta P_{dyn} \tag{2.41}$$

where ΔP_{dyn} is the contribution of the mean power due to the dynamics, see [22], as compared to the quasi stationary average $\langle P_s(V)+u'(t)\rangle = P_s(V)+\lambda_2\langle u'^2(t)\rangle$. If (2.41) is compared with (2.32) the function G, of ansatz [17, 18], is obtained as

$$\tilde{G}(f_i,V) \;\equiv\; \lambda_2 G(f,V)=\lambda_2+\Delta P_{dyn}. \tag{2.42}$$

And following with this the time averaged power output is arrived [22]

$$\overline{\langle P(t)\rangle} \;=\; P_s(V)+\sum_{i=1}^{N}\Delta f\; S(f_i)\tilde{G}(f_i,V). \tag{2.43}$$

which describes the ansatz (2.32) shown by [17, 18] at the weak turbulence intensity.

Thus, in the low turbulence intensities the dynamic correction factor ΔP_{dyn} can be obtained analytically within the response model (2.33). Therewith the correction for the averaged power output (2.43) due to the turbulent winds and turbine dynamics is possible and important for the power assessment, see Ref. [9]. The numerical comparason of results given in [17, 18] with [22] shown that the response function $g(t)$ can be obtained in a unique way by the response model (2.33).

Chapter 3

Data

This chapter gives briefly the description of the measurement data. To show the deterministic dynamical behavior of the output power process involved at the wind turbine system during its power operation performance. The fluctuating power output generation states and their influences by the power controller in the system are shown. In order to give a more general view into the dynamics, the frequency characteristics of the output power generation process, given by the spectra analysis, is shown. The output power process is extremely influenced by complex and nonlinear oscillations responses which depend on the mechanical - electrical wind turbine construction and by the stochastic winds. In the analysis for the measured power curve, the power performance characteristics of a 2MW wind turbine given by the standard *IEC 16400-12* method is shown.

3.1 Tjæreborg wind turbine

The Tjæreborg wind turbine was located approximately 9Km southeast of the city of Esbjerg in Denmark, in the marshland between the small village, Tjæreborg and the coastline. The surrounding of the site belongs to the class of flat terrain, for more details see Ref. [23, 24, 25]. In Figure 3.1 the Tjæreborg wind turbine in the site is shown.

The single wind turbine was a 2MW prototype of horizontal-axis upwind three-bladed rotor with a diameter of 61.1m specifically designed for the purpose of experimental measurements for analysis of mechanical loads and wind climate on the site.

The wind turbine is equipped with a blade pitch-regulated system. The rated power output at 2 MW is controlled by a continuously variable blade pitch system, operating between 0 and 35 degrees in production mode. In idling or parking mode, the pitch angle is 55 degree

Figure 3.1: *The Tjæreborg wind turbine.*

or 90 degree, respectively. In the Table 3.1 the main technical data of the wind turbine generator system is listed, see Ref. [23, 24].

3.2 Measurement wind and power data

Since the Tjæreborg wind turbine was installed for experimental proposes, two meteorological mast of 90m height each one were installed for the measurement system. The mast Nr.1 (M1) was placed in front and mast Nr.2 (M2) behind the wind turbine referring to the

Table 3.1: *Technical data of the Tjæreborg wind turbine [23, 24].*

Rated power	2MW
Nr. of blades	3
Rotor diameter	61m
Hub height	60m
Power regulation	Full span pitch controll
Generator	Asynchronous, slip 2%
Gear box	Combined epicyclic, 1:68.4
Rotor speed	22.3 RPM
Meteorological towers	Height 90m, 2 masts

dominant wind sector. The distance between the met M1 and the wind turbine was about 120m which corresponds to two times of rotor diameter of the wind turbine. The details about of the measurement instrumentation in the masts and in the turbine can be found in Ref. [25]. In Figure 3.2 a) the site layout of the turbine and the M1 and M2 masts are shown.

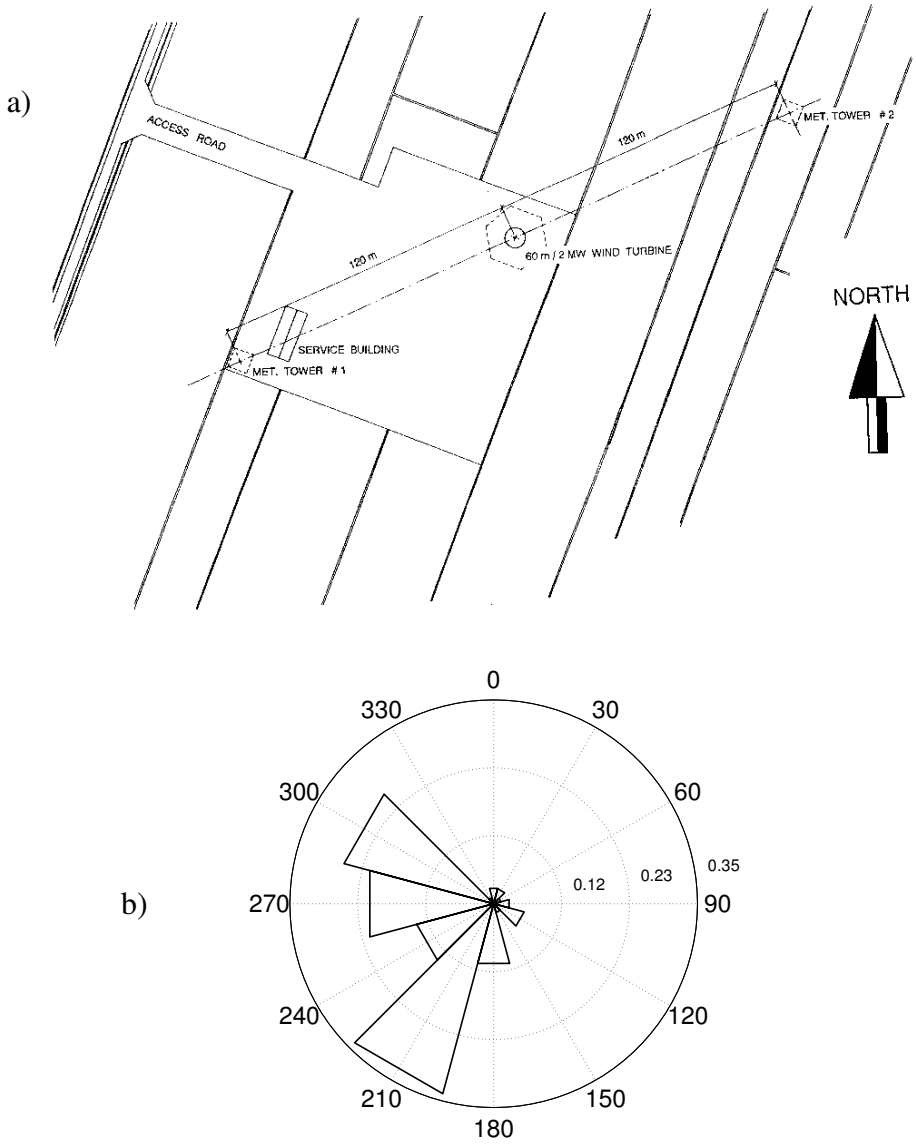

Figure 3.2: *In a) Layout of the Tjæreborg wind turbine and the meteorology M1 and M2 masts. In b) Wind-direction frequency of the measured data are shown [25].*

Regarding that the IEC-standard, given in [26], for the allowed location in relation to the turbine being measured, the disturbed wind-direction sectors on the site due to wake of the wind turbine and the M2 mast on the M1 mast were in the interval of 15-119 degrees. In

Figure 3.2 b) the frequency of the measured wind-direction, corresponding to the selected data, is shown. Thus, from this measurements we verify that the wind speed was mainly taken from zones were the sectors are undisturbed.

From those measurements, wind data collected from a cup-anemometer located at 60m height of the meteorological M1 mast, and the corresponding electrical output power of the wind turbine generator system were used for the later analysis of this work. These data correspond of about 2.3×10^6 sampled data. The sampling rate of the measurement data was 25Hz. The data are a collection of different 10min data sets (24hrs. in total) which correspond to the years of 1991-1992. The measured mean wind turbulence intensity was about 9%.

3.2.1 Time series analysis

As it was introduced in Chapter 2, the power performance of a wind turbine is a highly fluctuating source of energy because their power operation system depends on the wind speed variations and on the dynamics wind turbine characteristics (responses).

In order to get insight on the dynamics, in the time-domain, of the measured output power data of the Tjæreborg wind turbine system. Figures 3.3 show the typical operating states of the electrical output power (power generated) at full load and partial load that the power operating system (power controller) determined during their power performances. In Figure 3.3 a) the fluctuating output power at the full load operating state is presented. In Figure 3.3 c) the changing of different operating state phases at full load output power process in order to controll power were performed in time intervals of 10 minutes. In Figure 3.3 e) the well-known output power process at partial load are shown. Figures 3.3 b) c) d) show the corresponding wind speed respectively.

In general, the figures show that the dynamics of the output power of the Tjæreborg wind turbine varies very highly. It can be seen that the output power fluctuations at partial load are much higher than the full load, see Figures 3.3 a) and c). This typical behaviour is the resulted of the power controller system operation by fixed pitch regulation, which at partial load the wind turbine extracts the maximum power (optimal operation) from the wind and cannot effectively damp the output power variations. Unlike at full load operation where the fluctuating output power are better damped by active pitch regulations, see Ref. [9, 10, 23].

In Figure 3.3 b) the full load power generation with gradual switching power operations 1.51, 1.26, 1.00 and 2.00 MW phases are shown. The time period of those switching power operations was performed at 10min. The reason of this controlled power generation behaviour might had been due to increases of the measured wind speed conditions on the

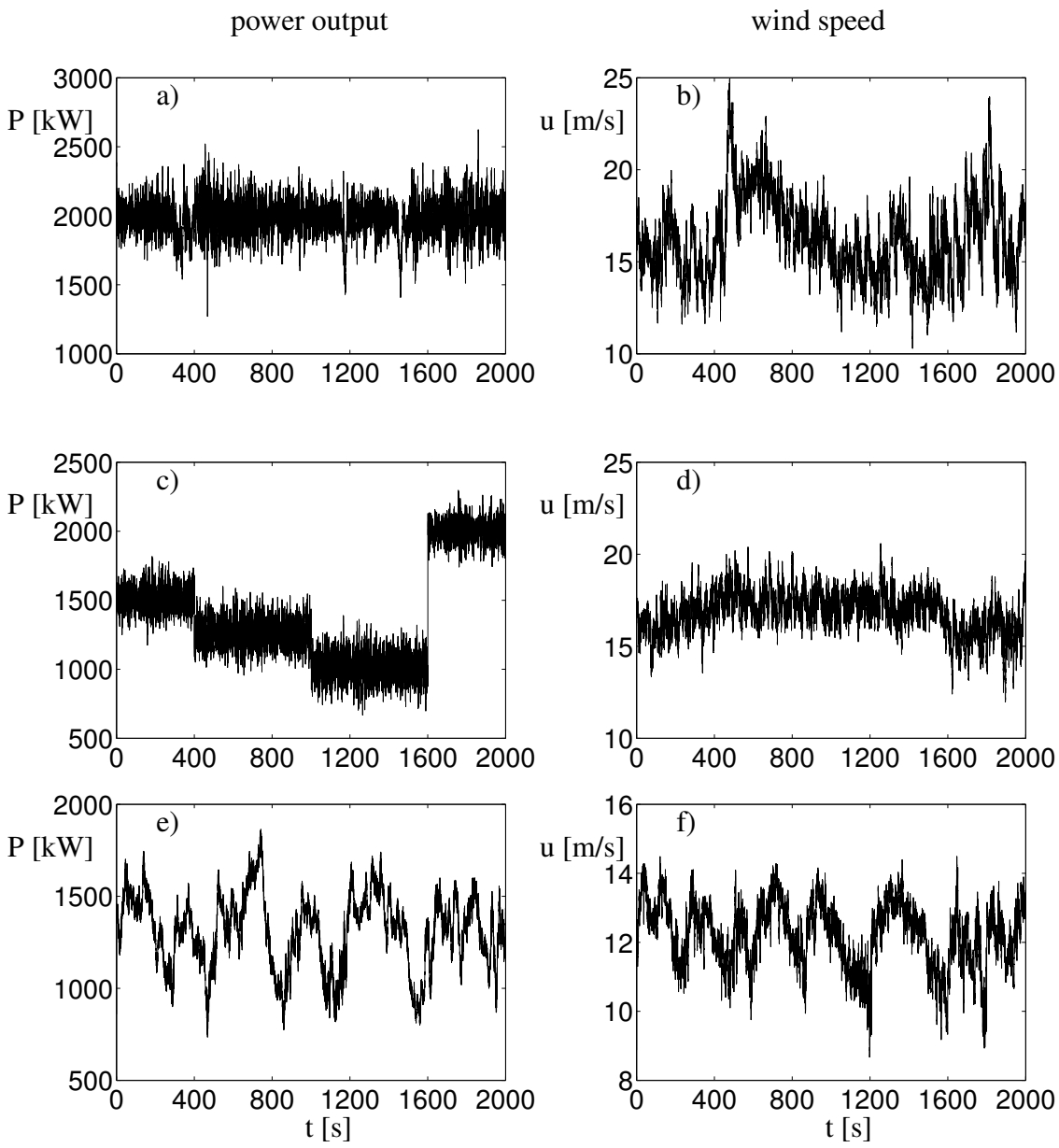

Figure 3.3: *Fluctuating output power generation by Tjæreborg wind turbine (left) and the corresponding wind speed (right). In a) b) Power generation at full load operation at a wind speed equal to 16.3 m/s. In b) c) the full load power generation operated also at 1.51, 1.26, 1.00 and 2.00 MW phases. The averall mean wind speed is equal to 17.0 m/s. The time period of those switching operations was 10min (600s). In e) f) Power generation in partial load at a wind speed equal to 12.2 m/s.*

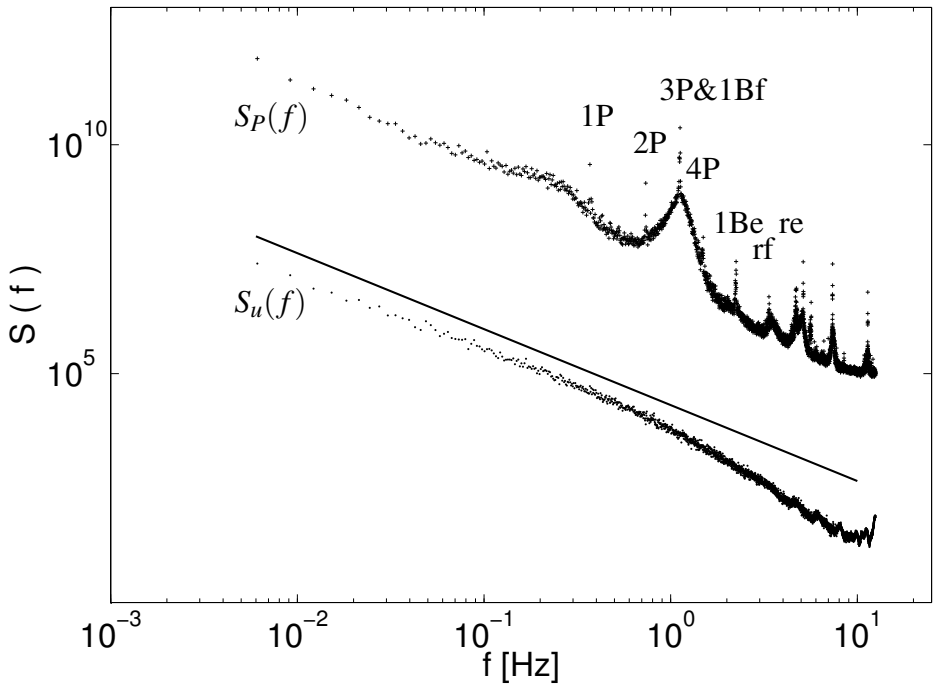

Figure 3.4: *Power spectra $S_P(f)$ of the output power production $(+)$ of the Tjæreborg wind turbine showing their eigenfrequencies. In addition the power spectra $S_u(f)$ of the corresponding wind speed from the M1 mast is plotted as $(\cdot)$ and the expected $S(f) \propto f^{-5/3}$ power law approach shown as $(-)$ solid line [27].*

power controller system which drived gradually to the wind turbine performance to the safe mode operation by regulating active pitch, [23].

All those dynamical behaviours of the output power, described above, show us clearly that the power controller of the wind turbine system is crucial in the power generation.

3.2.2 Spectral analysis

In the next, a more general view of the dynamics of the wind turbine output power production at the frequency-domain is given by the power spectra analysis. Following the previous analysis shown above, the Figure 3.4 shows the overall frequency characteristics (or natural frequencies) involving to the fluctuating power output conversion process given by the Tjæreborg wind turbine generator system and, in addition, given by the wind field.

In general, the power spectral $S_P(f)$ distribution in frequency f space shows that without consider their peak amplitudes, the energy distribution of the fluctuating power output decays to smaller and smaller scales. This behaviour is similar to the wind spectra $S_u(f)$ in

the inertial range, where the energy distribution approximatly follows, after [27], to the expected $S_u(f) \propto f^{-5/3}$ power law, for details see [28, 29].

In the frequency phases between $0.1 - 0.6$ Hz, the energy spectra for the fluctuating power output $S_P(f)$ shows as a hummock a wideband amplitudes, which are due to a mechanical tower bending oscillation (longitudinal and lateral directions) of the wind turbine. Furthermore harmonics at frequencies 0.37Hz (1P) and 0.74Hz (2P) appear due to the dynamical blades rotation of the wind turbine.

In the range frequencies $0.65 - 1.9$ Hz, the energy spectra $S_P(f)$ shows clearly the strong convergence to the maximum frequency $f = 1.12$ Hz value, (3P), which represents the effects of the rotor blades passing in front of the wind turbine tower, this is the well known tower shadow effect[1], and the blade flapwise (1Bf) effects respectively [23]. Due to its large amplitud this is the main mechanical eigenswings characteristic in the wind turbine oscillation analysis [9, 10, 30],

Following at the frequency $f = 1.5$ Hz a (4P) harmonic is shown, which was induced, mechanically, by the gearbox transmission system [23].

In frequencies of 2.24 Hz, 3.36 Hz and 4.7 Hz, the contributions of the blade edgewise (1Be), the shaft rotor flap (rp) and rotor edge (re) are shown respectively.

In higher frequencies $f > 4.7$ Hz, still appear others oscillation resonances given to the power production process, which were induced by the drive train, yaw, tilt, rotor shaft, etc., and also by the electrical power system. All those higher frequencies are extremely non-linear and complex for the power process. Some of those measured natural frequencies are escential for the analysis of wind turbine systems, for example, in the aerolastic simulation of wind turbines [31].

3.2.3 Standard power Curve

As introduced in Chapter 2, the standard method to characterize the expected power output of a wind turbine is given by the ensemble averaging method (Standard IEC 61400-12), which is based on measured 10 min mean values of the electrical output power and the wind speed at the hub heigh as reference [26]. From those measured mean values the expected power production of the wind turbine is calculated by the functional relationship of the averaged power output and averaged wind speed, as shown above in (2.26).

In Figure 3.5 we show the standard power curve resconstruction for the 2MW Tjæreborg wind turbine generator system and their corresponding uncertainties, which were obtained

[1] The tower shadow effect is just a vortex tower interaction produced by blocking of the air flow by the tower results in regions of reduced wind speed both upwind and downwind of the tower.

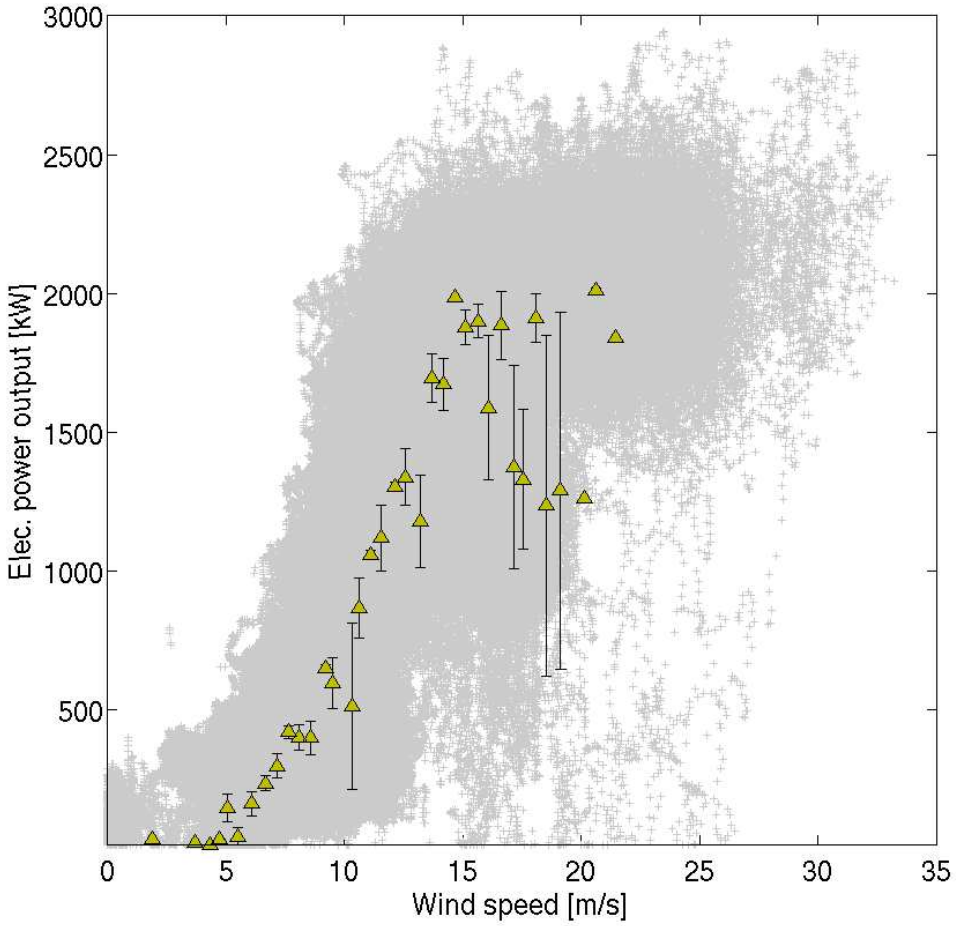

Figure 3.5: *Measurements of electrical power output and wind data (grey-lines) from a 2MW wind turbine [25]. The open-triangles (-△-) are mean values of 10 min data as recommended in [26]. Uncertainty of the estimations are plotted as bars. The sampling rate of the data was 25Hz.*

by their measured 10 minutes mean values. Due to the short overall time length still big scatter are found. Additionally, in Figure 3.6, we show the mean power output of wind speed bins of 0.5m/s calculated directly from the given data sets to show the nonlinear effects of the standard averaging method.

The technical details concerning to the power performance testing procedure under their special conditions is found in the standard *IEC 61400-12*, see Ref. [26]. We want to remark that this procedure does not take into account the overall dynamics behaviour of the wind turbine power performance to turbulent wind fields.

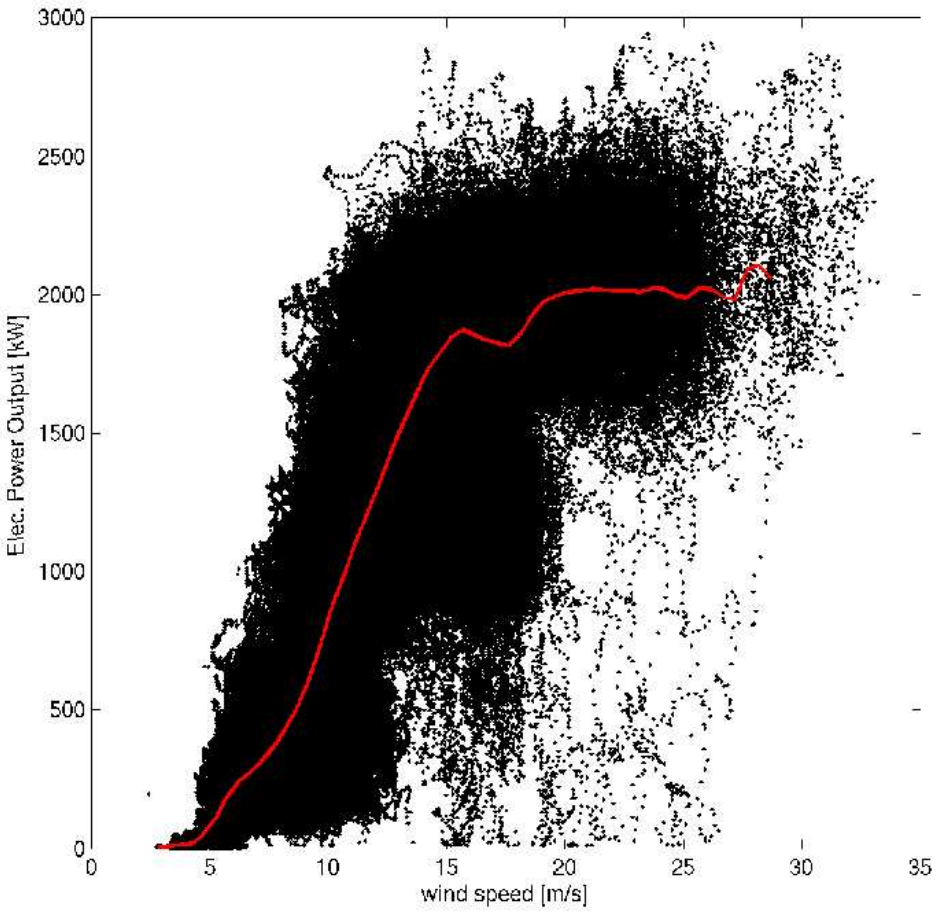

Figure 3.6: *Typical nonlinearity effects on measured power output data of a 2MW wind turbine [25]. A complex behaviour is observed by the dynamics response on sudden changes of wind velocity. The dots are instantaneous measured data and the solid line is the mean power output obtained for wind speed bins of* 0.5*m/s directly from the data sets. The sampling rate of the data was 25Hz.*

3.3 Meerhof wind data

In addition to the Tjæreborg data we also use measured wind data of a metmast of 100m heights located in front of a wind farm in the complex area of Meerhof close to Paderborn, Germany. The site is characterized by complex farms land and forest in the hills, especially at the east side of the measurements mast. The purpose of the measurements was for investigations on the energy output of wind turbines and wind turbulence, for details see Ref. [35]. In Figure 3.7 the location of the metmast is depicted.

The data were collected from an ultrasonic anemometer with sampling frequency of 50Hz located to the hub height of 98m. The measured mean wind turbulence intensity of the

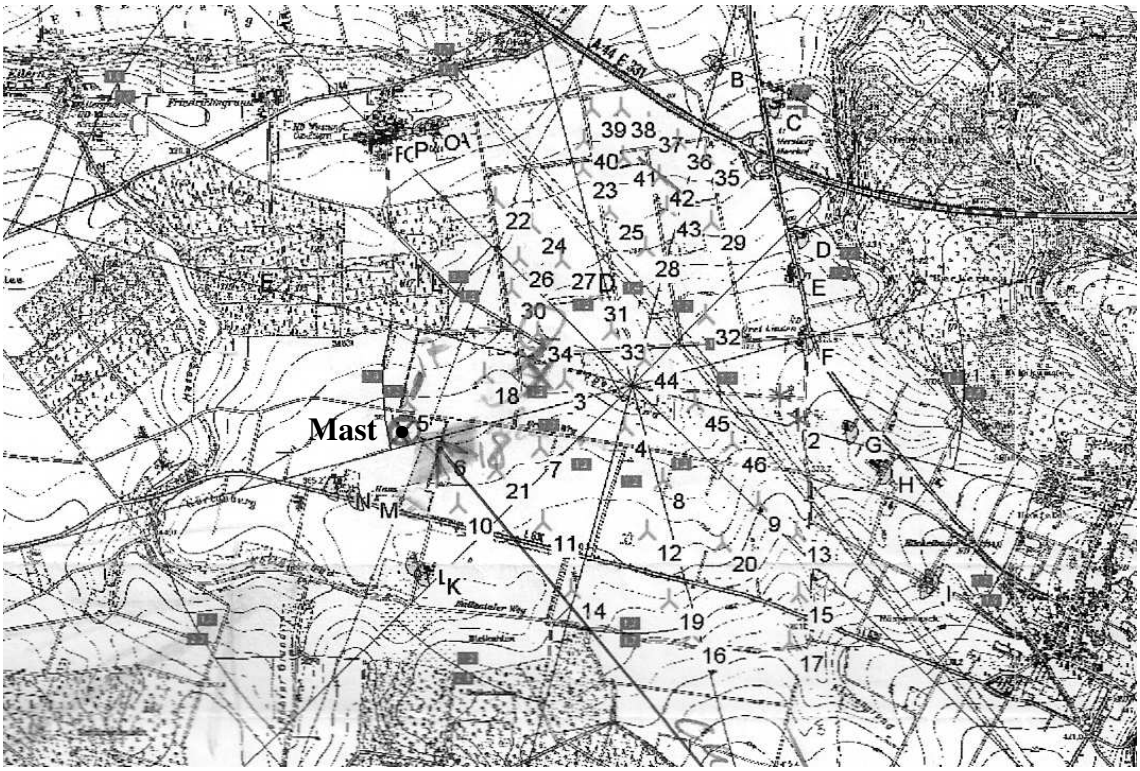

Figure 3.7: *Location of the measurement mast in the complex area of Meerhof, close to Paderbon, in Germany.*

wind data was about 14%. All data sets consist of more than $\times 10^6$ samples.

Chapter 4

Markovian Power Curves for Wind Turbines

(This chapter has been submitted for publication to *Wind Energy Journal* as:
Anahua E, Barth St, Peinke J.: Markovian Power Curves for Wind Turbines)

This Chapter shows a novel method to characterize the wind turbines power performance directly from the high frequency fluctuating measurements. In particular we show how to evaluate the dynamic response of the wind turbine system on fluctuating wind speed in the range of seconds. The method is based on the stochastic differential equations known as the Langevin equations of diffusive Markov processes. Thus, the fluctuating wind turbine power output is decomposed into two functions: i) the relaxation, which describes the deterministic dynamic response of the wind turbine to its desired operation state; and ii) the stochastic force (noise), which is an intrinsic feature of the system of wind power conversion.

As a main result we show that independently of the turbulence intensity of the wind the characteristic of the wind turbine power performance is properly reconstructed. This characteristic is given by their fixed points (steady-states) from the deterministic dynamic relaxation conditioned for given wind speed values. The method to estimate these coefficients directly from the data is presented and applied to numerical model data, as well as, to real world measured power output data.

The method is universal and not only more accurate than the current standard procedure of ensemble averaging (IEC-61400-12) but it also allows a faster and robust estimation of wind turbine's power curves.

4.1 Introduction

Among the great increase of the wind energy generation within the electricity grid the precise knowledge of the wind turbine power performance characteristics on turbulent winds is of primary importance in the economical planning of wind farms as well as in the deployment of other power stations on the network.

It is now well known that for the estimation of the annual energy production of wind turbines the relationship of standard averages of 10min measurements of wind speed at hub height and the electrical power output: $\langle u \rangle \rightarrow \langle P(u) \rangle$, where $\langle \cdot \rangle$ denotes the 10min ensemble-averages, as recommended in [9,26,32,33], does not describe precisely the power output characteristic. This is true because the high wind fluctuations are not dealt correctly by this procedure. It is well known that the standard averaging procedure depends on the terrain type of the test site. Note it is the terrain which strongly affects by the turbulent wind fields. Typical uncertainties of this procedure show levels of the order of $10\% - 20\%$ in their estimations [36, 38].

One important difficulty is caused by nonlinearities, like $P \propto u^3$, which already yields the following inequality $P(\langle u \rangle) \neq \langle P(u) \rangle$. Many authors propose additional linear and nonlinear methods to account those effects. For example the principal component analysis, that constitute the main tool for simplifying of secondary variables, or the class of artificial neuronal network has been proposed in [37, 39, 40, 41, 42]. To account the turbulence intensity of wind into time scales of 10min, [19] proposed the Taylor expansion for the averaged power output, see also Ref. [20, 21]. In spite of the progress achieved by those refined methods, there remain several challenges for a more advanced and detailed description. In particular aspects like the wind turbulence independent characteristics in the specific test site, the fast measurement period for the power performance assessment and the separation of wind and wind turbine's power output production has to be solved.

In this article we focus on a new method based on stochastic analysis of time series [48, 49, 58]. This method allows estimating *drift and diffusion coefficients* of nonlinear complex systems directly from the data sets. Some applications of the method have been widely validated in fields as traffic flows [57], noise analysis [64, 70], noise driven chaotic electric circuits [49, 58], turbulence flows [52], heart-rate dynamics [63], finance data [50, 60] and surface roughness [62]. Some first applications of this method for wind energy application has been presented in [67, 69, 70]. Our goal is to propose a novel method to characterize the wind turbine's power performance by the *fixed points* of the deterministic dynamics of the power output relaxation.

This paper is organized as follows. In Section 2 we illustrate the dynamics of a wind tur-

bine's electrical power output from measurement data. The standard analysis for the power performance is shown. We describe a simple stochastic model for the dynamics of the power output in Section 3. Also the numerical calculation of power data using a designed model together with empirical high frequency wind speed data is shown. In section 4 the procedure to reconstruct the Langevin equation from numerical and experimental data is described. In section 5 we show the method of the potential to reconstruct new power performance characteristics by the fixed points of the response dynamics. Conclusion and some open discussion are reported in section 6.

4.2 Wind and wind power data

The following analysis of the power output dynamics is based on measured data of about 2.3×10^6 samples of wind speed at 60m hub height and electrical power output of a single 2MW wind turbine. These data are a collection of different 10min data sets (24hrs. in total). The mean wind turbulence intensity was about 9%. The wind data were collected from a cup-anemometer with a sampling rate of 25Hz. The wind turbine was a horizontal-axis upwind three-bladed rotor with a diameter rotor of 61.1m. The used meteorological mast was located in a distance of 120m from the wind turbine according to [26] and was placed in the main direction of the wind. The test site was located in the flat terrain of Tjæreborg, Denmark. The results are based on the free available data obtained from the data base of Tjæreborg wind turbine, see Ref. [23, 25].

In Figure 4.1 the measured power output as function of wind speed has been plotted to show the real dynamics of the wind turbine power output. Furthermore the standard power performance characteristics and their uncertainties have been obtained for the 10min mean values (open-triangle) as suggested in [26]. Due to the short overall time length still big scatter are found. Additionally, we show the mean power output of wind speed bins of 0.5m/s calculated directly from the given data sets to show the nonlinear effects of the averaging method.

In addition to the Tjæreborg data we also use measured wind data from another location, namely, the more complex area of Meerhof in Germany, see Ref. [35]. The data were collected from an ultrasonic anemometer with sampling frequency of 50Hz located to the hub height of 98m. The mean wind turbulence intensity was about 14%. All data sets consist of more than $\times10^6$ samples.

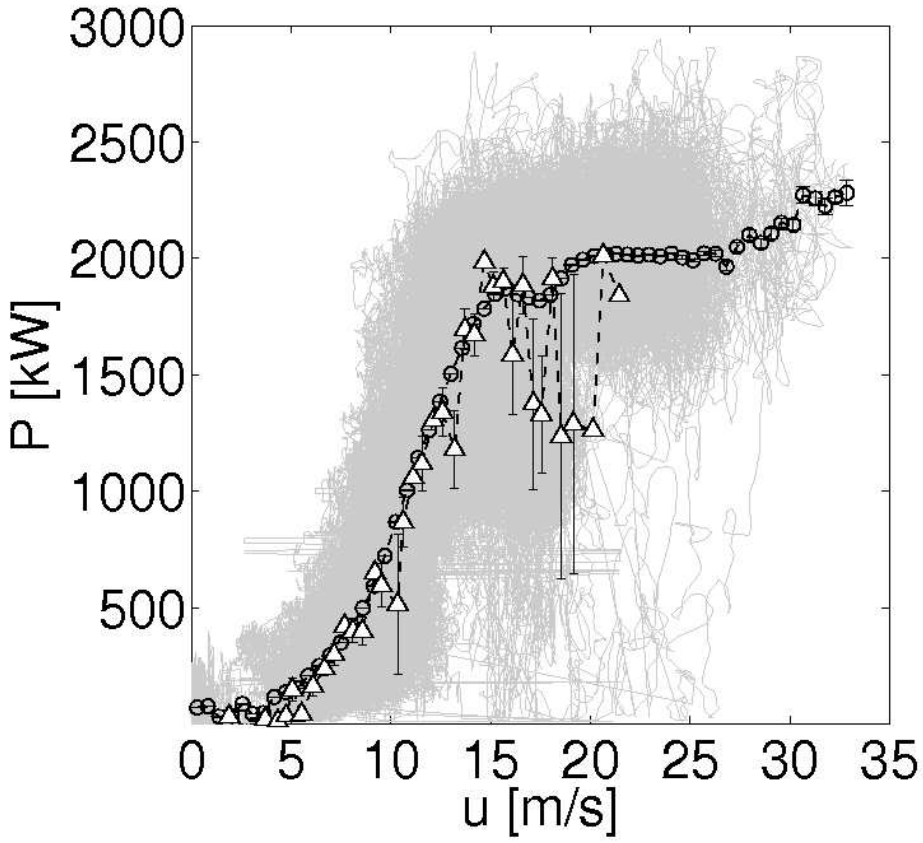

Figure 4.1: *Measurements of electrical power output and wind data (grey-lines) from a 2MW wind turbine [25]. The sampling rate of the data was 25Hz. The open-circles (-○-) present the mean power output obtained for wind speed bins of* 0.5*m/s directly from the data sets. The open-triangles (-△-) are mean values of 10 min data as recommended in [26]. Uncertainty of the estimations are plotted as bars.*

4.3 Simple relaxation model for the power output

In order to introduce our understanding of the dynamical electrical power output of a wind turbine converter we start with a simple stochastic model.

Firstly, to describe the dynamics, we focus only on the fluctuating electrical power output of the wind turbine $P = P(t)$ at time t. Thus we introduce the following general notation

$$P(t) = P_s(u) + p(t) \ , \tag{4.1}$$

where $P_s(u)$ denotes the steady state of the power output $P(t)$ as function of the wind speed. Note that also the wind speed is time dependent, $u = u(t)$, but for each instant there exists

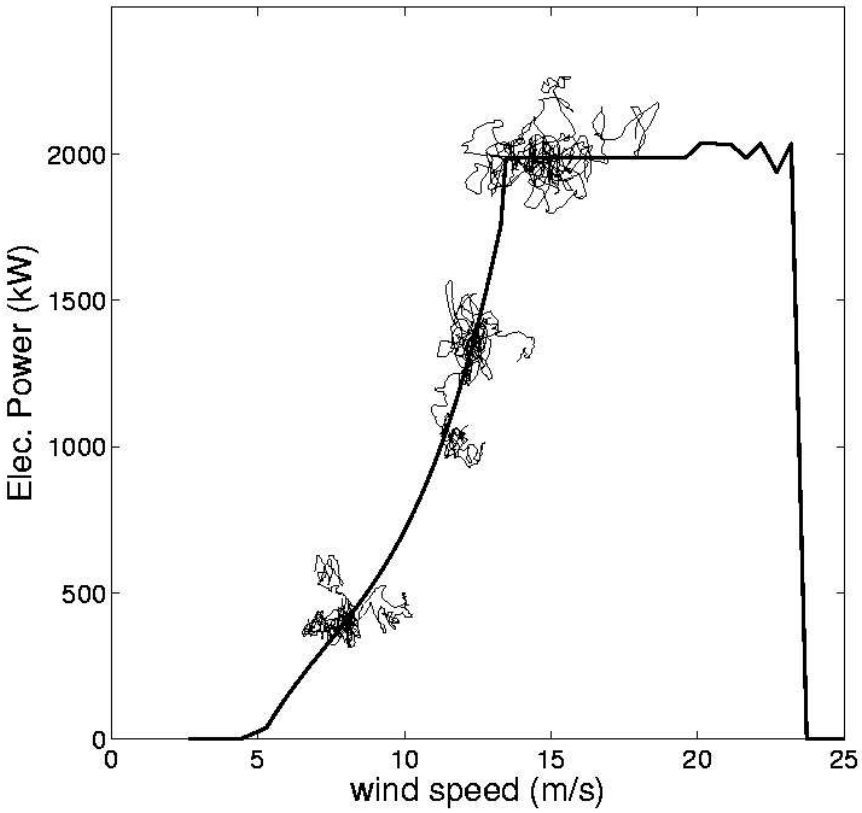

Figure 4.2: *Illustration of the dynamical power output as function of wind speed for several different sample paths (fine-lines) with typically 4sec duration taken from the data shown in Figure 4.1. In addition the steady power curve, $P_s(u)$ (thick-line) is shown.*

an ideal steady state power value P_s. In Figure 4.2 we show several short paths of the dynamical measured power output on different states of the steady power curve $P_s(u)$. The variable $p(t)$ denotes the noisy contribution.

Based on the time series (Figure 4.2) we propose a simple linear response model $-\alpha \cdot [P(t) - P_s(u)]$, which is perturbed by a noise term $\sqrt{\beta} \cdot \Gamma(t)$. Thus the following *Langevin equation* (for details see [5, 46])

$$\frac{d}{dt}P(t) \quad = \quad -\alpha \cdot [P(t) - P_s(u)] + \sqrt{\beta} \cdot \Gamma(t) \tag{4.2}$$

is proposed. The noise free solution is $P(t) \propto e^{-\alpha t}$.

In the stochastic wind turbine power output modeling the term $-\alpha \cdot [P(t) - P_s(u)]$ describes the simplest deterministic relaxation of the instantaneous $P(t)$, which decays and grows exponentially on sudden changes of the wind speed to the steady state $P_s(u)$. The relaxation

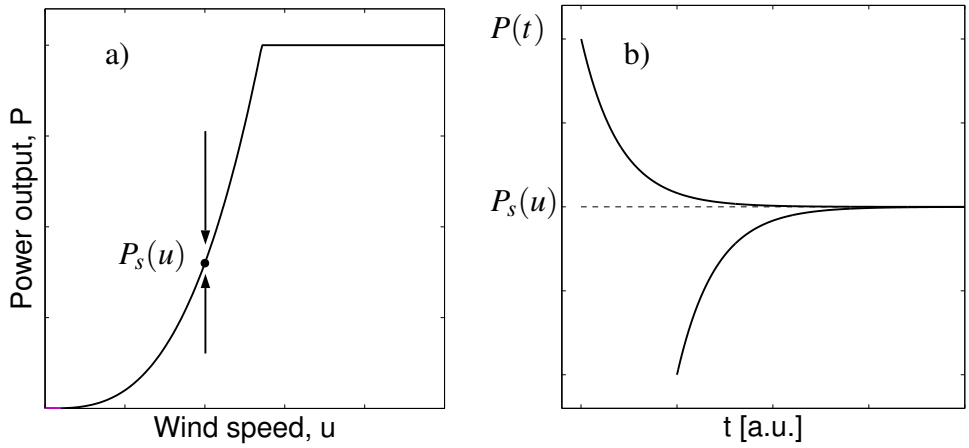

Figure 4.3: *a) Schematic illustration of the relaxation for the fluctuating power output $P(t)$ of a wind turbine at the fixed point $P_s(u)$. b) Attracted dynamics of the power to $P_s(u)$.*

factor α, is just constant in this approach but might be extended to a more advanced function of wind speed, i.e. $\alpha(u,P)$, as proposed in [22].

In Figure 4.3 the relaxation dynamics of the power output to a perturbation is shown schematically. The second important ingredient of our model is the noise term $\sqrt{\beta}\cdot\Gamma(t)$. Comparing Figure 4.3 and Figure 4.2 the necessity of the additional noise term becomes evident. The magnitude of this noise term is given by $\sqrt{\beta}$ and furthemore we assume that $\Gamma(t)$ is δ-correlated Gaussian distributed white noise in time: $\langle\Gamma(t)\rangle = 0$ and $\langle\Gamma(t)\Gamma(t')\rangle = 2\delta(t-t')$. In our ansatz $\sqrt{\beta}\cdot\Gamma(t)$ grasps all the dynamical noise contributions in the dynamical power conversion process. In particular it grasps the turbulent wind and possible noise effects like those caused by stall effects, pitch-angle controlling, yaw-angle deviations, power-grid instability, etc.. From Eq. (4.2) we see that the noise is damped dynamically by the damping factor α.

The Langevin equation (4.2) with this characteristics is called an *Ornstein-Uhlenbeck process* and is a simple case of a Langevin equation. The process is homogeneous, stationary with linear relaxation, [5, 46].

After we have defined the power conversion dynamics, one has to specify the wind speed $u(t)$ and the ideal power curve $P_s(u)$. Here we simply take for wind speed measurements at the hub high of the turbine [26]. The power output $P(u)$ values are calculated through of the following steady power curve function P_s

$$P_s(u) = \begin{cases} a\cdot u^3 & \text{, if } u < u_r \\ P_r & \text{, if } u \geq u_r \end{cases} \tag{4.3}$$

where a is a constant, u_r is the rated wind speed on the nominal power output P_r [70].

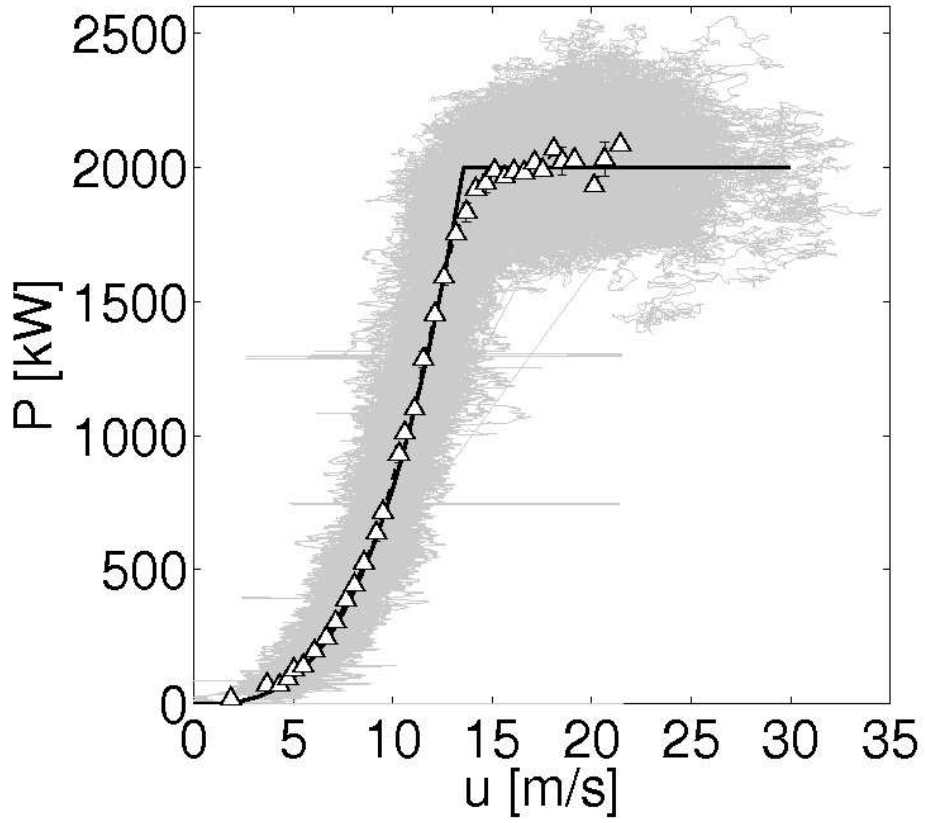

Figure 4.4: *Numerical power output data (grey-lines) obtained from the model (4.2) with parameters* $\alpha_n = 0.02$ *and* $\sqrt{\beta} = 0.021$. *The data of the plots are obtained from the measured wind data taken in the flat terrain of Tjæreborg site [25]. The sampling rate of the data were 25Hz. The theoretical power curve* P_s *(Eq. (4.3)) is shown as black-line and the reconstruction of the power curve by the standard method [26] is shown as open-symbols (-△-).*

The numerical solutions of Eq. (4.2) are solved by integrating recursively in equidistant small finite time steps, $dt = \tau$. Thus the resultant stochastic variable $P_n = P(t_n)$ for times $t_n = \tau\, n$ $(n = 0, 1, 2, ..., N-1)$ of the stochastic wind speed variable $u_n = u(t_n)$ are obtained by

$$P(t+\tau) \;\; = \;\; P(t) - \alpha \cdot [P(t) - P_s(u(t))]\,\tau + \sqrt{\beta \cdot \tau} \cdot w(t) \;\; . \tag{4.4}$$

The initial value at $t = 0$ is $P(0) = P_0$. $w(t)$ denotes an independent Gaussian-distributed random variable of the *Wiener* process with zero mean and variance 2, see [46, 47].

Next, we solve this model by using the above mentioned measured wind data with different degrees of turbulence. The input relaxation factor has been normalized to the sampling rate

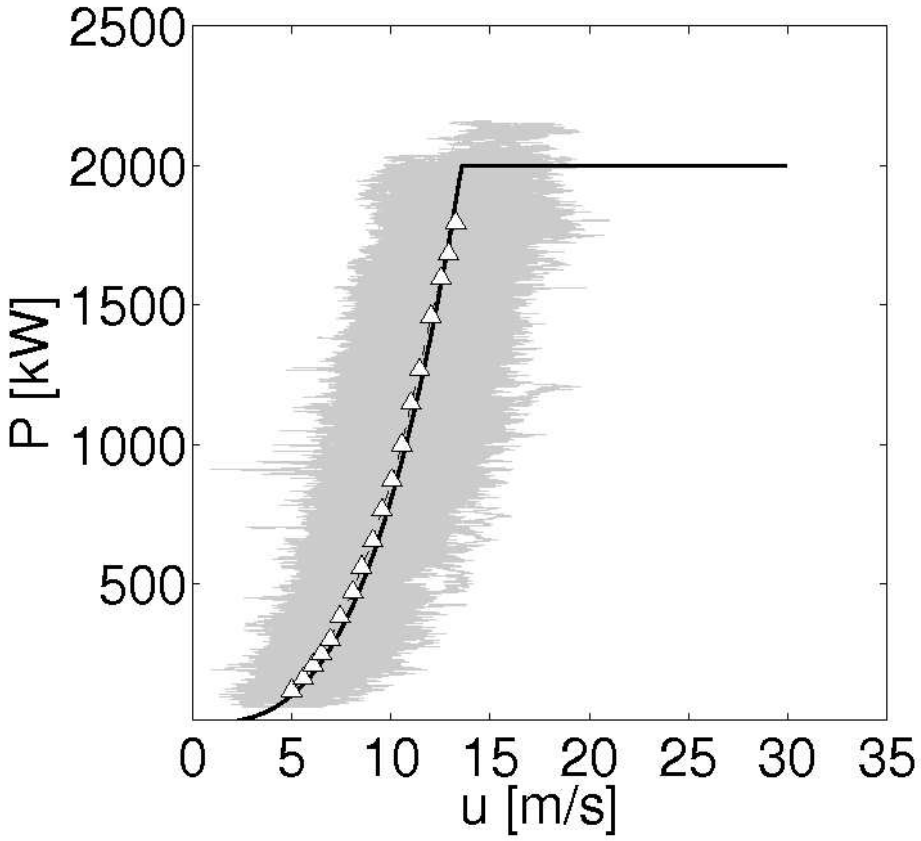

Figure 4.5: *Numerical power output data (grey-lines) obtained from the model (4.2) with parameters* $\alpha_n = 0.01$ *in and* $\sqrt{\beta} = 0.021$. *The data of the plots are obtained from the measured wind data taken in the complex terrain of Meerhof [35]. The sampling rate of the data were 50Hz. The theoretical power curve* P_s *(Eq. (4.3)) is shown as black-line and the reconstruction of the power curve by the standard method [26] is shown as open-symbols (-△-).*

of the data. Based on the result presented later on in this paper we choose as realistic values for wind turbines: $\alpha_n^{(1)} = 0.02$ and $\alpha_n^{(2)} = 0.01$ for the two measured data. The finite time steps of the integration of (4.4) was $\tau^{(1)} = 4 \times 10^{-2}$ for Tjæreborg data and $\tau^{(2)} = 2 \times 10^{-2}$ for the Meerhof data. The noise amplitude is set to $\sqrt{\beta} = 0.021$.

In Figures 4.4 and 4.5 numerical power output data obtained from the model (4.2) corresponding to these measured wind data are plotted. The difference in the amplitude of the stochastic power output $P(t)$ can be seen clearly. This is due to different turbulence intensity of the wind at the two different locations. Furthermore we show their standard averaged power curves [26]. Especially for smaller wind velocities, between $5-10$m/s, we clearly see significant differences in these mean values, which are due to different wind

situations, whereas the power conversion dynamics remains unchanged. This corresponds to the typical specific location dependence of the performance of a wind turbine.

4.4 Stochastic analysis

We consider the stochastic power output as dynamical Markov process like those introduced in Eq. (4.2). The condition of the Markov property demands that the dynamics of the process has no memory. This is described in terms of its conditional probability density function (pdf)

$$W(P_n,t_n|P_{n-1},t_{n-1};P_{n-2},t_{n-2};...;P_1,t_1) = W(P_n,t_n|P_{n-1},t_{n-1}) \ . \tag{4.5}$$

This definition is the characteristic property of a Markov process. The left-hand side describes the pdf at time scale t_n under the condition that the stochastic variable at the time $t_{n-1} < t_n$ was in the state P_{n-1}; at the time $t_{n-2} < t_{n-1}$ was in the state P_{n-2}; and so on. Thus, for Markov processes the conditional pdf depends only on the previous value P_{n-1} at the time t_{n-1}, see also [52]. The time evolution of $W(P,t|P',t')$ which is of interest, is governed by the Master equation and can be expressed by the *Kramers Moyal expansion* [46, 5]

$$\frac{\partial}{\partial t}W(P,t|P',t') = \sum_{n=1}^{\infty}\left(-\frac{\partial}{\partial P}\right)^n D^{(n)}(P,t)W(P,t|P',t'), \tag{4.6}$$

where $D^{(n)}$ are the *Kramers-Moyal coefficients* defined by

$$\begin{aligned} D^{(n)}(P) &= \lim_{\tau\to 0}\frac{1}{\tau}M^{(n)}(P,\tau)\,, \qquad \text{where,} & (4.7)\\ M^{(n)}(P,\tau) &= \int_{-\infty}^{+\infty}(\tilde{P}(t+\tau)-P(t))^n \times W(\tilde{P},t+\tau|P,t)d\tilde{P} \\ &= \left\langle(\tilde{P}(t+\tau)-P(t))^n\right\rangle|_{P(t)=P} \ . & (4.8) \end{aligned}$$

where $\langle\cdot\rangle$ denotes the ensemble averages. The condition $|_{P(t)=P}$ means that at time t the stochastic variable $P(t)$ is at the state P. The moments $M^{(n)}$ characterize the probabilities of $\tilde{P}$ conditioned on P and t: $W(\tilde{P},t+\tau|P,t)$ over a finite time scale $\tau = t-t' > 0$, see Eq. (4.5).

Next, the question arises whether the noise included in the process is Gaussian distributed. In the case of Markov processes with vanishing $D^{(4)}$, according to the Pawula's theorem

[46], the coefficients $D^{(n)} = 0, \forall n \geq 3$. In this case Gaussian noise is present in the process. Thus, Eq. (4.6) reduces to the *Fokker-Planck equation* [5,46] and leads by intengrating

$$W(P,t) = \int W(P,t|P',t')W(P',t')dP'$$

to the following expression of

$$\frac{\partial}{\partial t}W(P,t) = -\frac{\partial}{\partial P}D^{(1)}(P,t)W(P,t) + \frac{1}{2}\frac{\partial^2}{\partial^2 P}D^{(2)}(P,t)W(P,t) \ . \tag{4.9}$$

The Fokker-Planck equation corresponds to the generalized stochastic *Langevin equation* defined (in the Itô definition, see Appendix A) by

$$\frac{d}{dt}P(t) \ = \ D^{(1)}(P) + \sqrt{D^{(2)}(P)} \cdot \Gamma(t) \ . \tag{4.10}$$

The terms $D^{(1)}(P)$ and $D^{(2)}(P)$ are called the *drift* and *diffusion* coefficients and they describe the deterministic relaxation and stochastic (noise) temporal evolution respectively. The term $\sqrt{D^{(2)}(P)}$, as above shown $\sqrt{\beta}$, describes the amplitude of the *dynamical noise*, containing multiplicative noise if it depends on P otherwise additive noise. $\Gamma(t)$ as defined above is an independent δ-correlated Gaussian distributed white noise with zero-mean.

The definition of drift and diffusion coefficients, Eqs. (4.7,4.8), allows their estimations directly from given data via the conditional moments $M^{(n)}$, for further details see Ref. [48,49,51,54]. However the sampling rate of the measurements might be rather low in this case the conditional moments are better approximated by a *Taylor series expansion*, [47,53]

$$M^{(n)}(P,\tau) \ = \ \tau D^{(n)}(P) + O(\tau^2) \ . \tag{4.11}$$

The coefficients $D^{(1)}$ and $D^{(2)}$ are equal to $M^{(1)}$ and $M^{(2)}$ taken in the limit $\tau \to 0$. This limit is determined calculating linearly $M^{(1)}$ and $M^{(2)}$ over several scales τ where the Markov property would be validated. The Kramers-Moyal coefficients are just the slopes of the conditional moments as function of τ. In the case that the process is not Markov we note that the deterministic drift coefficient $D^{(1)}$ can be determined correctly, see Ref. [59]. Alternatively, advanced estimation methods of these coefficients can performed by minimizing of the Kullback-Leibler distances on pdfs as proposed by [65]. For the nontrivial evaluation of measurement noise contained in the process it is possible to distinguish it from the dynamical noise by just pure analysis on the conditional moments, see Ref. [58,64,70]. We note also that the analysis of the Langevin equation can easily be generalized to a larger dimensional case [46], where for example the power output and the wind speed vectors: $(P(t), u(t))$ are take as two independent dynamical variables.

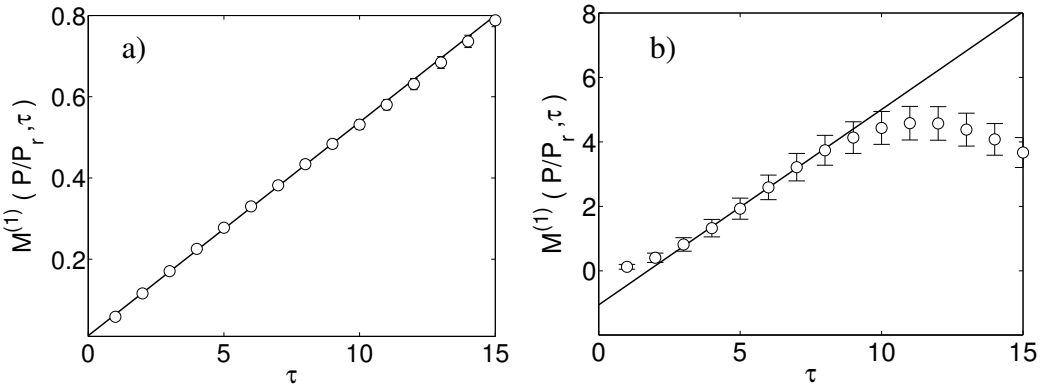

Figure 4.6: *Illustration of the estimation procedure of $D^{(1)}(P)$ in $u = 6.53$m/s for the numerical model (a) and measurement (b) data. The time-scales are given in units of 2×10^{-2}s and 4×10^{-2}s respectively. The coefficient $D^{(1)}$ is estimated in the range of $1 \le \tau \le 10$ for numerical data and $3 \le \tau \le 8$ for the measured data. Parametrization is shown as solid-line.*

4.4.1 Estimation of the Kramers-Moyal coefficients

Prior to the analysis we will normalize $P(t)$ defined in (4.1) by its nominal (rated) power output P_r. Thus, $P(t)$ as well as $M^{(n)}$ and $D^{(n)}$ are dimensionless. We consider stationarity in the interval: $u_{ij} \in (u_a, u_b)$, where u_{ij} is the jth stochastic wind speed in the ith interval. The corresponding P_{ij} is equally partitioned into 100 intervals: $P \in (P_c, P_d)$. For instance assuming wind speed bins of 0.5m/s with ranges between 0-50m/s the matrix for (u,P) is 100×100. Thus for about 10^6 data samples we expect 100 values in average in each bin.

As first step in the analysis the conditional moments $M^{(n)}(P,\tau)$ are estimated by the ensemble averages defined in (4.8). The Kramers-Moyal coefficients $D^{(n)}(P)$ are found by $\lim_{\tau\to0} M^{(n)}(P,\tau)$ as it is defined in (4.11). Next, for fixed values of P a straight line is fitted to the sequence of $M^{(n)}(P,\tau)$ on τ and extrapolated against $\tau = 0$, as shown for numerical and real data in Figure 4.6.

The uncertainty of the coefficients were performed empirically via their variance $\sigma^2_{M,P}$, which depends on the number of statistical events contributing to each estimation. Assuming that each bin of P containing N events has an intrinsic uncertainty

$$\begin{aligned} s_{M,P} &= \frac{\sigma_{M,P}}{\sqrt{N}} \\ \text{where,}\quad \sigma_{M,P} &= \sqrt{\langle[P_\tau(t) - \langle P_\tau(t)\rangle]^2\rangle}. \end{aligned} \tag{4.12}$$

Where $P_\tau(t)$ is just the vector $(P(t+\tau) - P(t))|_{P(t)=P}$ of eq. (4.8).

Next, the critical point in the coefficients estimation, one has to find the range of τ where the linear approach of Eq. (4.11) is valid. In particular one has to find the range of τ values

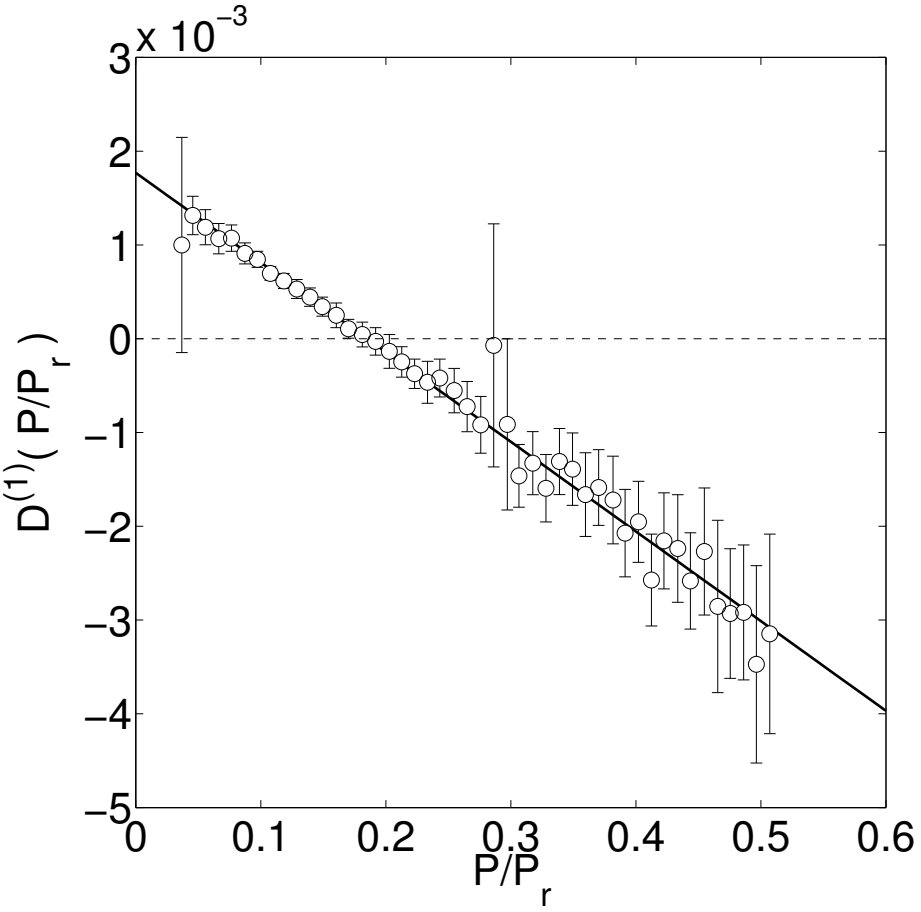

Figure 4.7: *Estimating drift coefficients for $u = 7.7 \pm 0.25$ of the numerical data. $D^{(1)}(P)$ (open-circles) showing a linear approach with slope ≈ -0.01. The reconstruction of $D^{(1)} \simeq D^{(1)}_{th}$, where $D^{(1)}_{th}$ is the theoretical relaxation α value given in the process.*

where the process follows the Markov properties, a task which provides further interesting features of the data like the Markov-Einstein length [54,55,56]. Here we simply search for a range (see Figure 4.6 b)) where a linear dependence of $M^{(n)}(P)$ is found.

It is clear that in all the time-scales τ, the Markov property is not universally fulfilled but commonly there exists a lower threshold. We estimate the coefficients $D^{(n)}(P)$ in the range of $1 \leq \tau \leq 10$ for the numerical data and $3 \leq \tau \leq 8$ for the measurement data.

With this procedure the coefficients $D^{(1)}$, $D^{(2)}$ and additionally $D^{(4)}(P)$, were evaluated.

In Figure 4.7 we have plotted the estimating drift coefficients $D^{(1)}(P)$ of the numerical data for a wind speed $u = 7.7 \pm 0.25$m/s. We show in this case that $D^{(1)}(P)$ is a linear function in P with a slope of ≈ 0.01, which is in accordance with the chosen α values for our numerical model above.

4.5 Markovian power curve: reconstruction

Based on the described procedure to reconstruct from a given data the underlying Langevin Eq. (4.10) we next discuss the determination of the idealized power characterization. The central point is that we search the fixed point of the power conversion dynamics. Fixed points are given by $D^{(1)}(P) := 0$. The stability of the fixed point is determined by the slope of $D^{(1)}(P)$ at $P = P_{fix}$, i.e. if the slope is negative the fixed point is attractive. An alternative way is the use of the potential $\Phi_D(P)$, where the fixed point is just the minimum value of the potential $\Phi_D(P)$

$$\begin{aligned} P_{fix}(u) &= \min(\Phi_D(P)) \,, \qquad \text{with} \\ \Phi_D(P) &= -\int^P D^{(1)}(P')dP' \,. \end{aligned} \tag{4.13}$$

This procedure is very useful not only to identify attractive $P_{fix}(u)$ but also to identify unstable states where also $D^{(1)}(P) := 0$, (e.g. [48, 57]).

In Figure 4.8 the potential $\Phi_D(P)$ of the numerical data is shown together with the minimum $P_{fix}(u)$. The estimated $P_{fix}(u) = 0.19 \pm 0.01$ agrees quite well with the theoretical expected value $P_s(u) = 0.18$.

In Figure 4.9 we have plotted $P_{fix}(u)$ in the local field of the power curve for the numerical data shown in Figure 4.4 and 4.5. For each wind speed u-bin we performed the $D^{(1)}(P)$ reconstruction to determine the fixed point $P_{fix}(u)$, see Appendix B. Furthermore we compare $P_{fix}(u)$ and the standard reconstruction (open-triangles). In Figure 4.9 c) d) magnification parts of Figure 4.9 a) b) are shown respectively. We clearly see that in contrast to the averaged values (open-symbols) our reconstruction (estimation) fixed points agrees well with the given dynamics of the wind power conversion, here given by Eq. (4.3). Note, that our method is not affected by different noise term, given here by different turbulent wind fields.

Next, in the case of measured power output data (Tjæreborg), we have plotted in Figure 4.10 and Figure 4.11 the estimated $D^{(1)}$, $\Phi_D(P)$, $D^{(2)}$ and $D^{(4)}(P)$ for two selected wind speeds.

In the case of $u = 13.6 \pm 0.25$m/s the drift term $D^{(1)}(P)$ shows a clear nonlinear behavior, see Figure 4.10 a) . The corresponding potential $\Phi_D(P)$, plotted in Figure 4.10 c), shows its absolute minimum value at $P_{fix}(u) = 0.99 \pm 0.03$ besides others minima at 0.73 and 0.63, which governed the dynamical equilibrium of P. The standard 10min average was 0.85 ± 0.04.

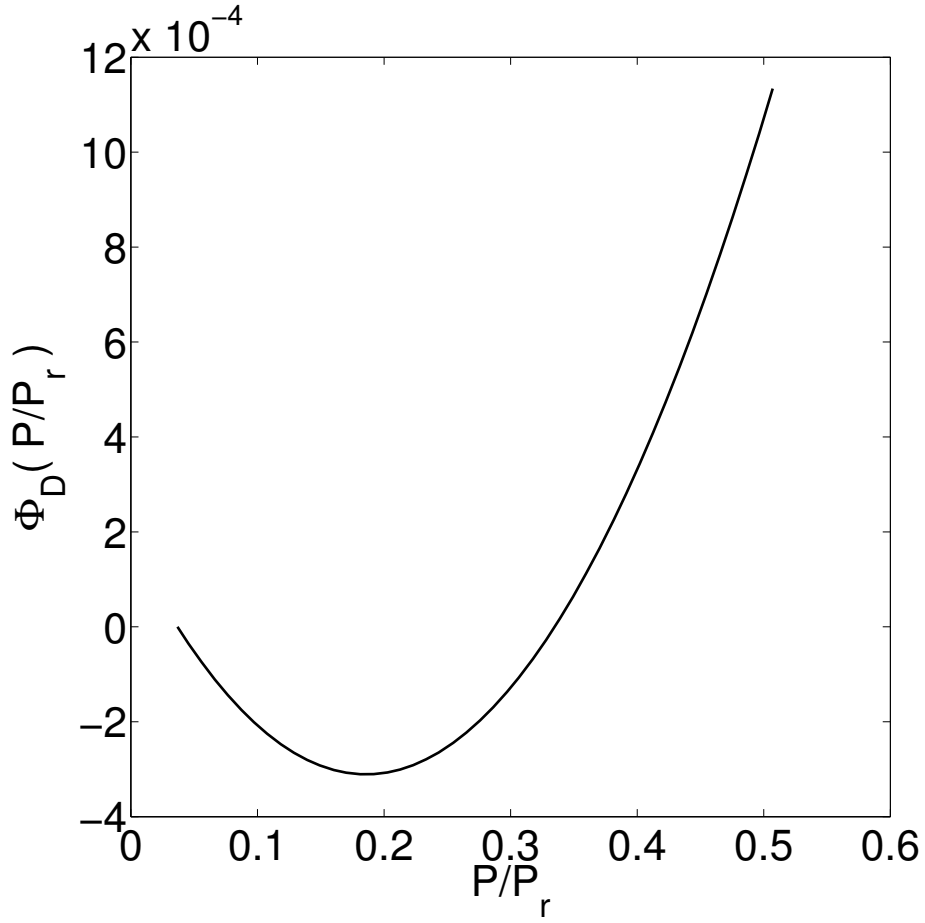

Figure 4.8: *Potential $\Phi_D(P)$ analysis for finding the fixed point P_{fix}. The estimated fixed point of Fig 4.7 is $P_{fix}(u) = 0.19 \pm 0.01$ and the theoretical $P_s(u) = 0.18$. The corresponding standard 10min mean value of the power characteristic is* 0.22 ± 0.01.

In Figure 4.11 a) the dynamical noise term $D^{(2)}(P)$ shows also a higher order behavior with less pronounced minima at the $P_{fix}(u)$ values. In the same plot $D^{(4)}(P)$ is presented to be very small compared to $D^{(2)}(P)$ from what we conclude that the Langevin approach is valid.

In the case of $u = 20.2 \pm 0.25$m/s the relaxation $D^{(1)}(P)$ shows approximately a linear behavior similar to the model, see Figure 4.10 b). In Figure 4.10 d) $\Phi_D(P)$ presents the clear minimum value at $P_{fix}(u) = 1.01 \pm 1.4 \times 10^{-3}$.

In Figure 4.11 b) the dynamical noise term $D^{(2)}(P)$ shows a quadratic form. The noise amplitude in this case is larger than in the first case Figure 4.11 a). In the same plot $D^{(4)}(P)$ is again small compared to $D^{(2)}(P)$.

The different power conversion dynamics just found for $u \sim 14$m/s and ~ 20m/s can be attributed to special effects of the power characteristics. Looking at Figure 4.12, we see $u =$

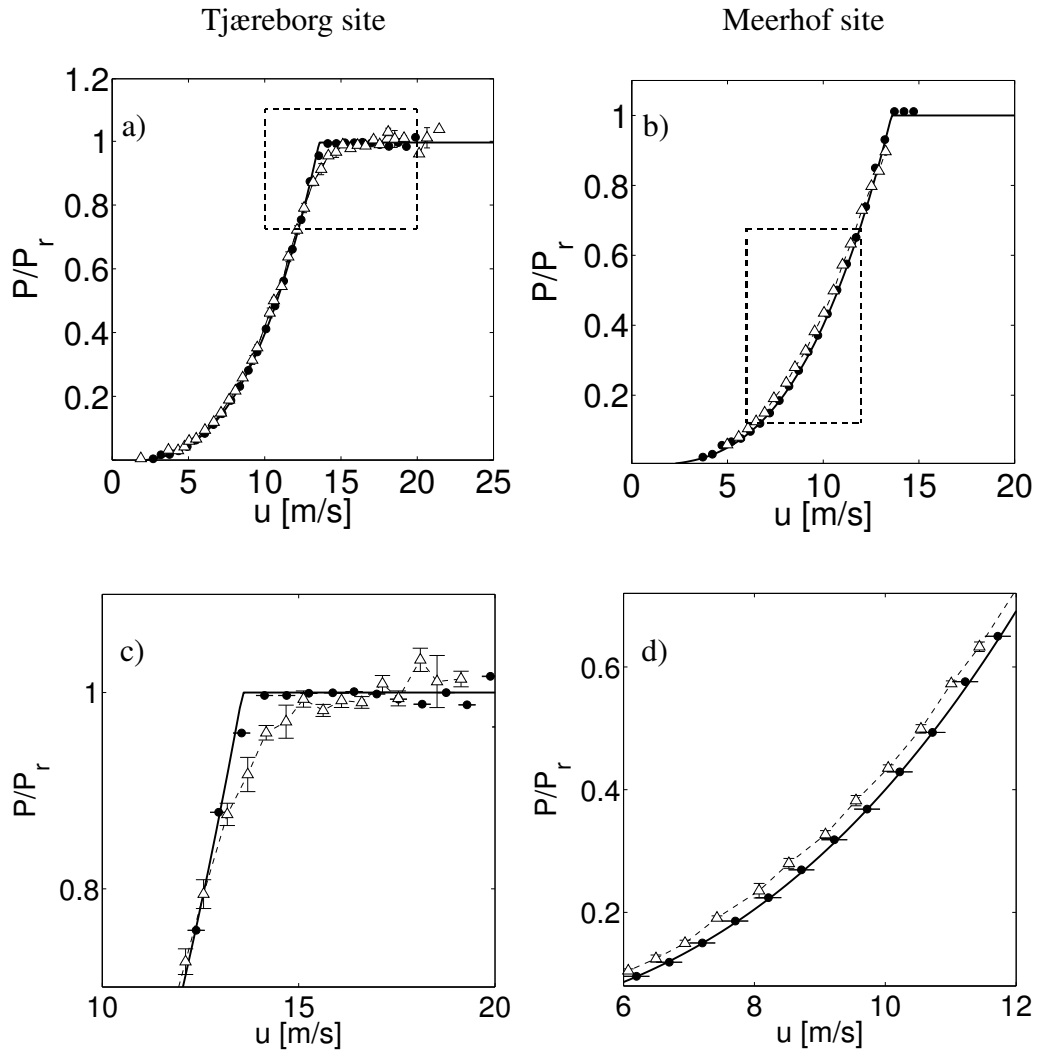

Figure 4.9: *Reconstruction of power curves in the local field for the numerical data, see Figure 4.4 and 4.5. The attractive $P_{fix}(u)$, are the black-points (•) and $P_s(u)$ the theoretical power curve as black-line. In a) b) $P_{fix}(u)$ is compared to the standard reconstruction of power curves shown as open-triangle (-△-). In c) d) Zoom-in of the regions marked in a) b) are shown respectively. Uncertainty estimations are plotted as bars.*

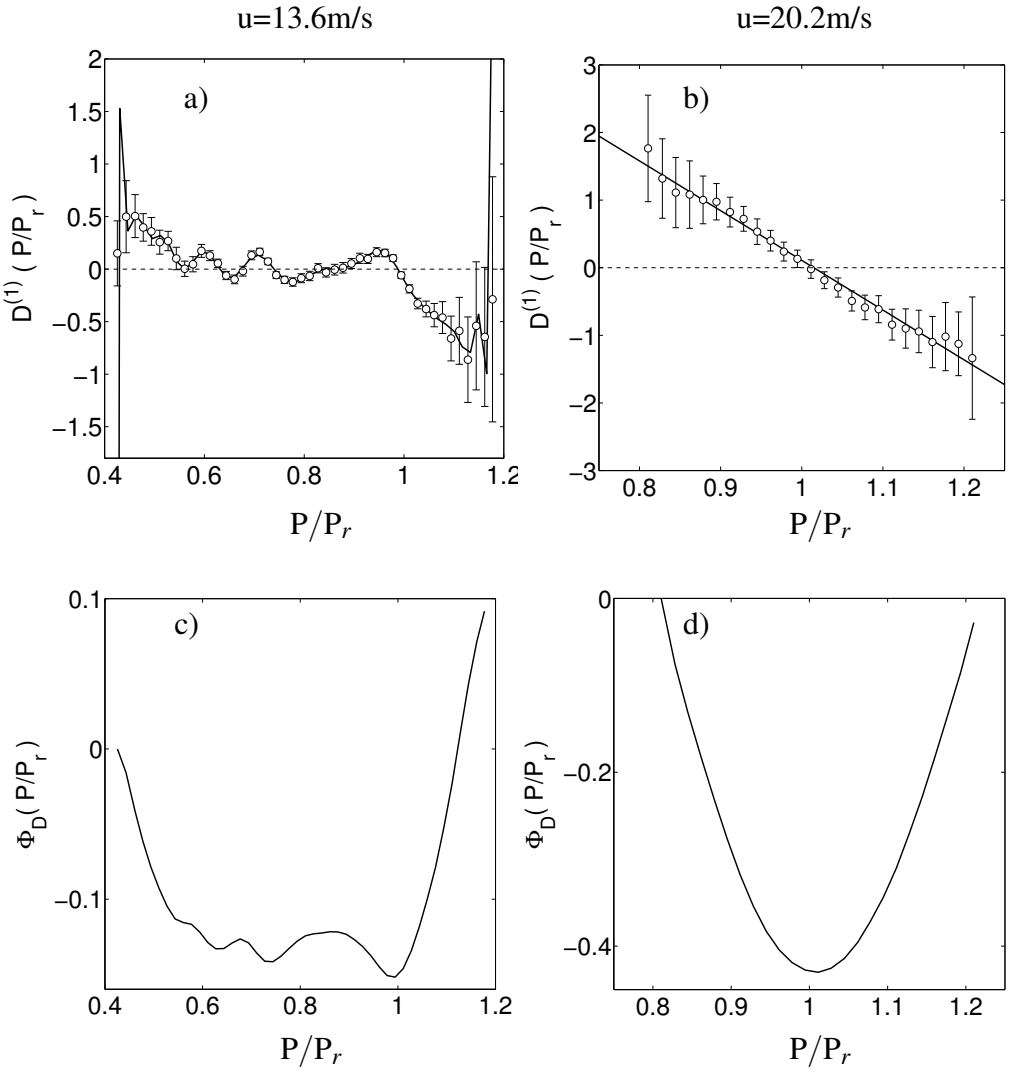

Figure 4.10: *Estimated drift and potential coefficients for $u = 13.6 \pm 0.25$m/s and $u = 20.2 \pm 0.25$m/s of the measured data (Tjæreborg). In a) b) drift coefficients $D^{(1)}(P)$ shown as open-circles ($\circ$); in c) d) Potentials $\Phi_D^{(1)}(P)$. Parametrizations of the pointwise values are shown as lines. Uncertainty is shown as bars.*

14m/s is close to the transition states of the rated power. Here typically control dynamics is crucial. As a consequence of the multiple fixed points (see Figure 4.10 a)), we found on the corresponding probability density of the power output $W(P, u = 13.6\text{m/s})$ a distribution with several local maxima. Note by the knowledge of $D^{(1)}$ and $D^{(2)}$ there is an analytical solution for the stationary case of Eq. (4.9), see also Ref. [46]. This solutions is given by a solid line in Figure 4.11 c) and d). Comparing this to the state of $u = 20.2$m/s, we see that the control dynamics is less complex, causing a narrower probability density $W(P, u = 20\text{m/s})$, as can be seen in Figure 4.11 d).

Next, in Figure 4.12 we have plotted the fixed values of the power production dynamics, $P_{fix}(u)$, which we obtained for the selected velocity bins with the method just mentioned. Additionally the dynamical relaxation to these fixed points can be obtained from values of $D^{(1)}(P)$. In Figure 4.12 a) and b) this relaxation is shown as arrows pointing to the fixed points. The size of the arrow is scaled with the value of $D^{(1)}(P)$, thus indicating the speed of the relaxation. The result shows clearly how the relaxation slows down in the vicinity of the fixed points. The comparison of the reconstructed fixed points with the standard power characteristic (open-triangles), see Figure 4.13, indicates clearly the progress achieved by the method proposed here.

In Figure 4.12 b) a magnification of a selected part of the dynamic power characteristic is shown. Most interestingly we find here a complex behavior given by a multi stability of the system, as it was indicated perviously by the potential, see Figure 4.10 b). In our interpretation such multi stability may arise from shifting of gears or the generator.

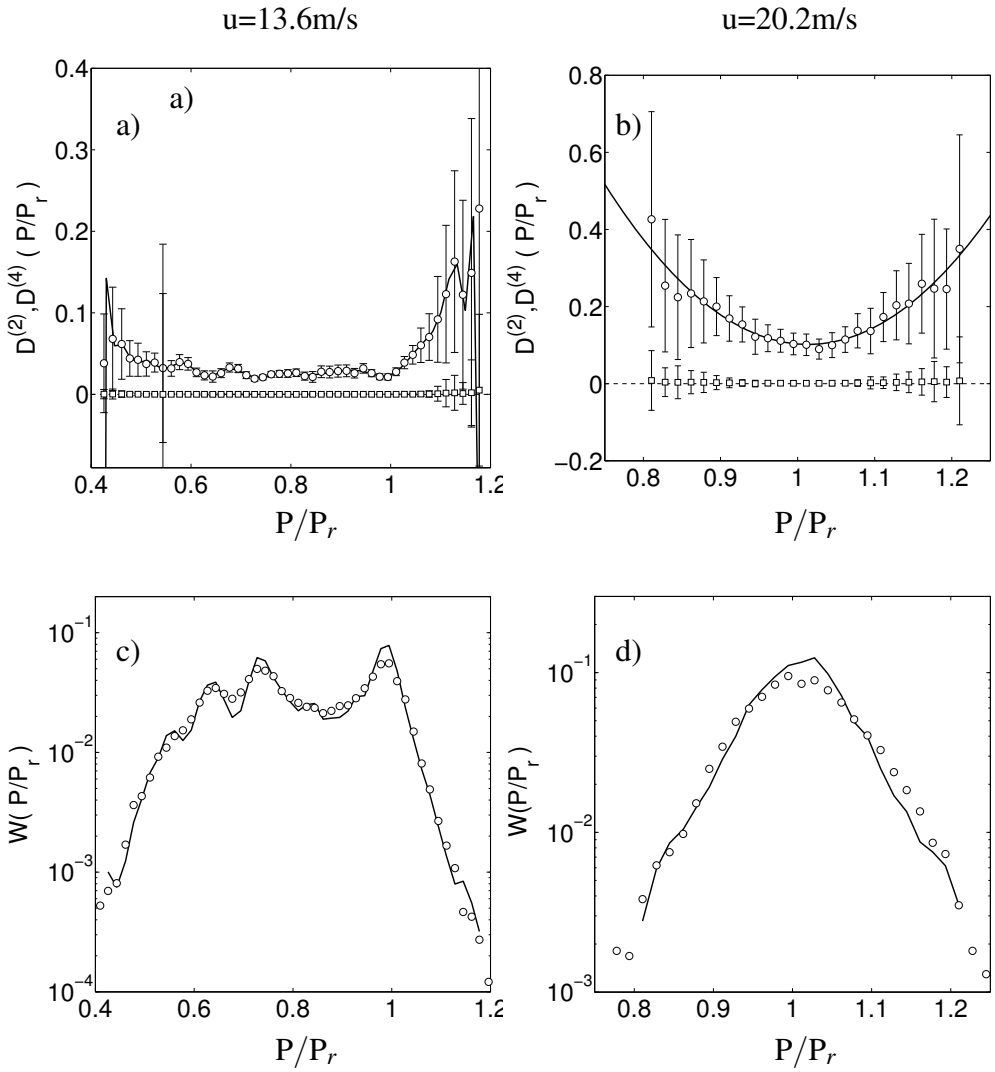

Figure 4.11: *In a) b) diffusion coefficients $D^{(2)}(P)$, see Figure 4.10 shown as open-circles ($\circ$), and additionally the coefficients $D^{(4)}(P)$ shown as squares. In c) d) Comparation of the stationary numerical solution of the Fokker-Planck-Equation (solid line), given by Eq. (4.9), with the probability density functions $W(P)$ of the measured power output data (open-circles). Parametrizations of the pointwise values in a) b) are shown as lines. Uncertainty is shown as bars.*

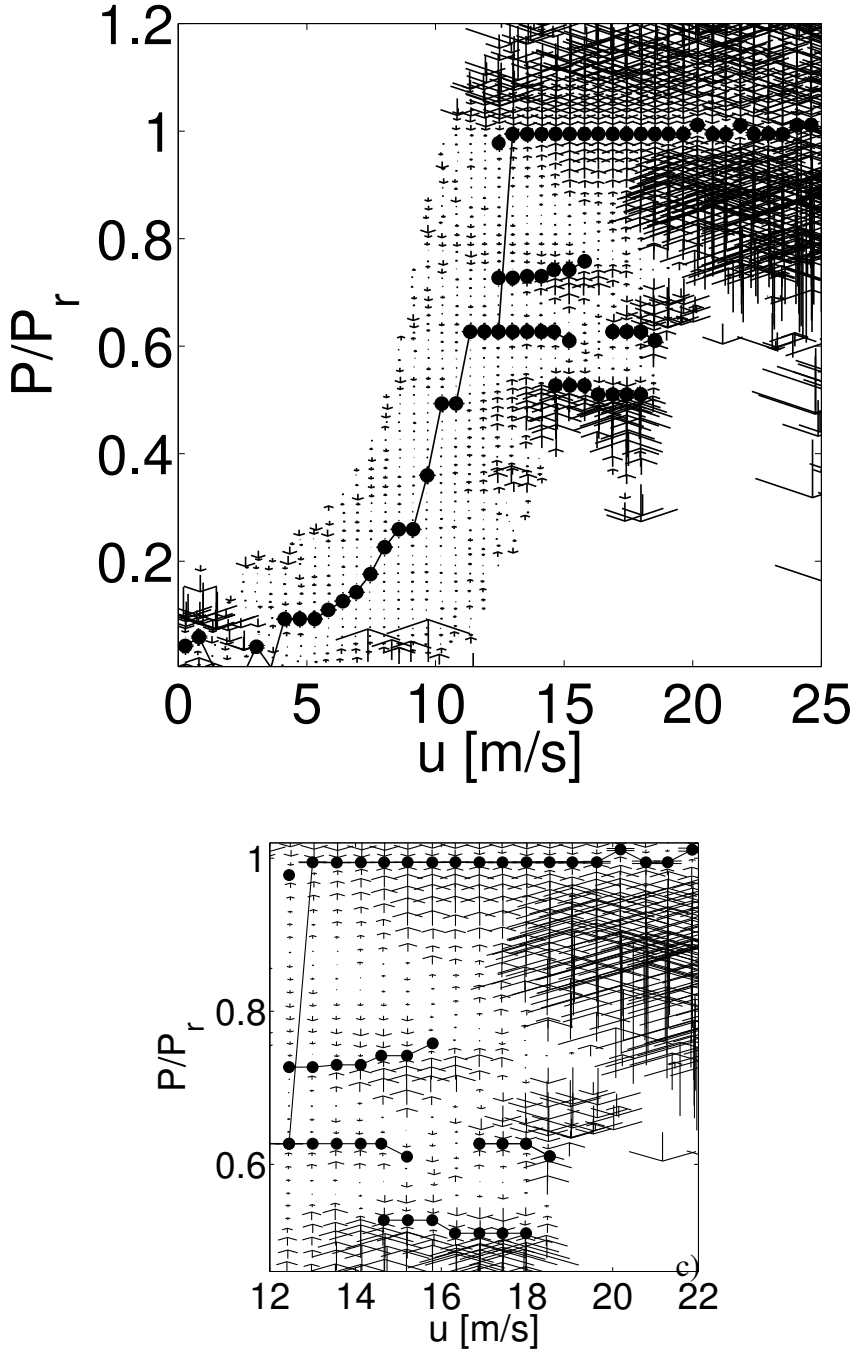

Figure 4.12: *Reconstruction of the power characteristic in the local field for the measured power output data of the Tjæreborg wind turbine, see also Figure 4.1. In a) the dynamics of the power conversion, given by $D^{(1)}(P)$, is shown as arrows together with the attractive $P_{fix}(u)$ (•). In b) Zoom in of part a) showing several local attractive $P_{fix}(u)$ in the range of 12m/s< u <19m/s.*

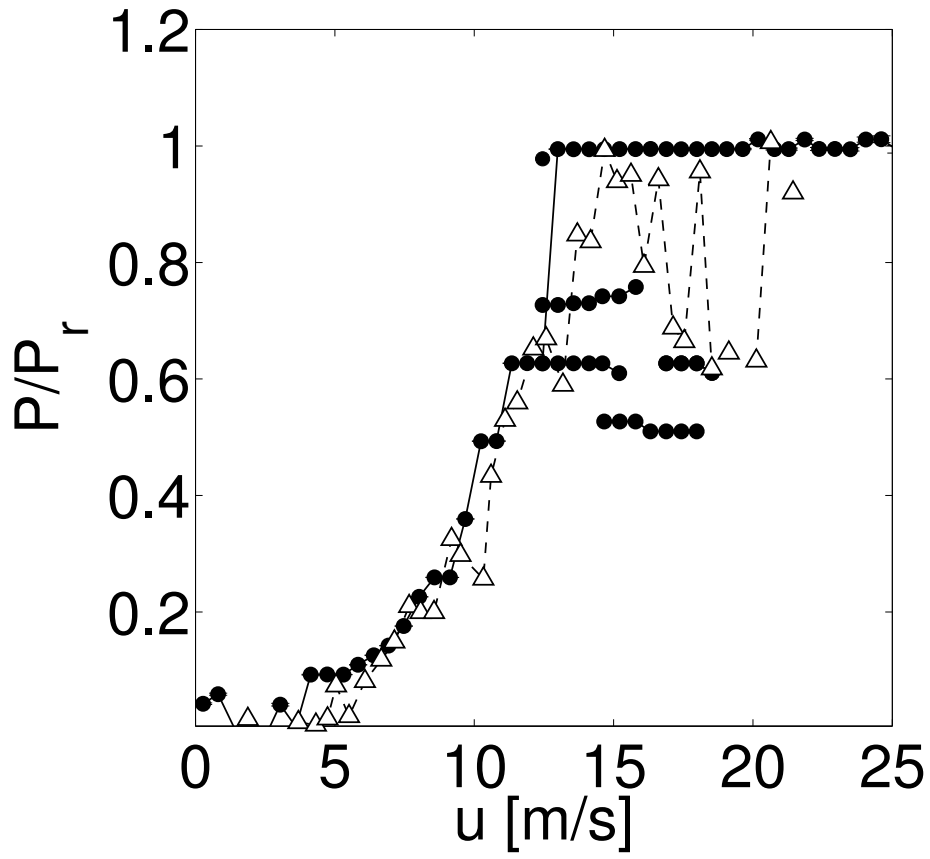

Figure 4.13: *Reconstruction of the power characteristic in the local field for the measured power output data of the Tjæreborg wind turbine. The power characteristics obtained by the standard procedure is shown as (-△-) [26] and the new procedure presented in this paper is shown as (•).*

4.6 Discussion and conclusion

The stochastic power output of a wind turbine has been described by the Langevin equation, which enables to describe relaxation effects as well as the influence of noisy driving forces. Based on this ansatz a new concept of a power characteristic of a wind turbine could be proposed. Instead of the evaluation of some time averaged mean performance, we propose to define the power characteristic as the power production, which is obtained, if no fluctuating wind condition is given. This ideal power production corresponds to the so-called dynamical fixed points. To introduce our new approach and to verify our methods a simple stochastic model for the power conversion of high frequency wind data has been shown. Two time series of wind data from locations with different complexity have been used. The procedure to estimate the Kramers-Moyal coefficients of the Langevin equation from such data has been presented. In both cases the reconstruction of the new power

curves from numerical data has been qualitatively shown by the fixed point analysis. The concept to extract those fixed points from the potential of the deterministic drift coefficient (relaxation part) has been proposed alternatively.

Besides the artificial model data we have investigated also measured data of the Tjæreborg wind turbine. The Kramers-Moyal coefficients of the power output, see Figs. 4.10 and 4.11, have been reconstructed. In the particular case of wind speed of 13.6m/s (close to the rated power) the relaxation function shows a more complex behavior than the one of wind speed of 20.2m/s. In the potential analysis we have found several fixed points between ranges of 12m/s $< u <$ 19m/s which revealed the complex control dynamics of the wind turbine system for optimal operating states (maximal power extraction) on changes of the wind speed, see also Figure 4.12 [9, 10].

These features of the wind power conversion of this wind turbine can not be seen by the standard reconstruction [26], especially if one is interested in the behavior of the turbine close to the kink range of the power curve, see Figure 4.4, 4.5. Furthermore we could show that already data from about one days suffices to get quite precise information of the power conversion, whereas the information of the mean values, used for the standard power characteristic evaluation, are still very unprecise.

To finalize, we point out that the presented novel Markovian method characterize more accurately the wind turbine power performance independent of site specific parameters as the turbulence intensity. The presented procedure is faster in measurement time than the current procedure, because the stochastic analysis is able to deal properly with high frequency fluctuating data. In the case of errors in the measurement data commonly denotes as outliers, the proposed procedure is more robust and more accurate. Furthermore large dynamical noise or transient states in the process yield constructive information for the reconstruction of the system dynamics and does not automatically prevent the estimation of the fixed points, Ref. [66].

Chapter 5

Phenomenological Response Theory to Predict Power Output

The investigations of this Chapter follow closely the phenomenological response theory for the average power output of wind turbines on turbulent winds as proposed in [22, 43]. In this approach the effects of the longitudinal wind speed fluctuations on the power output through a delayed response by the wind turbine are considered. To describe an empirical stationary wind-turbine power curve directly from measurement the extreme principle was proposed by Rauh *et al.* in [43]. This method is similar but not identical to the attractor principle, as previously shown, in Chapter 4, by the Markovian power curve anaylsis.

As example, we will show in sections 5.4-5.6 the relaxation in the special case of constant power in order to derive the delayed response from measurement data.

In the following sections 5.1-5.3 are quoted from [43].

5.1 Introduction

This contribution is on power prediction of wind energy converters (WEC) with emphasis on the effect of the delayed response of the WEC to fluctuating winds. Let us consider the wind speed - power diagram, Figure 5.1 a), with a typical power curve of a 2 MW turbine.

Suppose at time t_0 the system is at some working point $\{u_0, P_0\}$ outside the power curve with a wind speed u_0 which keeps constant for a long time. Then, for $t > t_0$, the system will move towards the power curve, either from above or from below. The power curve acts as an attractor [67]. What happens in a fluctuating wind field? Let us follow a short time series in the wind-speed power diagram, see Figure 5.1 b). We start at some time t_0

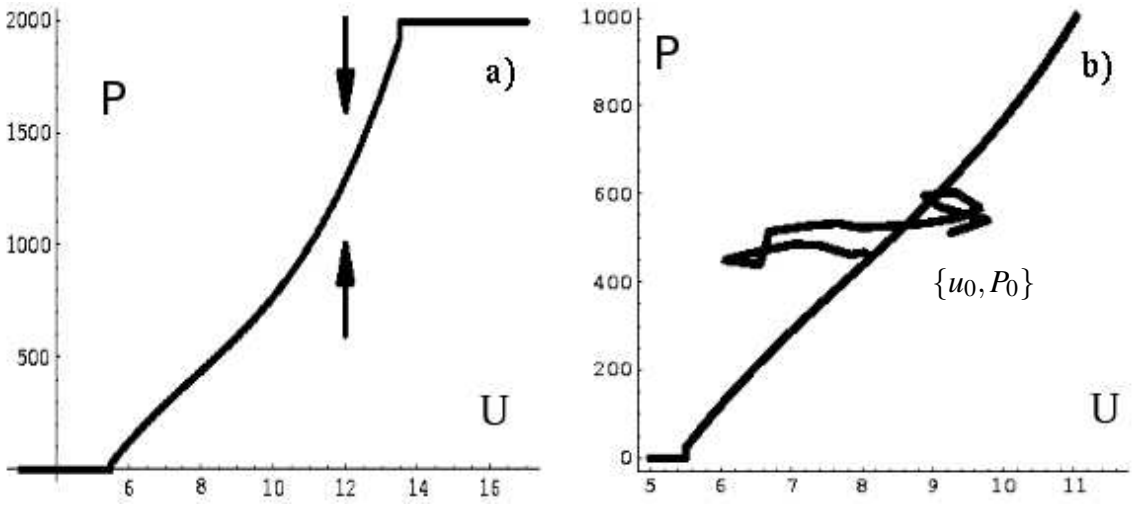

Figure 5.1: *a): Schematic power curve as an attractor. b): 20-second (u,P) trajectory in relation to the power curve. Horizontal and vertical units are m/s and kW, respectively [67].*

with a wind speed $u(t_0)$ and a power output $P(t_0)$. At the next time step, one observes a jump to the point $\{u(t_1), P(t_1)\}$, then to the point $\{u(t_2), P(t_2)\}$, and so on. In plot 5.1 b), consecutive points are connected by straight lines to form a trajectory. In the ideal case of an instantaneous response of the turbine, and in the absence of noise, all points would lie on the power curve. Actually, the turbine reacts with a delayed response to the wind speed fluctuations. The timely changes of the wind speed, $\dot{u}$, together with a finite response time hamper accurate power prediction by means of the power curve alone. The application of a suitable reponse theory may help to properly include the influence of turbulent wind in the power assessment. In Figure 5.2 we show a typical point cluster which is broadly spread around the power curve.

In the following we will discuss in some detail the main idea of a previously published phenomenological response theory [22]. We also will propose an extremal principle to establish an empirical power curve from measurement data [25]. The method is similar but not identical to the attractor principle applied elsewhere [67]. In addition we present an elementary theorem on power prediction in the case of a constant relaxation time of the WEC.

5.2 Power curve from measurement data

An inspection of the point cluster in Figure 5.2 suggests to define an empirical power curve by the location where, in a given speed bin, the maximal density of points $P(t_i)$ is found. This extremal property is expected, if the power curve is an attractor. In previous work [67],

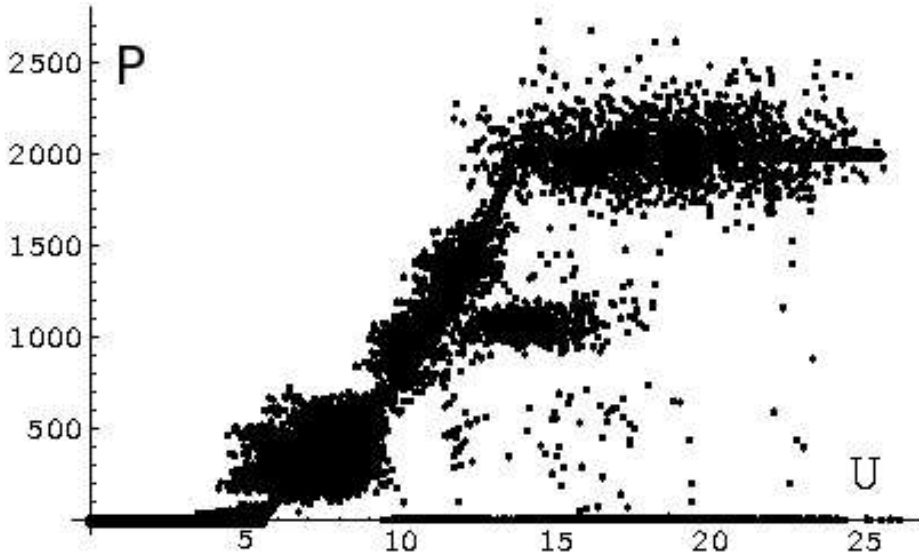

Figure 5.2: *Cluster of* 10^4 *one Hz points (2 MW turbine at Tjæreborg)*

the following expectation values were considered $\Delta_{jk} := < P(t_{i+1}) - P(t_i) >_{u_j,P_k}$ with the suffix u_j, P_k denoting the restriction to the speed and power bin, u_j and P_k, respectively. For a given speed bin u_j, the corresponding point on the power curve was defined by the power bin $P_{k(j)}$ where $\Delta_{jk(j)}$ changes sign. In practice this may cause a problem, if for a given speed bin there are several locations with sign change. The maximum principle, on the other hand, should give a unique result after properly defining the bin sizes:

$$k(j): \quad N_k := \sum_i P(t_i)|_{P_k,u_j}; \quad N_{k(j)} \geq N_k. \tag{5.1}$$

In words: For a given speed bin j, one determines the number N_k of events in the k-th power bin. The power bin $k(j)$ with the maximal number of events gives the point $\{u_j, P_{k(j)}\}$ of the power curve.

With N_k being the number of events in the k-th power bin, with speed u_j fixed, the statistical error is of the order $\sqrt{N_k}$. After adding these uncertainties to the measured ones $\tilde{N}_k := N_k \pm \sqrt{N_k}$, the intervals $\tilde{N}_k$, possibly, can no longer discriminate between different bins k. In this case one has to increase the bin width and thus the number of events in the bins. The widths of the bins then indicates the likely uncertainty of the curve.

The empirical power curve $P_s(u)$ as shown in Figure 5.1 and 5.2 was extracted, by means of the maximum principle, from data of the 2MW turbine at Tjæreborg which were sampled at a rate of 25 Hz over about 24 hours [25]. The data were averaged over 1 second which resulted in 87000 points $\{u(t_i), P(t_i)\}$. 520 1-second data points with negative power output and 137 cases with negative wind speed were set to zero, respectively. The width of the

speed bins was 1 m/s, with values chosen in the midle of the intervals at 3,5, 4.5, 5.5, ... The width of the power bins was variable, in the range from 10 kW to 50kW, depending on the number of events. The cut-in and cut-out speeds were chosen at 5.5 m/s and 31.5 m/s, respectively, where the latter value was the largest power value of the data set. In the interval $5.5 \leq u \leq 13.5$ the points were fitted by a cubic polynomial. In the interval $13.5 \leq u$, the power was set constant.

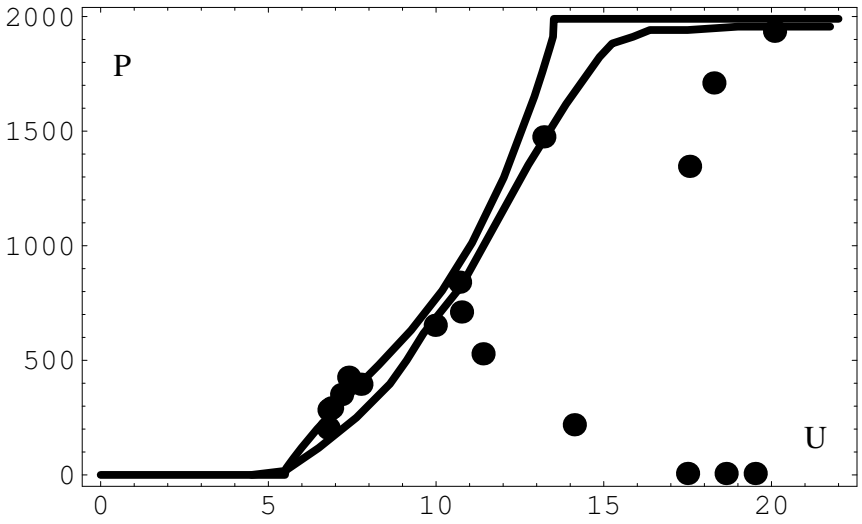

Figure 5.3: *Averages of Fig.2 over 10 minutes without exclusion of shutdown events. Upper and lower curve depict our empirical and the Tjæreborg [25] power curve, respectively.*

Which average power output is predicted by our empirical power curve? To this end, we adopt the standard method by first averaging the data points over 10-minutes. In Figure 5.3 such averaged points are plotted corresponding to Figure 5.2; as should be noticed, Figure 5.2 depicts the points of a part interval only of length 2.8 hours. Next we estimate the power output in two different ways. First the 10-minute speeds $\bar{u}_i$ are inserted into the empirical power curve function:

$$< P >_s = \frac{1}{N_1} \sum_{i=1}^{N_1} P_s(\bar{u}_i); \quad N_1 = N/600. \tag{5.2}$$

Pictorially, this amounts to shifting the points of Figure 5.3 vertically onto the power curve. This average is compared with the true average of the measured 1-second powers $P(t_i)$, or equivalently the average of the 10-minute values $\bar{P}_i$ ($N_1 = N/600$ be an integer):

$$< P >_{exp} = \frac{1}{N} \sum_{i=1}^{N} P(t_i) = \frac{1}{N_1} \sum_{i=1}^{N_1} \bar{P}_i. \tag{5.3}$$

An inspection of Figure 5.3 indicates that P_s significantly overestimates the power output $< P >_{exp}$, in particular since in the region of the plateau most data points have to be shifted

by a relatively large distance from below onto the power curve. As a matter of fact, due to safety reasons, power output is kept limited near the rated power. Also in the large time interval of 24 hours our power curve average overestimates $< P >_{exp}$, by 17%. In comparison with this, the Tjæreborg power curve, available in the world wide web [25], overestimates the same 24-hours data by about 8%.

One reason for this difference may lie in the fact that our 24h data base for establishing the power curve is rather small. However, in both cases neglection of the finite response time causes systematic errors.

5.3 Relaxation model

In order to include the delayed reponse of the WEC to power prediction, we recently proposed the following relaxation model [22]:

$$\frac{\mathrm{d}}{\mathrm{d}t}P(t) = r(t)\,[P_s(u(t)) - P(t)]; \quad r(t) > 0, \tag{5.4}$$

where P_s denotes the power curve and $u(t), P(t)$ the instantaneous wind speed and power, respectively. Because the relaxation function $r(t)$ is positive, the above model exhibits the attraction property of the power curve. In principle, the model could be nonlinearly extended by adding uneven powers of $P_s(u(t)) - P(t)$ with positive coefficients to preserve attraction.

In the simplest case, we may choose $r(t) = r_0 =$ constant. Defining the mean power as usual by the time average one finds that

$$< P(t) > = < P_s(u(t)) > [1 + o(\frac{1}{r_0 T})]. \tag{5.5}$$

Thus, the average based on the power curve predicts the true mean power output, provided the averaging time T is much larger than the relaxation time $\tau := 1/r_0$. To see this, one integrates Eq.(5.4) from time $t = 0$ to T:

$$\frac{P(T) - P(0)}{T r_0} = < P_s(u(t)) > - < P(t) >, \tag{5.6}$$

which implies that the left hand side of the equation tends to zero in the limit of large T.

In reality, a constant relaxation is not observed, see e.g. [18]. In order to implement a frequency dependent response to wind fluctuations, we made the following linear response ansatz [22]:

$$r(t) = r_0(\bar{u}) + r_1(\dot{u}); \quad r_1(\dot{u}(t)) = \int_{-\infty}^{t} \mathrm{d}t'\, g(t - t')\, \dot{u}(t'). \tag{5.7}$$

Here, r_0 describes relaxation at constant wind speed with $\dot{u}(t) = 0$, compare Figure 5.1a). The dynamic part $r_1(t)$ of the relaxation function takes into account the delayed response to wind speed fluctuations $\dot{u}(t)$. The function $g(t)$, which simulates the response properties of the turbine, principally may include the control strategies of the turbine at various mean (10-minute) wind speeds $\bar{u}$; thus one will generally set $g(t) = g_{\bar{u}}(t)$, see also [18]. In view of the convolution integral in Eq.(5.8), one has factorization in frequency space with

$$\hat{r}(f) = \hat{g}(f)\,[2\pi I\,\hat{u}(f)]; \quad I = \sqrt{-1}. \tag{5.8}$$

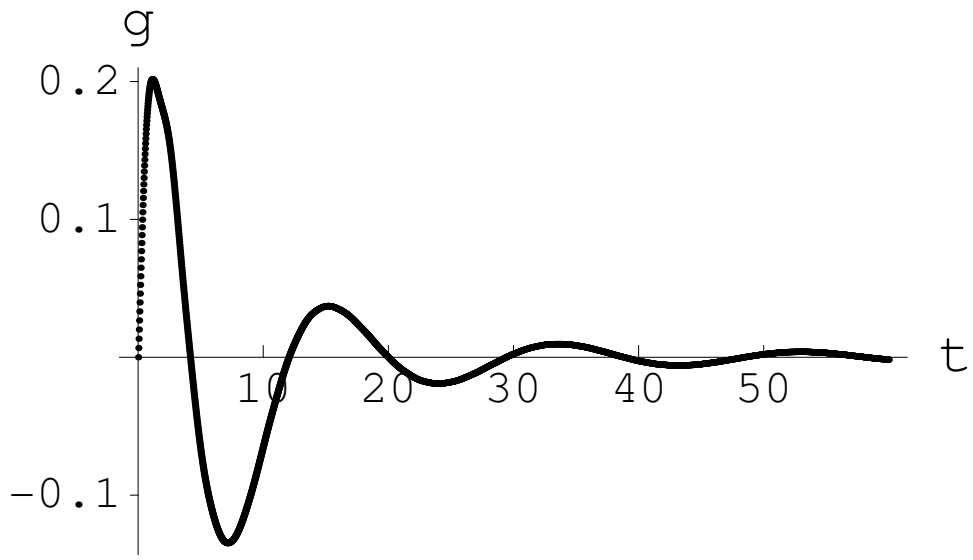

Figure 5.4: *Response function $g(t)$ for the 150 KW turbine Vestas V25 in Beit-Yatir for mean wind speed $\bar{u} = 8$ m/s, derived in ref. [22] from data of ref. [18]. Time t and g are in units of seconds and reciprocal meter, respectively.*

If the response function $g(t)$ is known together with the power curve, then the average power output can be predicted within this model after an elementary numerical integration of system (4) with a given wind field as input. Formally, the dynamic effect can be defined as a correction term, D_{dyn}, to the usual estimate by means of the power curve:

$$< P(t) > = < P_s(u(t)) > \left(1 + D_{dyn}\right). \tag{5.9}$$

For low turbulence intensities the dynamic correction factor D_{dyn} can be obtained analytically within our model [22]. It has the same structure as the dynamic correction introduced in an ad hoc way in [18]. The comparison with their results [18] allowed us, to deduce the response function $g(t)$ in a unique way, for details see [22]. The response function is shown in Figure 5.4.

We remark that the ad hoc ansatz made in [18] is limited to small turbulence intensities, whereas our response model can deal, in principle, with arbitrary wind fields.

5.4 A simple example for constant power

In order to get insight into the dynamics response model (5.4) we analyse the relaxation of the fluctuating power $P(t)$ of a wind turbine to wind speed fluctuations at the especial case of constant power P_0 value. In this case the relaxation function (5.4) in the wind speed interval with constant P_0 can be as seen as follows

$$-\frac{d}{dt} ln\,|P_0 - P(t)| = r(t), \tag{5.10}$$

which gives the relaxation $r(t)$ function in terms of a natural logarithm function. From Eq. (5.4) we evaluate the two possible cases for the logartithm term:

$$\begin{aligned} \frac{d}{dt}P(t) &= r(t)\,[P_0 - P(t)], \qquad \text{for } P_0 > P(t), \\ \frac{d}{dt}P(t) &= -r(t)\,[P(t) - P_0], \quad \text{for } P_0 < P(t). \end{aligned}$$

Thus preserving positive values for the argument of the logarithm function we denote the relaxation function in terms of its amplitude

$$-\frac{d}{dt} ln\,|P_0 - P(t)| = r(t). \tag{5.11}$$

Note that on this base the relaxation function is evaluated. The integral of this expression is bounded in time:

$$-\,ln\frac{|P_0 - P(t_1)|}{|P_0 - P(t_0)|} = \int_{t_0}^{t_1} dt\; r(t). \tag{5.12}$$

If the relaxation $-\int_{t_0}^{t_1} dt \frac{d}{dt} ln|P_0 - P(t)|$ is constant, i.e. $r(t) = r_0$, see also Eq.(5.5), the solution of Eq. (5.11) exponentially converges to P_0 as

$$P(t_1) = P_0 + [P(t_1) - P_0] exp[-(t_1 - t_0) r_0],$$

for a large time interval: $(t_1 - t_0) \to \infty$.

Now if we define the variable as $F(t) = ln|P_0 - P(t)|$ we check the relaxation r function by its Fourier transform. For convenience, we writte f by the angular frequency $\omega = 2\pi f$. Thus the Fourier transform for the case of Eq. (5.11) reads

$$\int dt \left[-\frac{d}{dt}F(t)\right] exp[i\omega t] = \int dt\; r(t) exp[i\omega t],$$

with the following derivative terms into the integral

$$\int_{t_0}^{t_1} dt \left(-\frac{d}{dt}\left[F(t)exp[i\omega t]\right] + F(t)\frac{d}{dt}exp[i\omega t] \right) \quad = \quad \tilde{r}(\omega). \tag{5.13}$$

In this equality we evaluate the integration over a finite interval of time. Here, we assume that $F(t) = 0$ outside this interval. Hence the first term of the integral (5.13)

$$\int_{t_0}^{t_1} dt - \frac{d}{dt}\left[F(t)exp[i\omega t]\right] = -F(t_0)exp[i\omega t_0] + F(t_1)exp[i\omega t_1] \rightarrow 0, \tag{5.14}$$

vanishes over time intervals where $t \leq t_0$ and $t \geq t_1$.

Thus the integral is reduced to the form of

$$\begin{aligned} \int dt F(t)\frac{d}{dt}exp[i\omega t] &= \tilde{r}(\omega), \\ iw\int dt\, F(t)exp[i\omega t] &= \tilde{r}(\omega), \end{aligned}$$

which leads to

$$i\omega\,\tilde{F}(\omega) \quad = \quad \tilde{r}(\omega).$$

5.5 Deriving the response function from data

In the following we attempt to derive a response $g(t)$ function from measurement data for the case of constant power P_0 of a wind turbine, as introduced above in section 5.2. In this case, to derive an empirical response $g(t)$ function we evaluate the relaxation $r(t)$ on the base of (5.11), from measured 0.5-sec mean power values. In this analysis the data has been previously selected to the specific mean wind speed $V = 16$m/s, which were taken over a measurement period of 10-min, to evaluate the relaxation $r(t)$ at the nominal power of the turbine, which is stationary and constant, i.e. $P_0 = P_r$, see Eq. (4.3). The stationary power curve P_s corresponds, in this case, to the empirical measured power curve that has been extracted by means of the extreme principle, Eq. (5.1), as shown the results in section 5.2. As alternative we have shown recently a new method of stochastic analysis to extract the deterministic law of a physical noised magnitud value. The application of this method for reconstructing power curves properly from given data has been shown in Chapter 4.

In the Fourier transform analysis we have deconvoluted the response function $\hat{g}(f)$, as given by Eq. (5.8), over averaged values with a length of $N = 2^6$ as duration time of responses in the order of seconds. The averaged $\hat{g}(f)$ values are based on about 20 smaller pieces of data, whose 10min data, about 1250 discrete samples of 0.5 sec means, has been brocken

up into small sections and then zero padded[1] at all the ends of those short sets of values in order to treat the end effects of each section for better resolution of Fourier transform results, as shown in (5.14). We remark that the deconvolution procedure used for Eq. (5.8) has been performed in this way in order to reduce as well as posible the noise effects of the input data.

Due to the restriction to the constant part of the power curve, i.e. in the wind speed interval $13 \leq u \leq 19$, only 1 data set of 10-min was evaluated, unfortunately.

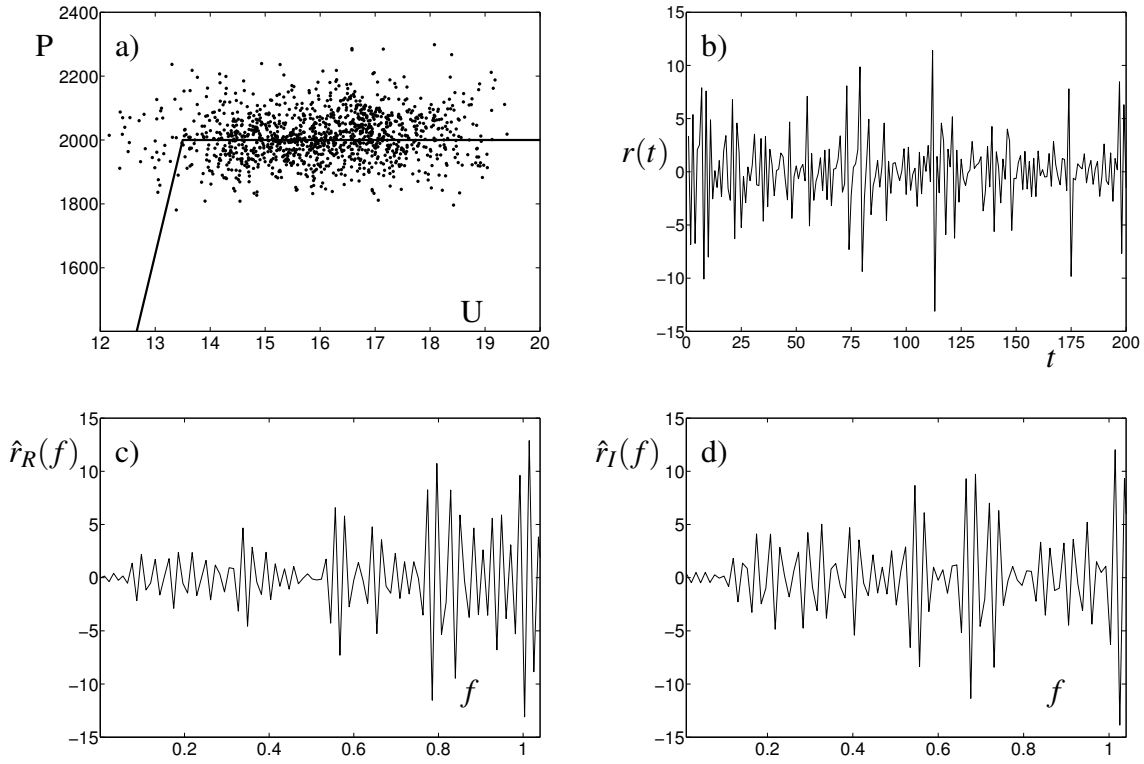

Figure 5.5: *a) The measured 0.5 sec mean power output data (dotted points), at the case of mean wind speed $V = 16$m/s, and the stationary power (solid) curve of Tjæreborg turbine [25]. Horizontal and vertical units are m/s and kW, respectively. b) Relaxation function as time series extracted from the data. The averaged relaxation value is $\langle r \rangle \approx 0.04 sec^{-1}$ and the corresponding relaxation time is $1/\langle r \rangle \approx 26 sec$. In c) d) the real and imaginary parts $\hat{r}_R$ and $\hat{r}_I$ are shown respectively.*

In Figure 5.5 a) the analyzed 0.5 sec mean data are shown as spread points, for the case of mean wind speed $V = 16$m/s, and the constant stationary power P_s as a curve. Figure 5.5b) depicts the relaxation function in the time space, which has been extracted from those mean values. The mean value of the relaxation function was $\langle r \rangle \approx +0.04 sec^{-1}$ which

[1]Zero padding consist to appening zero values to a signal in the time domain, which improves the resolution of the numerical Fourier calculation by an ideal interpolation in the frequency domain, see Ref. [72].

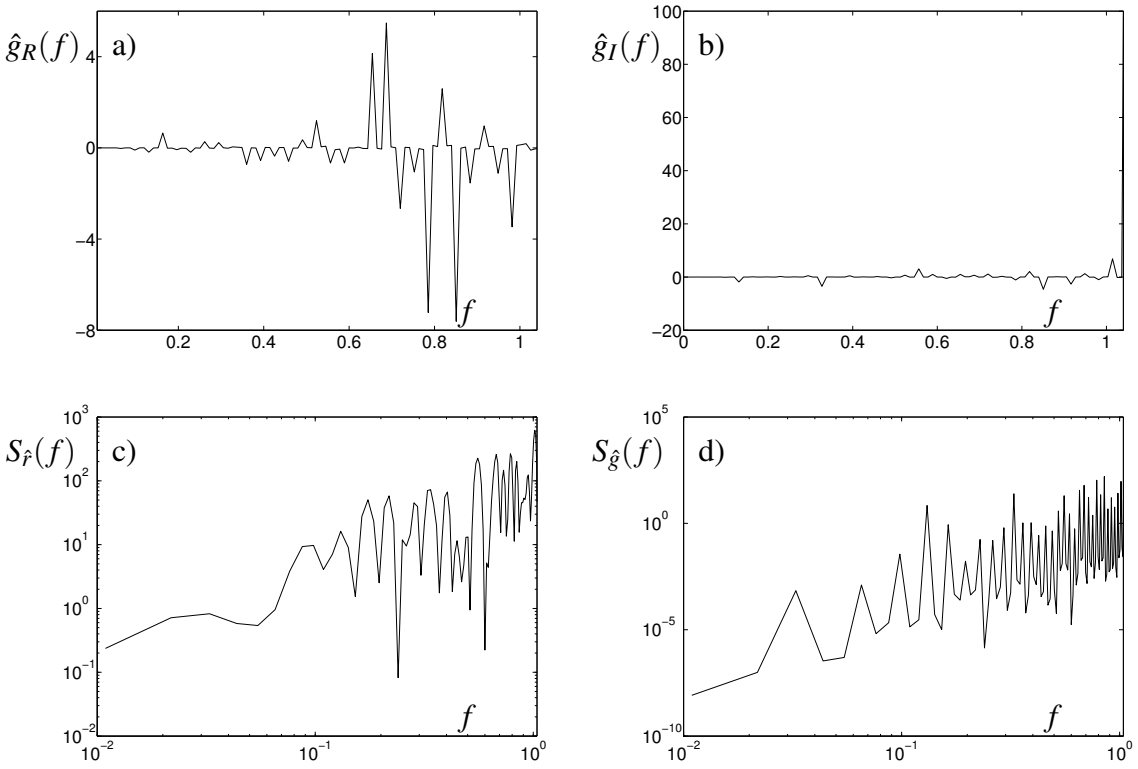

Figure 5.6: *In a) b) the real and imaginary parts $\hat{g}_R$ and $\hat{g}_I$, see Figure 5.5, are shown respectively. In c) d) the spectral density functions S_R and S_G are shown in log plots respectively. In all plots the horizontal axis are the frequency f in units of Hz.*

corresponds to a relaxation time: $\tau := 1/\langle r \rangle \approx 26sec$. The Figures 5.5 c) d) show the real and imaginary parts of the relaxation function $\hat{r}_R$ and $\hat{r}_I$ at the frequency space respectively.

Next, in Figures 5.6 a) b) we have plotted the deconvoluted real and imaginary parts of the response functions $\hat{g}_R$ and $\hat{g}_I$, respectively. In addition, Figure 5.6 c) d) shows the corresponding spectral density functions $S_{\hat{r}}$ and $S_{\hat{g}}$ in the frequency space f, respectively.

The result of the measured data evaluation for the response function $g(t)$ of the Tjæreborg wind turbine is plotted in Figure 5.7. In the given case, we see that the response $\hat{g}(t)$ function oscillates periodically at the frequency $\approx$ 1Hz with spikes amplitudes at the frequency 0.5Hz, see Figure 5.6 d). Note that in this case the response function does not decay to zero at some time later, as shown recently by numerical evaluation in [22], see Figure 5.4.

5.6 Discussion and conclusion

In this Chapter the analytical relaxation model for the average power output in stochastic wind fields has been evaluated in order to derive the response function by wind turbine

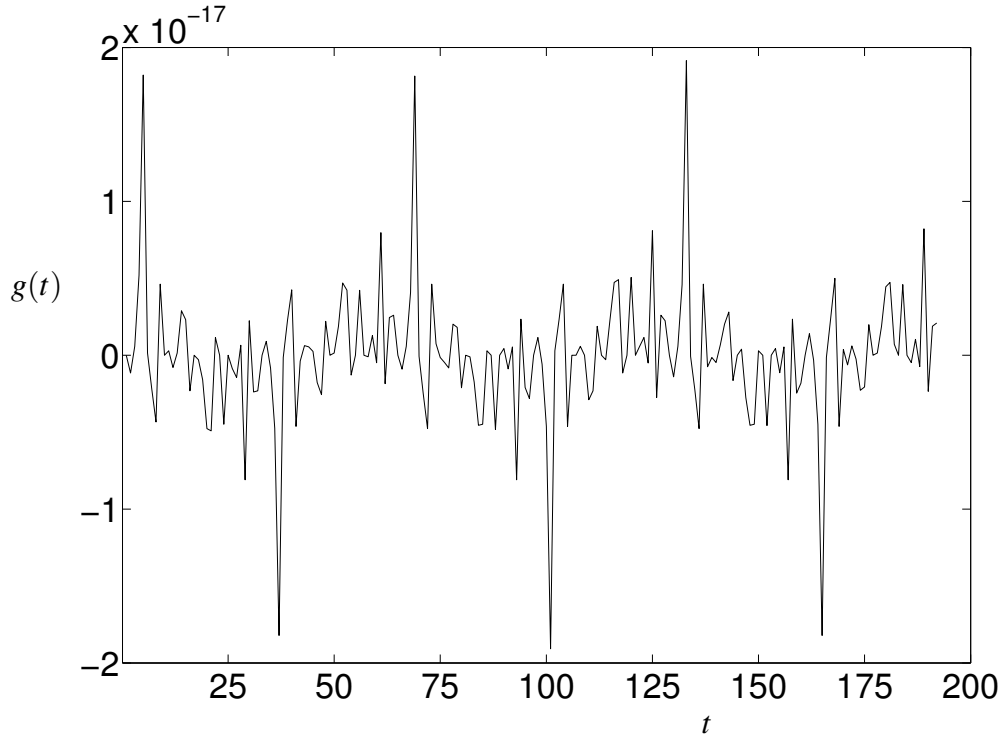

Figure 5.7: *Response function $g(t)$ for the 2 MW Tjæreborg turbine for mean wind speed $V = 16$ m/s. Time t and g are in units of seconds and reciprocal meter, respectively.*

from the measuring data [25]. In the simple case of constant power the response function $g(t)$ is analyzed by solving Eq.(5.4) in order to evaluate optimally $r(t)$ and determining $r(t_i)$ from $P(t_i)$ and $P_r(u(t_i))$.

As is seen, e.g. from Figure 5.6a, the deconvolution method for $\hat{g}(f)$ is quite sensitive to noise. Especially, if one is attemping to unfold wind turbine responses into their complex control dynamics, as for example, by the power controller, pitch control, yaw angle, etc., as shown in Chapter 4. Therefore it is important to use more data in order to calculate significant results, what was by far not available for this investigation. In addition, one may include in the deconvolution method alternative methods such as optimal filtering to treat the noise problem, see Ref. [72].

In the response evaluation it turns out that the measurement data used in this analysis is much too small. This is due to the fact that the all available measurement data (about 1 day), which were taken in data sets of periods of 10 minutes, are too short to evaluate responses in the range of seconds, see Figure 5.6 a)b) and 5.7. Therefore to achive a proper evaluation of the response it one requires 10000 minutes of data or at least 100 data sets of 10 minutes as measurement period, in order to estimate our results to a relative error of 1% of error. Furthermore to examine the response to turbulent wind fields the data has to be

in order to average out noise pre-selected according to their mean V values and turbulence intensity I_u because g depends on these quantities, as shown in [18, 22]. Thus the 100 data sets of 10 minutes have to be selected from a much larger data set.

Another problem is that at the Tjæreborg site, wind speed is measured relatively far away from the turbine, at a distance of 120 m, which poses the question whether the relevant wind fluctuations acting in the rotor plane are still sufficiently correlated with the wind speed fluctuations measured far away, especially in view of the response times of the order of a couple of seconds. Therefore, it is important to improve the measurement method in order to take into account the proper distance between the measure met mast and the wind turbine in order to provide consistency and accuracy on measurement of fluctuating data.

In conclusion we have shown, that an empirical power curve can be extracted from high frequency measurements of only one day. Second, we demonstrated that for a proper power output prediction effects of delayed response have to be considered. As example we shown the relaxation for the simple case of constant power in order to derive the delayed response from measurement data, which however was not satisfactory due to the lack of a sufficiently large data set.

Chapter 6

Conclusions and Outlook

In this work the stochastic power output production of a single wind turbine generator system on fluctuating winds is investigated in detail. The main idea is to describe the overall dynamical power responses of the wind turbine to introduce two basic components: the relaxation, which describes the deterministic dynamic response of the wind turbine to its desired operation state; and the stochastic force (noise), which is an intrinsic feature of the system, and, in addition, analyse the true steady-states of the wind power conversion.

As expected power mean values are strongly affected by fluctuating winds this work aims to provide a new method to characterize wind turbulence independent power curves in the specific test site, fast measurement period for the power performance assessment and the separation of wind and wind turbine's power output production.

The investigation focus only on contributions of the fluctuating power output to its desired stationary operation states. This is due to its basic physical non-linear response characteristic of the system that in combination with turbulent winds the power output of a given wind turbine generator system is crucial for power performance assessment. In order to concentrate on the fundamental effects of the dynamical delayed power output to fluctuating winds a method based on stochastic differential equations known as the Langevin equations of diffusive Markov processes is used. This method enables to describe relaxation effects as well as the influence of noisy driving forces. Based on this ansatz a new concept of a power characteristic of a wind turbine is proposed. Instead of the standard evaluation of some time averaged mean power output value, we propose to define the power characteristic as the power production, which is obtained, if no fluctuating wind condition is given. This ideal power production corresponds to the so-called dynamical fixed points.

In order to introduce this new approach and to verify our methods a simple stochastic model for the wind turbine power conversion of high-frequency wind measurements, i.e. for time

scales $\geq$ 1Hz, is shown. The investigations were achieved basically at the flat and complex terrain locations in order to include the complex local wind turbulence intensity effects that characterizes the specific sites on which wind turbines are installed.

The main result of the Markov power curves shows that independently of the wind turbulence intensity of the specific site the characteristics of the numerical power curves is properly well reconstructed. This characteristics is given by their fixed points analysis that have been extracted from the potential of the deterministic relaxation. The procedure to estimate the Kramers-Moyal coefficients of the Langevin method from such data is shown in detail and applied, as well as, to real measurement data of power output of a 2MW wind turbine. The reconstruction of these coefficients from that measurements showed, for example, that in the particular case of close to the rated wind speed, where power dynamics are usually difficult to describe, the relaxation function has a more complex behavior than the one of the full load. In the potential analysis several fixed points are found which show the complexity of the wind turbine system for optimal power operation on changes of the wind speed. Hence, these results show that the Markovian method can successfully be applied to describe the dynamical features of the wind power conversion of the wind turbines than the well-known standard reconstruction method: standard IEC-61400-12, especially if one is interested in the behavior of the turbine close to the rated wind speed of the power curve. Furthermore the Markovian method on fluctuating data of about days are enough to assess quite precise information of the power conversion, whereas the information of the mean values, used for the standard power characteristic evaluation, are still very unprecise.

Hence, the Markovian power curve method is not only more accurate than the current standard procedure of ensemble averaging but it also allows a measurement period much faster, about days, because the stochastic analysis is able to deal properly with high frequency fluctuating data. In the case of error in the measurement data (e.g. shutdown or power-on states, failure, etc. values commonly dennoted as outliers) the method is most robust to the estimation of wind turbine's power curves.

Actually the wind turbine reacts by some delayed dynamic response to the wind speed fluctuations. The short-time changes of these wind fluctuations together with a finite response time hamper accurate power prediction due to the non-linear power curve characteristic. In particular, the fluctuating winds that contribute to the dynamical responses of the wind turbine due to power control strategies at various mean wind speed conditions are dependent and lead to a non-linear relaxation function that are typically observed by wind turbine simulations. In this sense the application of a suitable response theory has been introduced properly in order to include the influence of turbulent wind in the power prediction. As a result an empirical stationary wind-turbine power curve can be directly extracted, as alternative, from high-frequency measurement data by the extreme principle. Also an ele-

mentary theorem on power prediction for the simplest case of a constant relaxation time of the wind turbine the true-mean power can be calculated.

6.1 Outlook

In the application of the stochastic Langevin equation for the wind turbine power output modeling it has been investigated in a first approach that numerical solutions over measured wind data can be possible to describe ideal power output dynamics. However those first results have to be confirmed by further investigations with more data. In particular, the method of stochastic analysis that has been used here is more reliable if measurements data over several days (or some weeks) are used. Hence, future work is required here to improve the statistical significance of the results.

In the stochastic power output model we have used the Ornstein-Uhlenbeck process as the simplest case of the Langevin equation. However, more investigation on the characteristic relaxation α and noisy β parameters, see Eq. (4.2), are required. In particular, the multiplicative (colored) noise of the wind power productions, which in this case was included by wind turbulence, has to be investigated. Hence, additional work is required to improve the noisy of the power output process which is very important characteristic parameter not addressed here.

In the investigations of the response theory for the averaged power output of wind turbines on turbulent winds we have shown that the delayed response function can be derived from measurement data. However, the analysis for constant power shows that the response function of the wind turbine is quite influenced by noise in the measurement data. This lead to the conclusion that improvements in the deconvolution procedure could be achieved by additional statistical methods, such as optimal filtering, in order to treat the noise problem. Furthermore the procedure of fluctuating measurement data have far not obtained an high attention by the wind energy standards as the measurements of averaged values. Hence, further improvements are focused on the noise treatment of the data and the measurement method for fluctuating data, which have to be explored in the near future.

Appendix A

General Langevin Equation

The generalized form of the **Langevin-Equation** eqn. (4.2) is written (in the Itô definition) in terms of the Kramers-Moyal coefficients $D^{(k)}$ by [5, 46, 47],

$$\frac{d}{dt}q_i(t) \;=\; D_i^{(1)}(\mathbf{q}) + \sum_{j=1}^{n}\left(\sqrt{D^{(2)}(\mathbf{q})}\right)_{ij}\cdot\Gamma_j(t), \quad i=1,...,n. \tag{A.1}$$

where, $\mathbf{q}(t)$ denotes the n-dimensional stochastic state vector. The terms $D_i^{(1)}(\mathbf{q})$ and $D_{ij}^{(2)}(\mathbf{q})$ are called the *drift* and *diffusion* coefficients and they describe the deterministic relaxation and stochastic (noise) temporal evolution respectively. The term $\sqrt{D_{ij}^{(2)}(\mathbf{q})}$ describes the amplitude of the dynamical noise containing multiplicative noise if it dependents on $\mathbf{q}$ otherways additive noise. $\Gamma_j(t)$ is an independent δ-correlated Gaussian distributed white noise with zero-mean: $\langle\Gamma_i(t)\rangle = 0$, $\langle\Gamma_i(t)\Gamma_j(t')\rangle = 2\delta(t-t')$.

The drift coefficient $D_i^{(1)}$ is derived over a finite time step τ by the limit $\tau\to 0$ via the conditional moments $M_i^{(1)}$

$$D_i^{(1)}(\mathbf{q},t) \;=\; \lim_{\tau\to 0} M_i^{(1)}(\mathbf{q},t,\tau)\,, \qquad \text{where,} \tag{A.2}$$

$$M_i^{(1)}(\mathbf{q},t,\tau) \;=\; \int_{-\infty}^{+\infty}(q_i'(t+\tau)-q_i(t))\times w(q',t+\tau|q,t)\cdot\prod_n dq_n' \tag{A.3}$$

$$M_i^{(1)}(\mathbf{q},t,\tau) \;=\; \left\langle q_i'(t+\tau)-q_i(t)\right\rangle|_{q_i(t)=\mathbf{q}} \tag{A.4}$$

and the diffusion coefficient $D_{ij}^{(2)}$ by the conditional moments $M_{ij}^{(2)}$

$$D_{ij}^{(2)}(\mathbf{q},t) \;=\; \lim_{\tau\to 0}\frac{1}{\tau}M_{ij}^{(2)}(\mathbf{q},t,\tau)\,, \tag{A.5}$$

where,

$$M_{ij}^{(2)}(\mathbf{q},t,\tau) = \int_{-\infty}^{+\infty} (q_i'(t+\tau) - q_i(t)) \times (q_j'(t+\tau) - q_j(t)) \times w(q',t+\tau|q,t) \cdot \prod_n dq_n', \;\; n = 1,2,...n \tag{A.6}$$

$$M_{ij}^{(2)}(\mathbf{q},t,\tau) = \frac{1}{\tau} \left\langle (q_i'(t+\tau) - q_i(t)) \times (q_j'(t+\tau) - q_j(t)) \right\rangle |_{q(t)=\mathbf{q}} \tag{A.7}$$

where, $\langle \cdot \rangle$ denotes the ensamble averages. The term $|_{q(t)=\mathbf{q}}$ means that at time t the stochastic variable $q(t)$ is at the state $\mathbf{q}$. The moments $M_i^{(1)}$ and $M_{ij}^{(2)}$ characterizes the probabilities $w(q',t+\tau|q,t)$ over a finite time scale $\tau = t' - t > 0$.

Appendix B

Reconstruction of Markovian Power Curves

This appendix illustrates the reconstruction of the power characteristic in the local field for the numerical power data shown in Figures 4.4, 4.5, 4.9 and measured data shown in Figure 4.1.

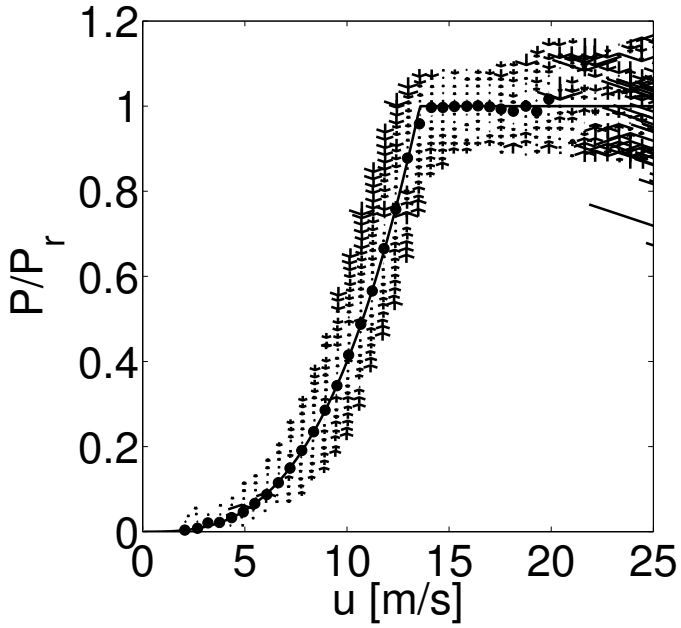

Figure B.1: *Reconstruction of the power characteristic in the local field for the numerical power output data of the Tjæreborg site, see also Figure 4.4. The dynamical relaxation of the power conversion, given by $D^{(1)}(P)$, is shown as arrows together with the attractive fixed points $P_{fix}(u)$ (•). The theoretical power curve $P_s(u)$ is shown as black-line.*

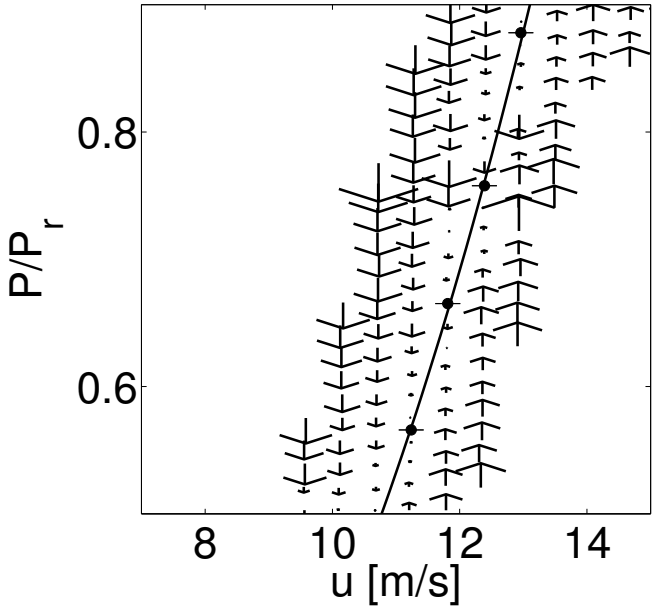

Figure B.2: *Zoom-in of a part of Figure B.1 showing several local attractive fixed points $P_{fix}(u)$ in the range of wind speeds of 7m/s< u <15m/s.*

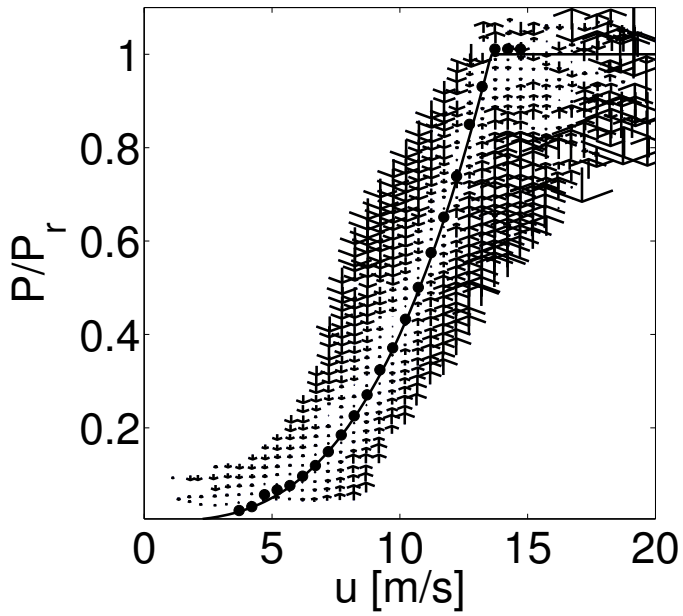

Figure B.3: *Reconstruction of the power characteristic in the local field for the numerical power output data of the Meerhof site, see also Figure 4.5. The dynamical relaxation of the power conversion, given by $D^{(1)}(P)$, is shown as arrows together with the attractive fixed points $P_{fix}(u)$ (•). The theoretical power curve $P_s(u)$ is shown as black-line.*

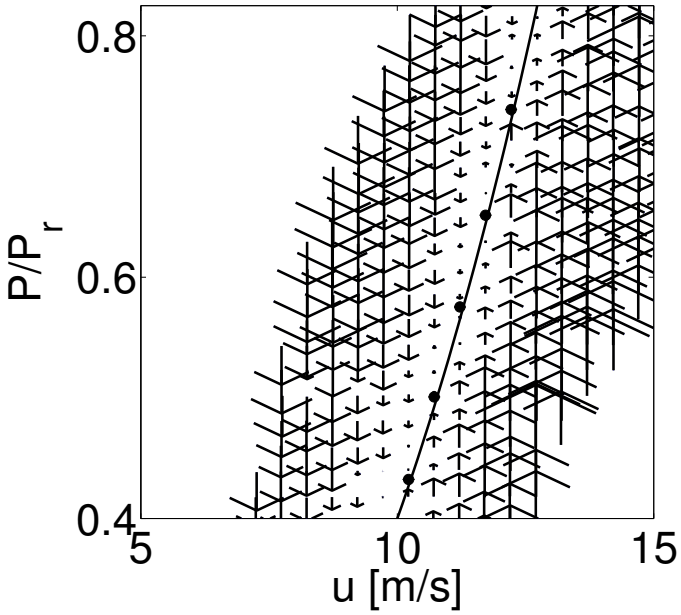

Figure B.4: *Zoom-in of a part of Figure B.3 showing several local attractive fixed points $P_{fix}(u)$ in the range of wind speeds of 5m/s< u <15m/s.*

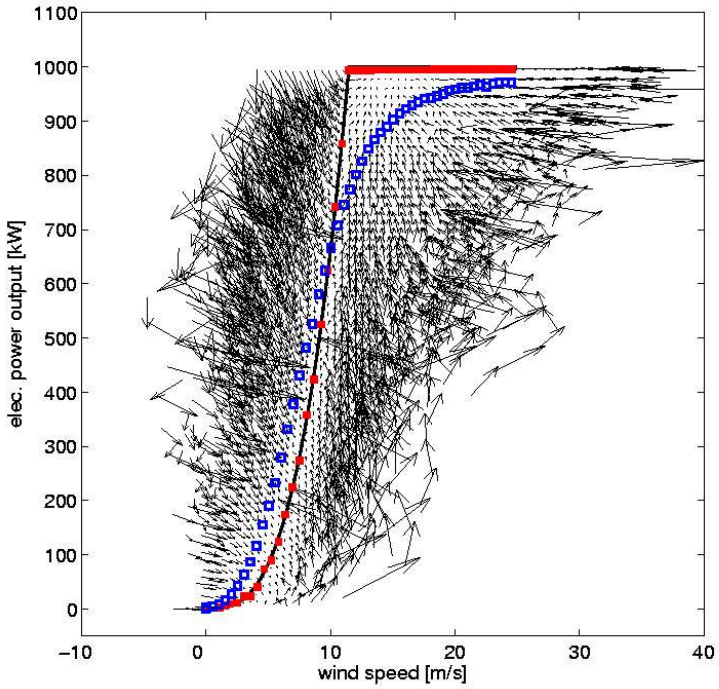

Figure B.5: *Reconstruction of the real power curve on numerical simulation, wind turbulence intensity of 30%, see Figure 2.2. The vector-fields are the deterministic fluctuations. The black-line is the real power curve. The open-squares are the power curve according to the IEC-standard. The filled-squares points are the stationary power curve given by the new method.*

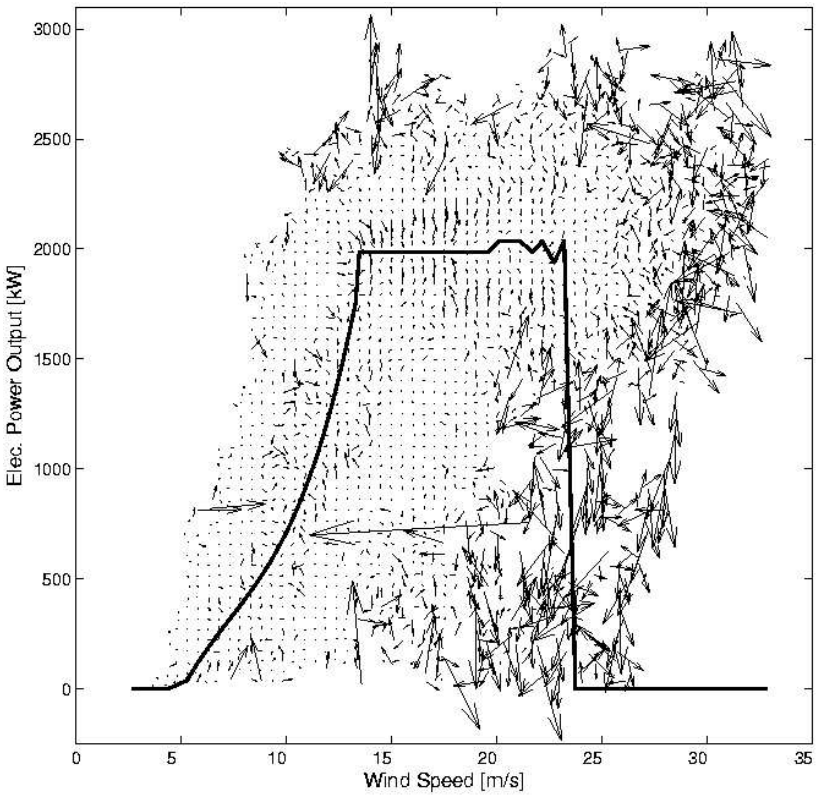

Figure B.6: *Stationary power curve given by the fixed points for all wind velocity intervals, black-line, see Ref. [69]. The arrow fields represent the deterministic dynamical relaxation of the power output given by a two-dimensional analysis,* $D^{(1)}(L,u)$.

Bibliography

[1] European Commision. Energy for the Future: Renewable Sources of Energy. *White Paper for a Community Strategy and Action Plan, COM(97)599 Final*: 1997.

[2] International Energy Agency. Renewables in Global Energy Supply - An IEA Fact Sheet. *OECD/IEA Fact sheet*: Paris, January 2007.

[3] Global Wind Energy Council, Greenpeace International. Global Wind Energy Outlook 2006. *IEA Report 2006*: September, 2006.

[4] Bendt JS, Piersol AG. *Random Data Analysis and Measurements*. John Wiley and Sons: New York, 1986.

[5] Gardiner CW. *Handbook of Stochastic Methods*. Springer: Berlin, 1985.

[6] Lueck St. *Skalenaufgeloeste Experimente und statistische Analysen von turbulenten Nachlaufstroemungen.* PhD Thesis, Carl-von-Ossietzky University of Oldenburg, 26111 Oldenburg, Germany, 2000.

[7] Kaimal JC, Finnigan JJ. *Atmospheric Boundary Layer Flows*, Their Structure and Measurement. Oxford University Press: Oxford, 1994.

[8] Rauh A, Seelert W. The Betz optimum efficiency for windmills. *Applied Energy journal.*; **17**: 15-23, 1984.

[9] Burton T, Sharpe D, Jenkins N, Bossanyi E. *Wind Energy Handbook*. Wiley: New York, 2001.

[10] Lubozny Z. *Wind Turbine Operation in Electric Power Systems*. Springer: Berlin, 2003.

[11] Hanse AD, Jauch C, Soerense P, Iov F, Blaabjerg F. Dynamic wind turbine models in power system simulation tool DIgSILENT. *Risø Report: Risø-R-1400(EN)*, Risø National Laboratory, 2003.

[12] International Electrotechnical Commission. *Wind Turbine Generator Systems, Part 12: Wind turbine power performance testing*. IEC 61400-12 International Standard, 1998.

[13] Boettcher F, Renner Ch, Waldl HP. Peinke J. On the statistics of wind gusts. *Bound.-Layer Meteor.*; **108**: 163-173, 2003.

[14] International Electrotechnical Commission. *Wind Turbine Generator Systems, Part 1: Safety requirements*. IEC 61400-1 International Standard, 1998.

[15] Boettcher F, Peinke J, Kleinhans D, Friedrich R. Handling system driven by different noise sources - Implications for power estimations. *Wind Energy* Springer: Berlin; 179-182, 2007.

[16] Bronstein IN, Semendjajew KA, Musiol G, Muehlig H. *Taschenbuch der Mathematik*. Verlag Harri Deustch: Frankurt am Main, 2005.

[17] Sheinman Y, Rosen A. A dynamical model of the influence of turbulence on the power output of a wind turbine. *J. Wind Eng. Ind. Aerodyn.*; **51**: 287-302, 1992.

[18] Rosen A, Sheinman Y. The average power output of a wind turbine in a turbulent wind. *J. Wind Eng. Ind. Aerodyn.*; **51**: 287-3002, 1994.

[19] Albers A, Hinsch Ch. Influence of different meteorological conditions on the power performance of large WECS. *DEWI Magazin*; **9**: 40-49, 1996.

[20] Van Radecke H. Turbulence correction of power curves. *DEWI Magazin*; **24**: 56-62, 2004.

[21] Keiser K, Langreder W, Hohlen H, Hϕjstrup W. Turbulence corrections for power curves. *Wind Energy* Springer: Berlin; 159-162, 2007.

[22] Rauh A, Peinke J. A phenomenological model for the dynamic response of wind turbines to turbulent wind. *Journal of Wind Engineering and Industrial and Aerodynamics*; **92**: 159-183, 2004.

[23] ELSAMPROJEKT A/S. The Tjæreborg Wind Turbine. *Final Report CEC, DG XII contract EN3W.0048; EP92/334*, 1992.

[24] ELSAMPROJEKT A/S. The Tjæreborg Wind Turbine. Internet: *http://www.afm.dtu.dk/wind/tjar.html*, 2002.

[25] Database on Wind Characteristics. Tjæreborg Wind Turbine Data: 1991-1992. Internet: *http://www.winddata.com*. Technical University of Denmark, Denmark.

[26] International Electrotechnical Commission. *Wind Turbine Generator Systems, Part 12: Wind turbine power performance testing*. IEC 61400-12 Ed.1 International Standard, 1998.

[27] Kolmogorov AN. The local Structure of Turbulence in incompressible viscous fluid for very large Reynolds number. *Doklady ANSSSR*; **30**: 301-304, 1941.

[28] Kaimal JC, Finnigan JJ. *Atmospheric Boundary Layer Flows, Their Structure and Measurement*. Oxford University Press: Oxford, 1994.

[29] Frish U. *Turbulence*. Cambridge University Press: Cambridge, 1995.

[30] Thiringer T. Periodic pulsations from a Three-Bladed Wind Turbine. IEEE Transaction on Energy conversion: **16** 2, 2001.

[31] Ahlstrom A. Influence of wind turbine flexibility on loads and power production. *Wind Energy*; **9** 3: 237-249, 2005.

[32] International Energy Agency. *Recommended practices for wind-turbine testing and evaluation: 1 Power performance Testing*. London, 1990.

[33] Akins RE. Performance evaluation of wind turbines. *Transportation Engineering Journal of ASCE*, New York; **106**: 19-29, 1980.

[34] Stull R. *An Introduction to Boundary Layer Meteorology*. Kluwer Academic Publishers: Netherlands, 1988.

[35] Anahua A, Gottschall J, Barth St, Boettcher F, Zacarias N, Peinke J. Analysis of Wind Turbine Characteristics and Wind Turbulence with respect to Improve Energy Output Prognosis. *ForWind Annual Report 2005*: 67-71, Germany, 2005.

[36] Frandsen S, Antoniou I, Hancen JH, Kristen L, Madsen HA. Redefinition power curve for more accurate performance assessment of wind farms. *Wind Energy*; **3**: 81-111, 2000.

[37] Hunter R, Pedersen TF, Dunbabin P, Antoniou I, Frandsen S, Klug H, Albers A, Lee WK. European Wind Turbine Testing Procedure Developments, Task 1: Measurement method to verify wind turbine performance characteristics. *Risø Report: Risø-R-1209(EN)*, Risø National Laboratory, 2001.

[38] Pedersen TF, Gjerding S, Ingham P, Enevoldsen P, Hansen JK, Joergensen HK. Wind Turbine Power Performance Verification in Complex Terrain and Windfarms. *Risø Report: Risø-R-1330(EN)*, Risø National Laboratory, 2002.

[39] Curvers APWM, Van der Werff PA. Identification of Variables for Site Calibration and Power Curve Assessment in Complex Terrain, SiteParIden JOR3-CT98-0257, Relative Power Curve Measurements in Complex Terrain Task 7. *ECN Report: ECN-C-01-102*, 2001.

[40] Li S, Wunsch DC, O'Hair E, Giesselmann MG. Comparative analysis of regression and artificial neural network models for wind turbine power curve estimation. *Journal of Solar Energy Engineering of ASME*; **123**: 327-332, 2001.

[41] Ernst B, Rohring K, Jursa R. Online-monitoring and prediction of wind power in german transmission operating centres. *First Join Action Symposium on Wind Forecast Techniques*; Norrköping: 125-145, Sweden, 2002.

[42] Kariniotakis G, Stavrakakis GS, Nogaret EF. Wind power forecasting using advanced neural network models. *IEEE Transaction on Energy Conversion*;**11 4**: 762-767, 1996.

[43] Rauh A, Anahua E, Barth St, Peinke J. Phenomenological response theory to predict power output. *Wind Energy* Springer: 153-158, Berlin, 2007.

[44] Boettcher F, Renner Ch, Wald HP, Peinke J. On the statistic of wind gusts. *Boundary-Layer Meteorology*; **108**: 163-173, 2003.

[45] Haken H. *Syenergetics: Introduction and Advanced Topics*. Springer: New York, 2004.

[46] Risken H. *The Fokker-Planck Equation*. Springer: Berlin, 1989.

[47] Kloeden PE, Platen E. *Numerical Solution of Stochastic Differential Solutions*. Springer: Berlin, 1999.

[48] Siegert S, Friedrich R, Peinke J. Analysis of data sets of stochastic systems. *Physics Letters A*; **243**; 275-280, 1998.

[49] Friedrich R, Siegert S, Peinke J, Lueck St, Siefert M, Lindemann M, Raethjen J, Deuschl G, Pfister G. Extracting model equations from experimental data. *Physics Letters A*; *271*: 217-222, 2000.

[50] Friedrich R, Peinke J, Renner Ch. How to quantify deterministic and random influences on the statistics of the foreign exchange market. *Physics Review Letters*; **84**: 5224-5227, 2000.

[51] Ragwitz M, Kantz H. Indispensable finite time corrections for Fokker-Planck equations from time series data. *Physics Review Letters*; **87**: 254501, 2001.

[52] Renner Ch, Peinke J, Friedrich R. Experimental indications for Markov properties of small-scale turbulence. *Journal of Fluid Mechanics*; **433**: 383-409, 2001.

[53] Friedrich R, Renner Ch, Siefert M, Peinke J. Comment on "Indispensable finite time corrections for Fokker-Plank equations from time series data". *Physics Review Letters*; **89**: 149401, 2002.

[54] Renner Ch. *Markowanalysen stochastisch flukturiender Zeitserien*. PhD Thesis. Carl-von Ossietzky Universitaet Oldenburg: Oldenburg, 2002.

[55] Friedrich R, Zeller J, Peinke J. A note in three point statistics of velocity increments in turbulence. *Europhysics Letters*; **41**: 153, 1998.

[56] Lueck St, Renner Ch, Peinke J, Friedrich R. The Markov -Einstein coherence length a new meaning fort he Taylor length in turbulence. *Physics Letters A*; **359**: 335, 2006.

[57] Kriso S, Peinke J, Friedrich R, Wagner P. Reconstruction of dynamical equations for traffic flow. *Physics Letters A*; **299**: 287-291, 2002.

[58] Siefert M, Kittel A, Friedrich R, Peinke J. On a quantitative method to analyze dynamical and measurement noise. *Europhysics Letters*; **61 (4)**: 466-472, 2003.

[59] Siefert M, Peinke J. Reconstruction of the deterministic dynamics of stochastic systems. *International Journal of Bifurcation and Chaos*; **14**, 2004.

[60] Peinke J, Boettcher F, Barth St. Anomalous Statistics, financial markets and other complex systems. *Annalen der Physik*; **13** 7: 450-460, 2004.

[61] Peinke J, Barth St, Boettcher F, Heinemann D, Lange B. Turbulence, a challenging problem for wind energy. *Physica A*; **338**: 187-193, 2004.

[62] Waechter M, Riess F, Schimmel Th, Wendt U, Peinke J. Stochastic analysis of different rough surfaces. *The European Physical Journal B*; **41**: 259, 2004.

[63] Kuusela T. Stochastic heart-rate model can reveal pathological cardiac dynamics. *Physics Review Letter E*; **69**: 0131916, 2004.

[64] Boettcher F, Peinke J, Kleinhans D, Friedrich R, Lind PG, Haase M. Reconstruction of complex dynamical systems affected by strong measurement noise. *Physics Review Letters*; **97**: 090603, 2005.

[65] Kleinhans D, Friedrich R, Nawroth A, Peinke J. An iterative procedure for the estimation of drift and diffusion coeffients of Langevin processes. *Physics Letters A*; **346**: 42-46, 2005.

[66] Van Mourik AM, Daffertshofer A, Beek JP. Estimating Kramers-Moyal coefficients in short and non-stationary data sets. *Physics Letters*; **351**: 13-17, 2005.

[67] Anahua E, Lange M, Boettcher F, Barth St, Peinke J. Stochastic analysis of the power output for a wind turbine. *Proceedings of the European Wind Energy Conference EWEC*, London, 2004.

[68] Anahua E, Lange M, Boettcher F, Barth St, Peinke J. Stochastic Analysis of the Power Output for a Wind Turbine. *Proceedings of the German Wind Energy Conference DEWEK*, Wilhelmshaven, 2004.

[69] Anahua E, Barth St, Peinke J. Characterisation of the power curve for wind turbines by stochastic modeling. *Wind Energy* Springer: 173-177; Berlin, 2007.

[70] Boettcher F, Peinke J, Kleinhans D, Friedrich R. Handling system driven by different noise sources - Implications for power estimations. *Wind Energy* Springer: 179-182; Berlin, 2007.

[71] Anahua E, Barth St, Boettcher F, Peinke J. Characterisation of the power curve for wind turbines by stochastic modeling. *Proceedings of the European Wind Energy Conference EWEC*, Athens, 2006.

[72] Press WH, Teukolsky SA, Wertterling WT, Flannery BP. *Numerical recipes in C++*. Cambridge University Press: Cambridge, 2002.

Acknowledgments

First of all, special acknowledgments I would like to give to two sponsors who provide the financial found. The European Commision who founded to the beginning of my research work within the project *HONEYMOON* under fifth framework programme and *The Federal Ministry of Education and Research (Bundesministerium für Bildung und Forschung, BMFB)* who founded the final part of this work under EWO project.

My personal acknowledgments, I would like to thank my promotor, Prof. Dr. Joachim Peinke. He not only gave me the scientific support and supervision that a student can expect from his professor, but he also allowed and encouraged me to take part of his Hydrodynamics and Wind Energy group and at the Center for Wind Energy Research (ForWind) of the Carl von Ossietzky University of Oldenburg. The full discussions and information's exchange by national and international conferences were always suggested and financed. Thanks to him, I have never been without a stimulated work and a friendly ear. Without those I would never have made it this far.

Prof. Dr. Alexander Rauh, for his disposition in accept as second expert in the examination of this thesis. Though his subject was mainly not in my work, his ideas, his research, specially in the wind energy field brought periodically full discussions and suggestions on which the last part of this thesis was built.

I would like to thank to Stephan Barth, Frank Boettcher and Julia Gottschall for the common work and helpfully discussions on physics and other topics, for the friendly work atmosphere while we were working together in the Energy Lab and on other occasions.

I am grateful to Andreas Nawroth for many discussions on the Kramers-Moyal coefficients, to David Kleinhans who helped with the numerical integration of the Ornstein-Uhlenbeck process to me and the all habitants of Energy Lab who provided a friendly winds during all those years.

Also I thanks to Matthias Lange who introduced me in the beginning of my work in the field of wind energy predictions. Though he left the university a little early than I expected I nevertheless benefit from his knowledges.

Moreover, I would like to thank Detlev Heinemann for his advice and sopport in carring out my initial work at the university.

The Tjæreborg measurement data was provided by the ”Database on Wind Characteristics”, internet: *http://www.winddata.com*, located at the Technical University of Denmark (DTU); and the Meerhof measurement data by ForWind where I thank, in particular, Norbert Zacharias, Arne Wessel and Peter Rieder (EWO Energietechnologie), for their support.

A list that has far too many names on it to mention separately is that all co-workers, group members, and roommates at the Institute of Physics of the University of Oldenburg that I have worked, talked, and lunched with over the years. My gratitude goes to all those colleagues and former colleagues at the ForWind; the Hydrodynamics and Wind Energy group; the Energy Meteorology group; the Energy and Semiconductor Laboratory (EHF) and all staff at the Postgraduate Programme Energy (PPRE). I treasure the memories.

I am, of course, particularly indebted to give a very big hearty thanks to my wife Florence and friends[1], for her help, friendship and enormous patience for the fact that they never gave in the to the temptation to make fun of my perennial thesis delays and delays... Well hardly ever.

A special thanks to my parents for their monumental, unwavering support and encouragements that they gave me in the beginning of this road. All they have truly been for me, and without them none of this would have been even possible.

[1] You know who you are.

Curriculum Vitae

Personal Data

Name	Edgar Anahua
Birthdate	17. November 1971
Birthplace	Tacna, Perú

Education

03.1990 - 03.1992	Industrial Engineering Student at the University of Tarapacá in Arica, Chile
03.1993 - 03.1999	Mechanical Engineering at the University of Tarapacá in Arica, Chile Thesis title: Design and implementation of a monitoring system for photovoltaic water pump system
09.2000 - 09.2001	Master of Science (MSc.) at the Postgraduate Programme Renewable Energy of the Carl von Ossietzky Universität Oldenburg Thesis guided by Prof. Dr. J. Peinke, with the title “Analysis of data, turbulence and wind power”

Research Work

10.2002 - 02.2005	Researcher at the Energy and Semiconductor Research Group and Researcher at the Center for Wind Energy Research (ForWind) of the Carl von Ossietzky University Oldenburg EU-funded Project HONEYMOON: Embedding short term prediction in numerical weather prediction model
since 03.2005	Researcher at the Center for Wind Energy Research (ForWind) of the Carl von Ossietzky University Oldenburg BMBF-funded Project: Analysis of wind turbine characteristics and wind turbulence with respect to improve energy output prognosis

Erklärungen

Ich erkläre hiermit, dass ich die vorliegende Dissertation selbst verfasst und nur die angegebenen Quellen und Hilfsmittel verwendet habe.

Oldenburg, den 04. July 2007

.....

(Edgar Anahua)

Publications

Articles and proceedings where mainly results of my work are published.

- ANAHUA E., BARTH S., PEINKE J. Markovian Power Curves for Wind Turbines *Wind Energy Journal* (recently submitted), 2007.

- ANAHUA E., BARTH S., PEINKE J. Characterization of the Power Curve for Wind Turbines by Stochastic Modeling *Wind Energy, J. Peinke, P. Schaumann, S. Barth (Eds.) (Springer: Berlin)*; pp. 173-177., 2007.

- ANAHUA E., GOTTSCHALL J., BARTH S., PEINKE J. Getting Wind Turbine Power Curves from Fluctuating Data *8th German Wind Energy Conference*, Proceedings of the DEWEK, 2006.

- ANAHUA E., BARTH S., BOETTCHER F., PEINKE J. Characterization of the Power Curve for Wind Turbines by Stochastic Modeling *European Wind Energy Conference*, Proceedings of the EWEC, 2006.

- ANAHUA E., LANGE M., BOETTCHER F., BARTH S., PEINKE J. Stochastic Analysis of the Power Output for a Wind Turbine *European Wind Energy Conference*, Proceedings of the EWEC, 2004.

- ANAHUA E., LANGE M., BOETTCHER F., BARTH S., PEINKE J. Stochastic Analysis of the Power Output for a Wind Turbine *7th German Wind Energy Conference*, Proceedings of the DEWEK, 2004.

Additional publications where I have contributed.

- RAUH A., ANAHUA E., BARTH S., PEINKE J. Phenomenological response theory to predict power output *Wind Energy, J. Peinke, P. Schaumann, S. Barth (Eds.) (Springer: Berlin)*; pp. 153-158, 2007.

- GOTTSCHALL J., ANAHUA E., BARTH S., PEINKE J. Stochastic Modeling of Wind Speed Power Production Correlations *PAMM 2006, Proceedings GAMM*; Vol.6: pp. 665-666, 2006.

- PEINKE J., ANAHUA E., RAUH A. Dynamic Response of Wind Turbines to Turbulent Winds *European Wind Energy Conference*, Proceedings of the EWEC, 2006.

- BARTH S., BOETTCHER F., GRUENEBERGER R., ANAHUA, E., PEINKE, J. Effects of Turbulence on Wind, Lift and Power *European Geophysics Union (EGU)*; Vol. 8, 04866, 2006.

- BOETTCHER F., SIEFERT M., ANAHUA E., PEINKE J. Analysis of noisy and deterministic contributions to the dynamics of measured data sets - applications to atmospheric wind speeds *European Geophysics Union (EGU)*; Vol.5, 05228, 2003.

- BOETTCHER F., ANAHUA E., PEINKE J. The Dynamical Behavior of Gusts *Global Windpower Conference*, Proceedings of the GWEC, 2002.

- BOETTCHER F., ANAHUA E., PEINKE J. Dynamische Eigenschaften von Windsund ihre Auswirkungen *6th German Wind Energy Conference*, Proceedings of the DEWEK, 2002.